

AD-A002 753

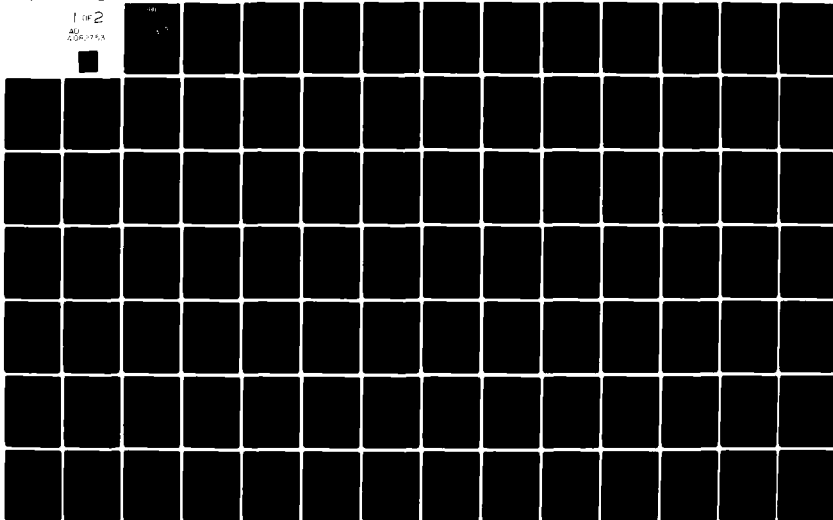
GENERAL ELECTRIC CO LYNN MA AIRCRAFT ENGINE GROUP F/G 21/5
HIGH BYPASS TURBOFAN COMPONENT DEVELOPMENT, PHASE II. DETAILED --ETC(U)
AUG 79 H MAUCH, T OLDAKOWSKI, D WELDON F33615-78-C-2060

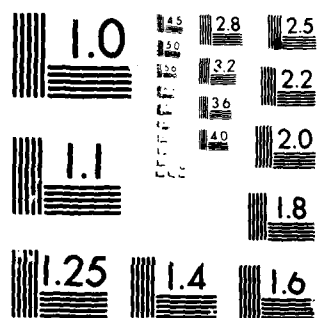
AFAPL-TR-79-2064

NL

UNCLASSIFIED

1 OF 2
AD
200707A





MICROCOPY RESOLUTION TEST CHART
NATIONAL BUREAU OF STANDARDS-1963-A

AFAPL-TR-79-2064

LEVEL

PS 10

ADA082753

HIGH BYPASS TURBOFAN COMPONENT DEVELOPMENT
PHASE II DETAILED DESIGN

Author(s)

H. Mauch
T. Oldakowski
D. Weldon

DTIC
ELECTE
APR 4 1980
S D C

Aircraft Engine Group
General Electric Co.
Lynn, Massachusetts 01910

August 1979

Technical Report AFAPL-TR-79-2064
Report for Period - 4 October 1978 - 25 May 1979

Approved for Public Release; Distribution Unlimited

AIR FORCE AERO PROPULSION LABORATORY
AIR FORCE WRIGHT AERONAUTICAL LABORATORIES
AIR FORCE SYSTEMS COMMAND
WRIGHT-PATTERSON AIR FORCE BASE, OHIO 45433

80 4 4 015

NOT FILED


NOTICE

When Government drawings, specifications, or other data are used for any purpose other than in connection with a definitely related Government procurement operation, the United States Government thereby incurs no responsibility nor any obligation whatsoever; and the fact that the government may have formulated, furnished, or in any way supplied the said drawings, specifications, or other data, is not to be regarded by implication or otherwise as in any manner licensing the holder or any other person or corporation, or conveying any rights or permission to manufacture, use, or sell any patented invention that may in any way be related thereto.

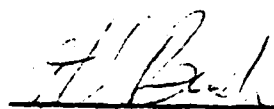
This report has been reviewed by the Information Office (OI) and is releasable to the National Technical Information Service (NTIS). At NTIS, it will be available to the general public, including foreign nations.

This technical report has been reviewed and is approved for publication.


LARRY W. GILL
Project Engineer


ERIK W. LINDNER
Tech Area Manager

FOR THE COMMANDER:


H. I. BUSH
Deputy Director

"If your address has changed, if you wish to be removed from our mailing list, or if the addressee is no longer employed by your organization please notify AFAPL/TBP, W-PAFB, OH 45433 to help us maintain a current mailing list".

Copies of this report should not be returned unless return is required by security considerations, contractual obligations, or notice on a specific document.

19 REPORT DOCUMENTATION PAGE		READ INSTRUCTIONS BEFORE COMPLETING FORM	
1. REPORT NUMBER AFAPL TR-79-2064 ✓	2. GOVT ACCESSION NO.	3. RECIPIENT'S CATALOG NUMBER 9	
4. TITLE (and Subtitle) HIGH BYPASS TURBOFAN COMPONENT DEVELOPMENT Phase II, Detailed Design 8041614L		5. TYPE OF REPORT & PERIOD COVERED Interim Technical Report, 4 Oct 78 - 25 May 79	
7. AUTHOR(s) H. Mauch T. J. Idakowski D. Weldon		8. CONTRACT OR GRANT NUMBER(s) 15 F33615-78-C-2068 ✓	
9. PERFORMING ORGANIZATION NAME AND ADDRESS Aircraft Engine Group ✓ General Electric Company Lynn MA 01910		10. PROGRAM ELEMENT, PROJECT, TASK AREA & WORK UNIT NUMBERS 62203F/3066/15 26 26 17	
11. CONTROLLING OFFICE NAME AND ADDRESS Air Force Aero Propulsion Laboratory (TBP) Wright-Patterson AFB, OH 45433		12. REPORT DATE Aug 1979	
14. MONITORING AGENCY NAME & ADDRESS (if different from Controlling Office) 12 138		13. NUMBER OF PAGES 129	
		15. SECURITY CLASS. (of this report) Unclassified	
		15a. DECLASSIFICATION/DOWNGRADING SCHEDULE	
16. DISTRIBUTION STATEMENT (of this Report) Approved for Public Release; Distribution Unlimited			
17. DISTRIBUTION STATEMENT (of the abstract entered in Block 20, if different from Report)			
18. SUPPLEMENTARY NOTES			
19. KEY WORDS (Continue on reverse side if necessary and identify by block number) High Bypass Turbofan Fan Aerodynamic Design Small Turbofan Fan Aeromechanical Design Fan Component Fan Mechanical Design Bird Strike Capability			
20. ABSTRACT (Continue on reverse side if necessary and identify by block number) A detailed aerodynamic, aeromechanical and mechanical design of the high bypass turbofan fan stage selected during Phase I of this program was satisfactorily completed. This fan design is the result of aero and aeromechanical iterations and trade-offs which achieved the objectives of meeting aerodynamic performance as well as the life and mechanical considerations of MIL-E-5007D. The resulting fan design compares very closely to the fan originally proposed.			

TABLE OF CONTENTS

<u>SECTION</u>	<u>PAGE</u>
I. SUMMARY	1
II. INTRODUCTION	2
III. DESCRIPTION AND RESULTS OF PHASE II - TECHNICAL WORK	3
3.1 FAN AERODYNAMIC PARAMETRIC STUDIES	3
3.1.1 Description of Parametric Studies	3
3.1.2 Parametric Studies Results	9
3.2 FAN AEROMECHANICAL PARAMETRIC STUDIES	32
3.2.1 Fan Aeromechanical Design Objectives	32
3.2.2 Parametric Studies	32
3.3 FAN AERODYNAMIC DESIGN	50
3.3.1 Effect of Birdstrike on Fan Performance	50
3.3.2 Design Point Selection	56
3.3.3 Flow Field Specification	56
3.3.4 Blading Definition	81
3.4 FAN AEROMECHANICAL ANALYSIS	106
3.4.1 Fan Rotor Design Analysis	106
3.4.2 Fan Stator Design Analysis	112
3.5 FAN MECHANICAL DESIGN	115
3.5.1 Fan Blisk Overall Design	115
3.5.2 Fan Blisk and Spinner Stress Levels	115
3.5.3 Fan Blisk Material Selection	119
3.5.4 Fan Exit Guide Vane Overall Design	119
3.5.5 Fan Exit Guide Vane Material Selection	119
3.5.6 Fan Weight	119
3.5.7 Compliance with MIL-E-5007 Requirements	122
3.6 TEST EQUIPMENT INTERFACE + DESIGN INTEGRATION	124
3.6.1 Design Philosophy	124
3.6.2 Fan Interface with Test Vehicle	124
3.6.3 Test Rig Preliminary Design	124
3.7 RELIABILITY, MAINTAINABILITY AND SYSTEMS SAFETY	126
IV. CONCLUSIONS	127
V. RECOMMENDATIONS	127
ABBREVIATIONS, ACRONYMS, AND SYMBOLS	128

LIST OF ILLUSTRATIONS

<u>Figure No.</u>		<u>Page</u>
1.	Rotor Tip Wheel Speed	10
2.	Flow Per Annulus Area	11
3.	Rotor Inlet Radius Ratio	12
4.	Rotor Discharge Axial Velocity (Rotor Area Convergence)	13
5.	Fan Discharge Mach No	14
6.	Rotor Aspect Ratio	15
7.	Stator Aspect Ratio	16
8.	Rotor Solidity	17
9.	Stator Solidity	18
10.	Rotor Tip Wheelspeed	21
11.	Flow Per Annulus Area	22
12.	Rotor Inlet Radius Ratio	23
13.	Fan Rotor Discharge Axial Velocity	24
14.	Fan Discharge Mach No.	25
15.	Flowpath Flaring Concept	27
16.	Effects of Flaring on Efficiency and Stall Margin	28
17.	Rotor Casing Flaring Effects	29
18.	Method for Airfoil 2/Rev Avoidance	35
19.	Method for Airfoil HCF Optimization	36
20.	Method for Airfoil Frequency Control	37
21.	Airfoil Pressurization Due To Bird Strike	40
22.	Bird Approach Angle and "Footprint"	41
23.	Slicing Action During Bird Impact	42
24.	Bird Impact Load/Stress Mode	43
25.	Severity of Bird Strike as a Function of Impact Location	45
26.	Method for Selecting Blade Thickness for Bird Strike	46
27.	Method for Selecting Blade Airfoil Attachment	49

LIST OF ILLUSTRATIONS

<u>Figure No.</u>		<u>Page</u>
28.	Velocity Vector Diagram Including Bird Path	51
29.	Airfoil Thickness Requirements to Satisfy Bird Strike Conditions	52
30.	Rotor Airfoil Thickness Axial Distribution	53
31.	Blade Passage Design Parameters	54
32.	Suction Surface Incidence Considerations	55
33.	Effect of Birdstrike Requirement on Blade Passage Design	57
34.	Wedge Angle for Various Fan Blade Shapes vs. Maximum Wedge Angle	58
35.	Final Aerodynamic Flow Path	65
36.	Rotor and Stator Discharge Profiles	67
37.	Rotor Total Pressure Loss Coefficients	68
38.	Stator Total Pressure Loss Coefficients	69
39.	Percent Cumulative Change in Total Temperature	70
40.	Percent Cumulative Change in Stator Air Angle	71
41.	Rotor Diffusion Factor	72
42.	Stator Diffusion Factor	73
43.	Rotor Inlet and Discharge Relative Air Angles	74
44.	Stator Inlet and Discharge Angles	75
45.	Rotor Relative Inlet Mach No.	76
46.	Stator Absolute Inlet Mach No.	77
47.	Stator Discharge Absolute Mach No.	78
48.	Ratio of Discharge to Inlet Axial Velocity Across Rotor	79
49.	Stator Axial Velocity Ratio Profile	80
50.	Radial Distribution Rotor Chord	82
51.	Rotor Solidity Radial Distribution	83
52.	Stator Chord Radial Distribution	84
53.	Stator Solidity Radial Distribution	85

Accession For	
NTIS	<input checked="" type="checkbox"/>
DDC TAB	<input type="checkbox"/>
Unannounced	<input type="checkbox"/>
Justification	<input type="checkbox"/>
By _____	
Distribution _____	
Availability _____	
Dist	Available for special

LIST OF ILLUSTRATIONS

<u>Figure No.</u>		<u>Page</u>
54.	Rotor Maximum Thickness/Chord Radial Distribution	86
55.	Stator Maximum Thickness/Chord Radial Distribution	87
56.	Rotor Incidence Angle Radial Distribution	88
57.	Stator Incidence Angle Radial Distribution	89
58.	Rotor Deviation Angle Radial Distribution	90
59.	Stator Deviation Radial Distribution	91
60.	Meanline Metal Angles	92
61.	Rotor Streamline Camber And Stagger Angles Distribution	94
62.	Rotor Tip Blade-to-Blade Passage Shape	95
63.	Rotor Pitch Blade-to-Blade Passage Shape	96
64.	Rotor Hub Blade-to-Blade Passage Shape	97
65.	Rotor Blade Passage Area Ratios	98
66.	Rotor Suction Surface Incidence Angle	99
67.	Stator Meanline Metal Angle	100
68.	Stator Streamline Camber And Stagger Angles	101
69.	Stator OD Blade-to-Blade Passage Shape	102
70.	Stator Pitch Blade-to-Blade Passage Shape	103
71.	Stator ID Blade-to-Blade Passage Shape	104
72.	Stator Passage Throat to Inlet Area Ratio	105
73.	Rotor Airfoil Aerodynamic And Geometric Description	107
74.	Rotor Airfoil Frequency Characteristics	108
75.	Rotor Airfoil Stability Margin	109
76.	Rotor Airfoil Stress Characteristics	110
77.	Rotor Airfoil Bird Impact Tolerance Capability	111
78.	Stator Airfoil Aerodynamic And Geometric Description	113
79.	Stator Airfoil Frequency Characteristics	114
80.	Fan Blisk Full Scale Cross Section	116

LIST OF ILLUSTRATIONS

<u>Figure No.</u>		<u>Page</u>
81.	Comparison Between Demonstrator and Flight Blisks	117
82.	Fan Blisk and Spinner Stress Distribution	118
83.	Exit Guide Vane Assembly Overall Design	121
84.	Fan Blisk and EGV Assembled in Test Rig	125

LIST OF TABLES

<u>Table</u>		<u>Page</u>
1.	Standards For Evaluation of Parametrics	4
2.	Aerodynamic Model	5
3.	List of Parameters Selected For Study	6
4.	Base Point Values For Aerodynamic Study	7
5.	Parametric Study Constants	8
6.	Effects of Parametric on Stall Margin and Efficiency	19
7.	Summary of Fan Parametric Effects	26
8.	Rotor Casing Flaring Effects Summary	31
9.	Mechanical Performance Requirements	33
10.	Aeromechanical Criteria	34
11.	Bird Ingestion Tolerance Design Criteria	38
12.	Bird Strike Problem/Solution Format	44
13.	Rationale for Blade Material Selection	48
14.	Impact of Meeting Bird Strike Requirement	59
15.	Final Selection of Aerodynamic Design Parameters	60
16.	Reasons for Final Design Selection	61
17.	Reasons for Final Design Selection	62
18.	Reasons for Final Design Selection	63
19.	Comparison of Important GE26/F4 Design Conditions With Proposal	64
20.	Fan Blisk Material Selection Factors	120
21.	Key Mil-E-5007D Requirements Evaluation	123

SECTION I

SUMMARY

This report describes those efforts expended by the Contractor in Phase II - Detailed Design of the High Bypass Turbofan under USAF Contract F-33615-78-C-2060.

With the completion of Phase II, eleven months of the twenty-seven months of effort associated with this program have been completed. The time to date spent on Phase I and Phase II has been devoted to preliminary design and detailed design respectively. The fabrication and test phase remains to be accomplished.

In Phase II, the subject of this report, the Contractor has been able to meld the aerodynamic and the mechanical requirements into a cohesive design which satisfies all of the aero, aeromechanical and mechanical requirements imposed and which, incidentally, comes quite close to the design originally proposed for this program.

The report which follows - the second Interim Technical Report associated with this Contract - documents fully the specific investigations carried out as part of the detailed design effort. The organization of the report is as follows:

- o Fan aerodynamic parametric studies
- o Fan aeromechanical parametric studies
- o Fan aerodynamic design
- o Fan aeromechanical analysis
- o Fan mechanical detail design

Other topics covered in this report include discussions of test equipment and reliability, maintainability and systems safety.

SECTION II

INTRODUCTION

The current primary trainer (T-37) fleet is approaching the end of its useful life and will necessitate the development of replacement aircraft in the near future. In light of the current awareness of life cycle cost and decreasing fuel reserves, the replacement aircraft must have a fuel efficient engine as the propulsion system, i. e., modern turbofan engine. Technology in the large turbofan engines has been well demonstrated, but little has been done in the size applicable to a twin-engine primary trainer aircraft. Today, there is sufficient effort to provide the necessary technology for the development of the engine with the exception of the fan component. It is the objective of this program to develop such a fan using the latest compressor technology.

Phase I - Preliminary Design was successfully completed, as reported in the first interim technical report, including the identification of fan design objectives required for a small turbofan engine intended to power the future Air Force Primary trainer.

This document presents the second interim technical report on the High Bypass Turbofan Program describing the technical work which was done under Phase II - Detailed Design in accordance with the Contract Statement of Work. Specifically, a detailed design of the fan component was generated based upon the Phase I preliminary design. Trade-off studies between aerodynamic design and mechanical design were performed. The detailed design addressed to the design requirements of MIL-E-5007D with special emphasis on foreign object tolerance, distortion and low cycle fatigue.

In recognition of the successful completion of Phase II Detailed Fan Design AFAPL has authorized the execution of Phase III - Fabrication and Test of the Detailed Fan Design.

SECTION III

DESCRIPTION AND RESULTS OF PHASE II TECHNICAL WORK

The following subsections provide details of the technical work performed in accordance with Phase II of the Statement of Work and the significant results obtained.

3.1 FAN AERODYNAMIC PARAMETRIC STUDIES

This subsection describes the aerodynamic parametric studies and trade-offs which were carried out to achieve the performance objectives in a practical and cost effective manner.

3.1.1 Description of Parametric Studies

The first phase of the detailed design of the High Bypass Fan was to perform parametric studies of the important aerodynamic design parameters. The objective of these fan aerodynamic parametric studies are the following:

- o Determine effect of fan design parameters on fan performance.
- o Utilize aerodynamic parametric study trends for trade-off studies with aeromechanical and mechanical parametric studies.
- o Select values of fan design parameters for best balanced fan design.

The standards used to evaluate each of the fan design parameters are listed in Table 1 and reflects a desire to select the best balanced fan design for the trainer engine configuration as defined in Phase I.

The parametric studies utilized a pitchline compressor model to estimate the effect of the design variables on fan efficiency and stall margin. The details of the aerodynamic model used in the parametric study are described in Table 2.

Eleven parameters were selected for the parametric study. These are listed in Table 3. The range studied reflects judgement based on GE experience with other fans and the results of the preliminary parametric studies used for the proposal.

The base point values for the aerodynamic parametric studies are compared to those in the proposal in Table 4. The values were selected to be in the center of the range studied.

Certain parameters were held constant during the parametric studies. These are listed in Table 5. The correct airflow and average pressure ratio were selected in Phase I of the High Bypass Fan contract. The fan does not have an inlet guide vane to reduce cost and complexity. Fan discharge swirl was set equal to 0° for good duct performance. Rotor tip clearance reflects GE experience with similar fan designs.

TABLE 1. STANDARDS FOR EVALUATION OF PARAMETRICS

PARAMETRIC STUDY: STANDARDS OF "GOODNESS"

- o HIGH EFFICIENCY
 - EQUAL TO OR BETTER THAN PROPOSAL EFFICIENCY (.855)
- o STALL MARGIN
 - 20% OR BETTER @ 100% $N/\sqrt{\theta}$
- o MEET MECHANICAL AND AEROMECHANICAL DESIGN OBJECTIVES
- o DESIGN COMPATIBLE WITH TRAINER ENGINE CONFIGURATION
 - INNER DUCT
 - DISCHARGE MACH NO.
 - DISCHARGE HUB RADIUS
 - TURBINE
 - RPM
 - CORE COMPRESSOR

TABLE 2. AERODYNAMIC MODEL

GE COMPRESSOR MODEL FOR PARAMETRIC STUDIES

- Pitchline Compressor Model
 - Approximate Hub and Tip Calculations
- Estimates Efficiency Potential Considering:
 - Blade Profile Losses

Utilizes Compressible Boundary Layer Theory to Extend Lieblein's Equivalent Diffusion Factor Model to Higher Mach No. Region.
 - Shock Losses Due to Passage Shocks and Bow Shocks.
 - End Wall Losses Due to Boundary Layer and Clearance.
- Estimates Stall Margin Potential
 - Utilizes term "Effectivity" Defined as Ratio of Static Pressure Rise Coefficient to Maximum Static Pressure Rise Coefficient Possible at Stall.
 - Based on Empirical Correlations Comparing Compressor Performance to 2-D Diffuser Performance.
 - Similar Technology Compressors Utilized to Establish Appropriate Level of "Effectivity".

TABLE 3. LIST OF PARAMETERS SELECTED FOR STUDY

PARAMETRIC STUDY: RANGE OF VARIABLES

- o Rotor Tip Speed - Varied from 1400 to 1500 ft/sec
- o Flow/Annulus Area - Varied from 41 to 44 lbm/sec/ft²
- o Inlet Radius Ratio - Varied from .31 to .43
- o Stator Discharge Mach No. - Varied from .5 to .6
- o Ratio of Rotor Annulus Area Convergence to Stage Annulus Area Convergence - Varied from .6 to .9
- o Rotor Pitch Solidity - Varied from 1.7 to 2.05
- o Stator Pitch Solidity - Varied from 1.4 to 1.7
- o Rotor Aspect Ratio - Varied from 1.0 to 1.5
- o Stator Aspect Ratio - Varied from 1.6 to 2.3
- o Rotor Tip Flaring (RTOUT/RTIN) - Varied from 1.0 to 1.05
- o Stator Tip Flaring (RTOUT/RTIN) - Varied from 1.0 to 1.05

TABLE 4. BASE POINT VALUES FOR AERO DYNAMIC STUDY

HIGH BYPASS FAN

PARAMETRIC STUDIES: BASE POINT

<u>Variable</u>	<u>Base Point</u>	<u>Proposal</u>
Rotor Tip Speed (ft/sec)	1450	1455
Flow/Annulus Area (lbm/sec/ft ²)	42.5	43.0
Inlet Radius Ratio	.37	.36
Stator Discharge Mach No.	.55	.55
Ratio of Rotor Annulus Area Convergence to Stage Annulus Area Convergence	.75	.8
Rotor Pitch Solidity	1.9	2.04
Stator Pitch Solidity	1.56	1.71
Rotor Aspect Ratio	1.26	1.27
Stator Aspect Ratio	1.9	2.3
Rotor Tip Flaring (RTOUT/RTIN)	1.0	1.0
Stator Tip Flaring (RTOUT/RTIN)	1.0	1.0

TABLE 5. PARAMETRIC STUDY CONSTANTS

PARAMETRIC STUDY: PARAMETERS HELD CONSTANT

Corrected Airflow	41.6 lbm/sec
Pressure Ratio	1.758
No Inlet Guide Vane	
Discharge Swirl	0°
No Shroud	
Clearance	.018 0 (supported on both ends)
Surface Finish	24 RMS
Blade Thickness	.03/.096 .09/.05
	Rotor (Tip/Hub) Stator (OD/ID)

Stator clearance was set equal to zero since the stator was supported at both ends. The blade/vane surface finish was selected to be 24 RMS to assure good performance at a reasonable cost. The blade thickness reflects a preliminary aeromechanical analysis made for the proposal.

3.1.2 Parametric Study Results

The effect of each fan design parameter on fan stall margin and efficiency was determined by individually varying each parameter about the baseline values to the limit of the range. The results of these perturbations are presented in the following figures:

<u>PARAMETER</u>	<u>FIGURE</u>
Rotor tip wheelspeed	1
Flow per annulus area	2
Rotor inlet radius ratio	3
Rotor discharge axial velocity (rotor area convergence)	4
Fan discharge Mach No.	5
Rotor aspect ratio	6
Stator aspect ratio	7
Rotor solidity	8
Stator solidity	9

The effects of various fan parameters on fan stall margin and efficiency are summarized in Table 6. Lowering the flow per annulus area improved stall margin and efficiency. Efficiency is improved by lowering rotor tip wheelspeed, rotor discharge axial velocity or rotor solidity, but at the expense of stall margin.

A review of the internal details of the fan flow field indicated that flow conditions were most severe in the hub region. Therefore, special attention was directed towards reducing the severity of conditions in the hub which could increase the risk of not meeting the performance predicted by the model. These conditions examined are:

- o Rotor hub discharge relative angle
- o Stator hub inlet Mach No.
- o Stator hub diffusion factor

It is desirable that the rotor hub discharge relative air angle be positive. The combination of a high stator hub inlet Mach No. and high stator hub diffusion factor was considered risky and so either one or both should be reduced to improve efficiency. Reducing the stator hub diffusion factor would also help stall margin potential.

The fan performance should be balanced against inner duct performance to assure good engine performance. The prime considerations would be:

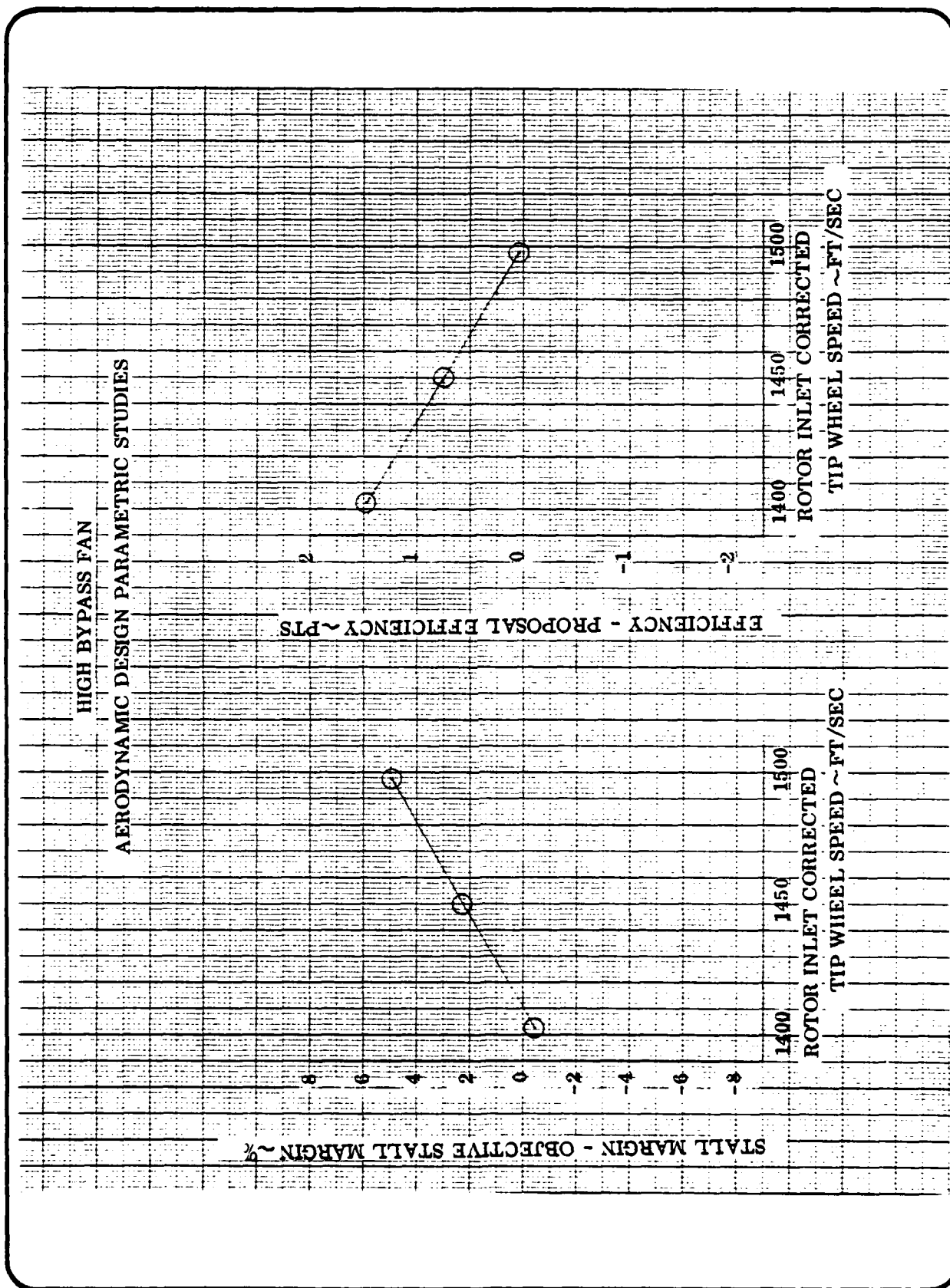


Figure 1. Rotor Tip Wheel Speed

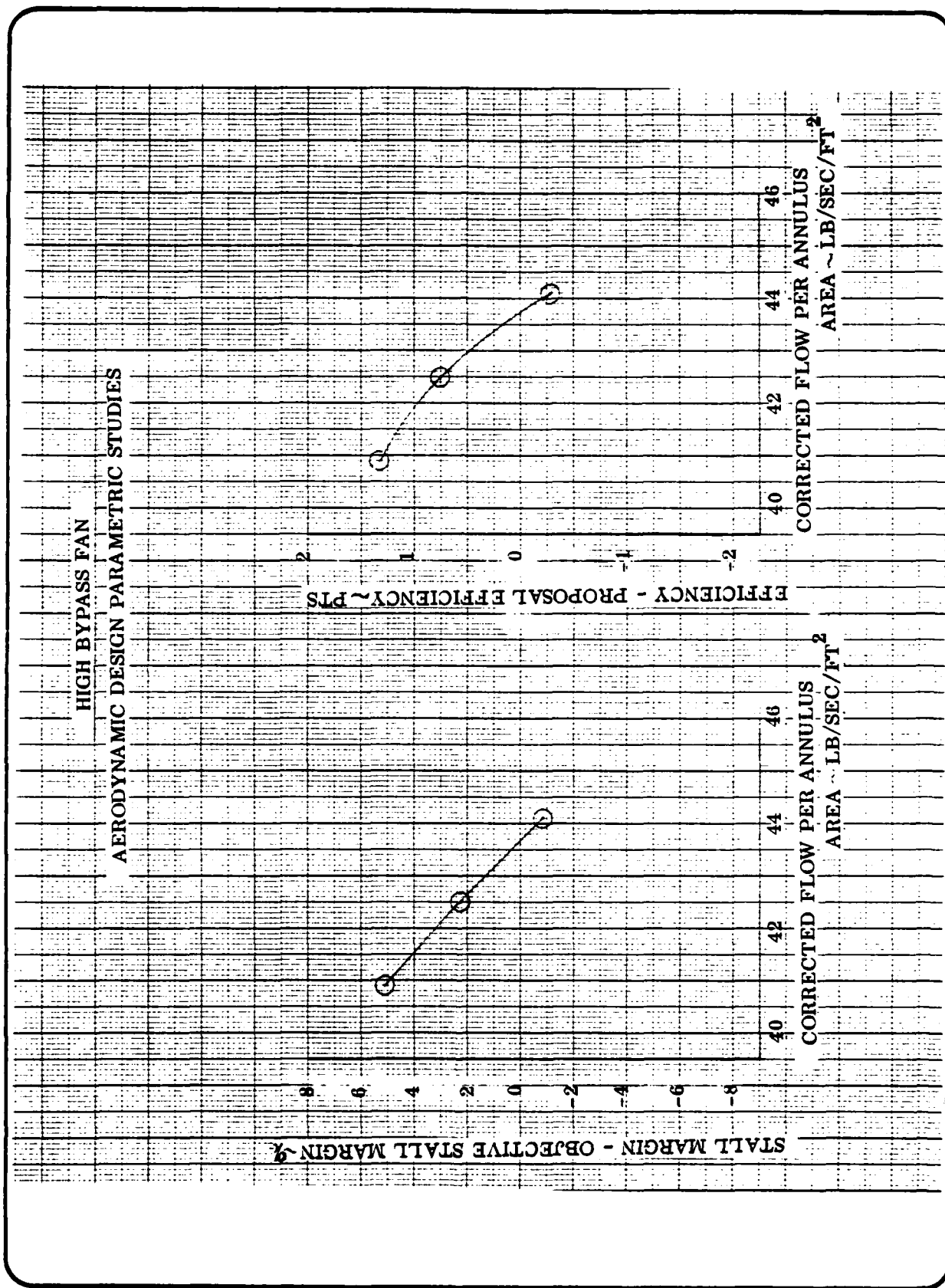


Figure 2. Flow Per Annulus Area

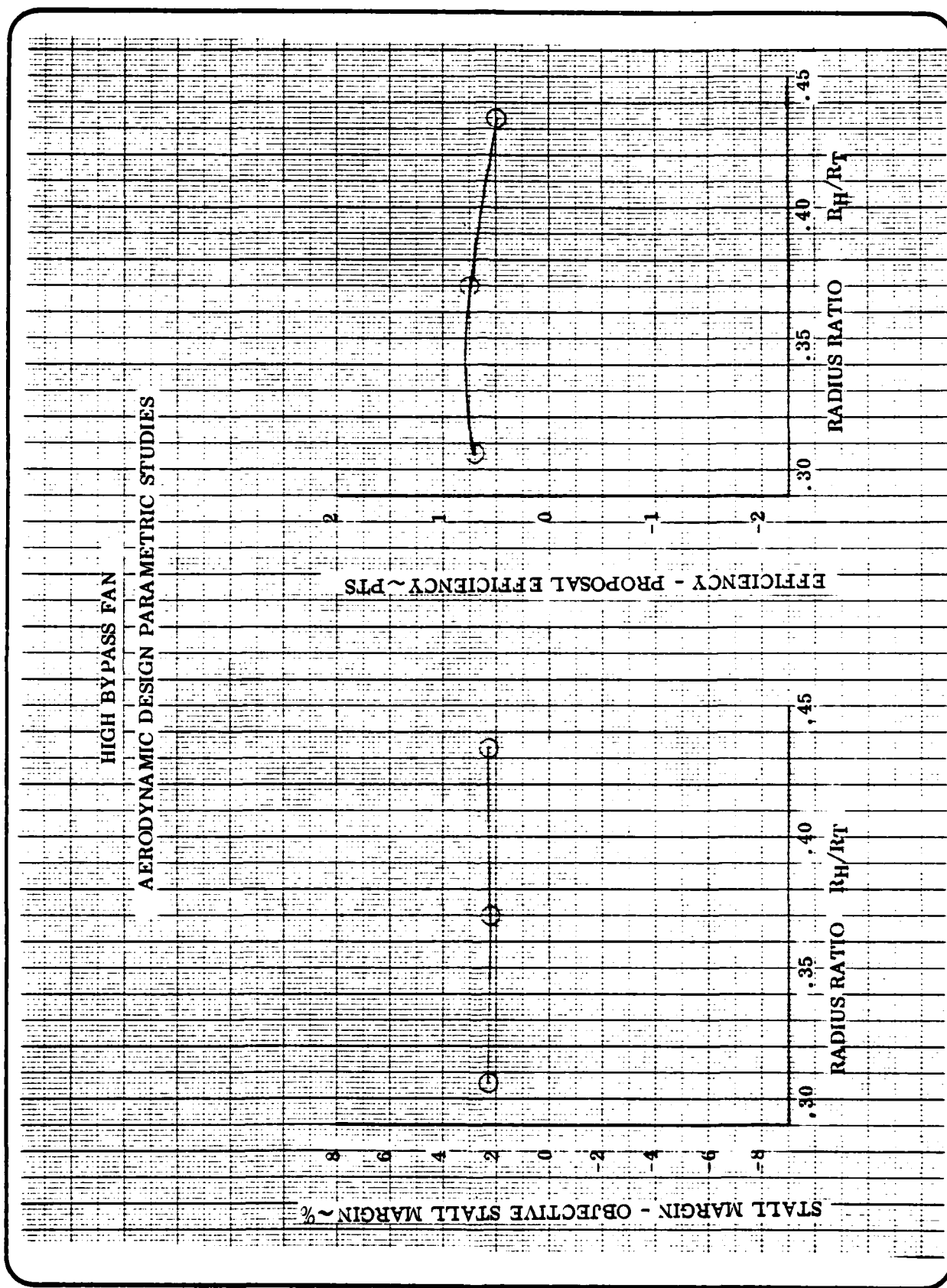


Figure 3. Rotor Inlet Radius Ratio

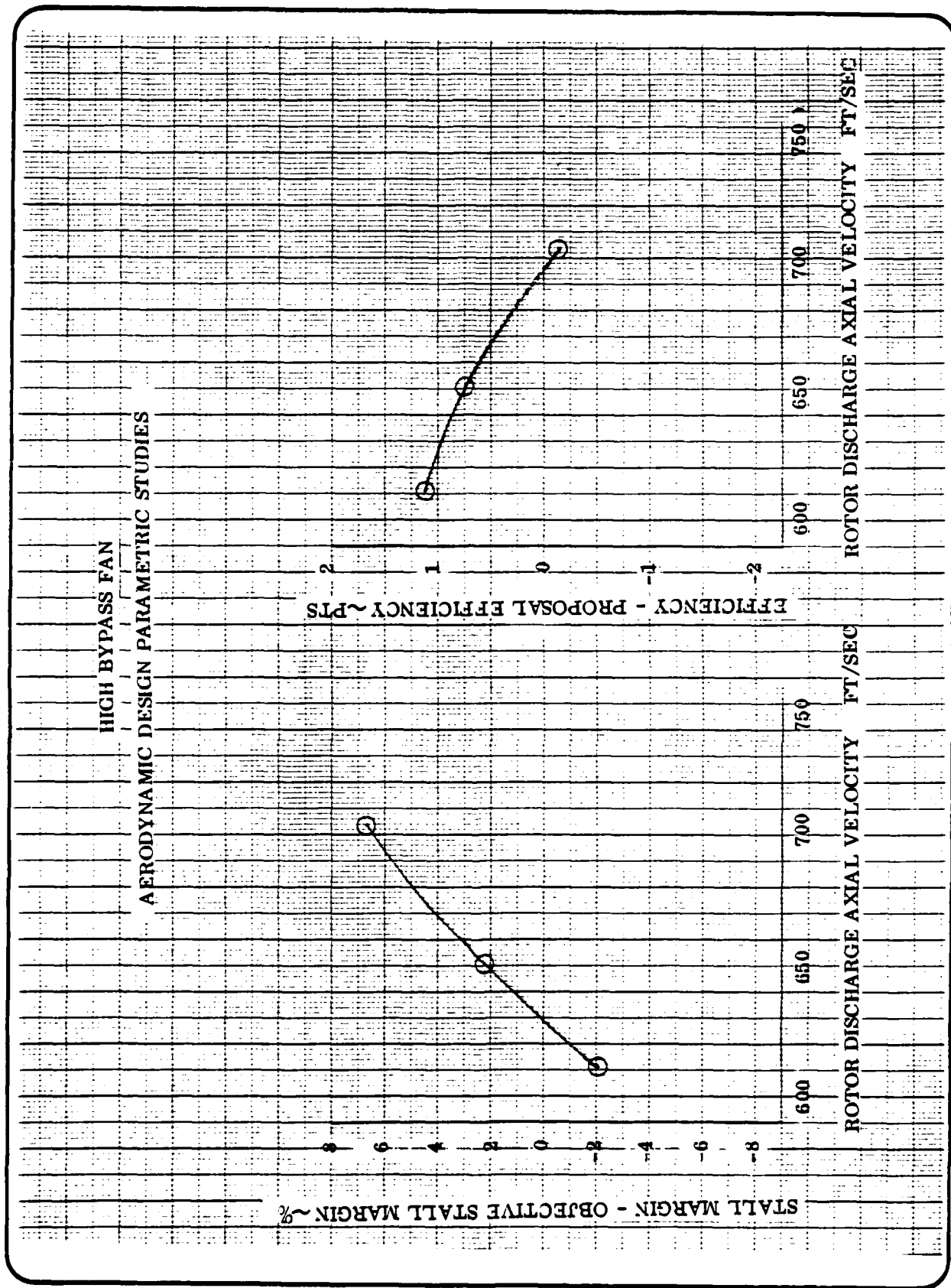


Figure 4. Rotor Discharge Axial Velocity (Rotor Area Convergence)

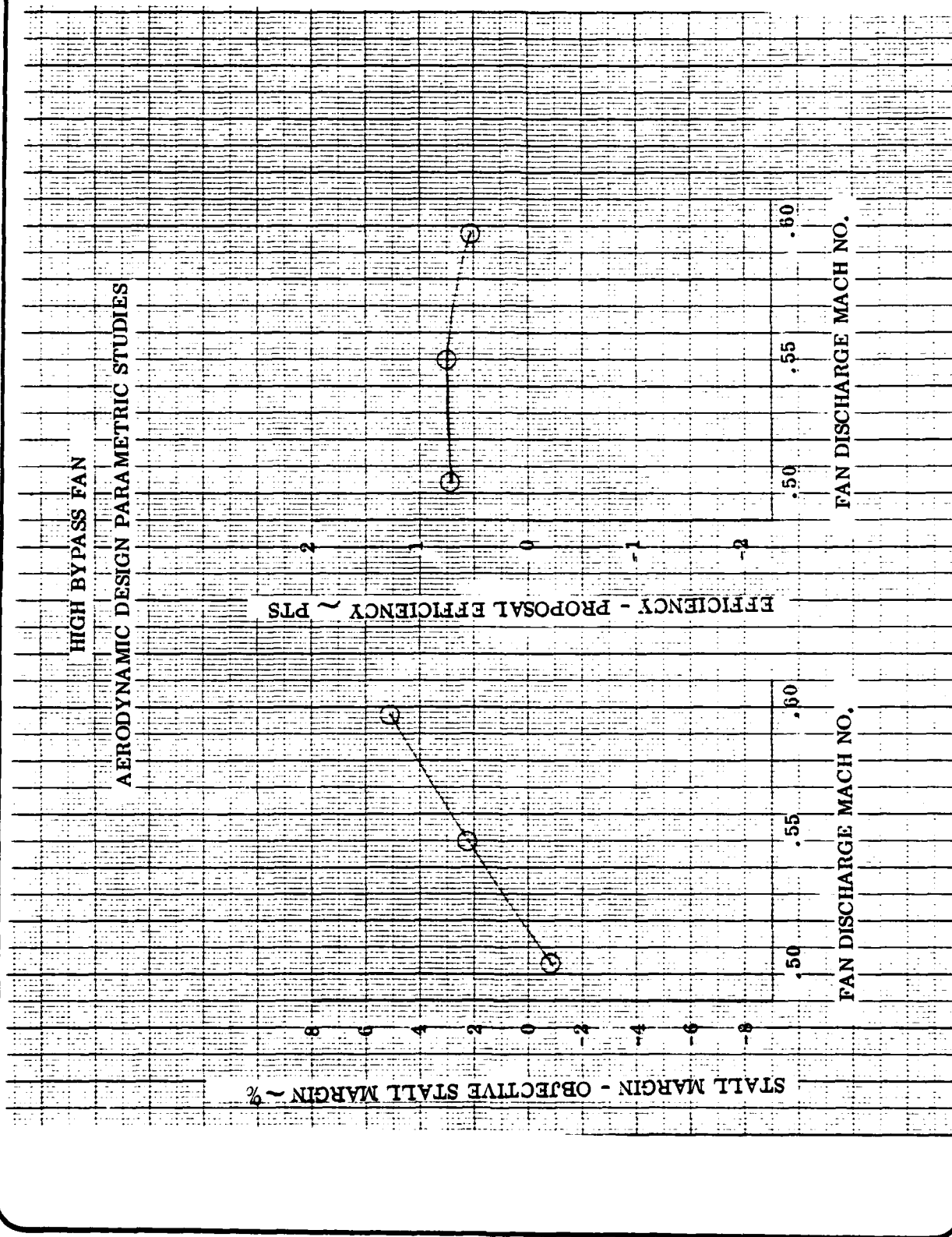


Figure 5. Fan Discharge Mach No

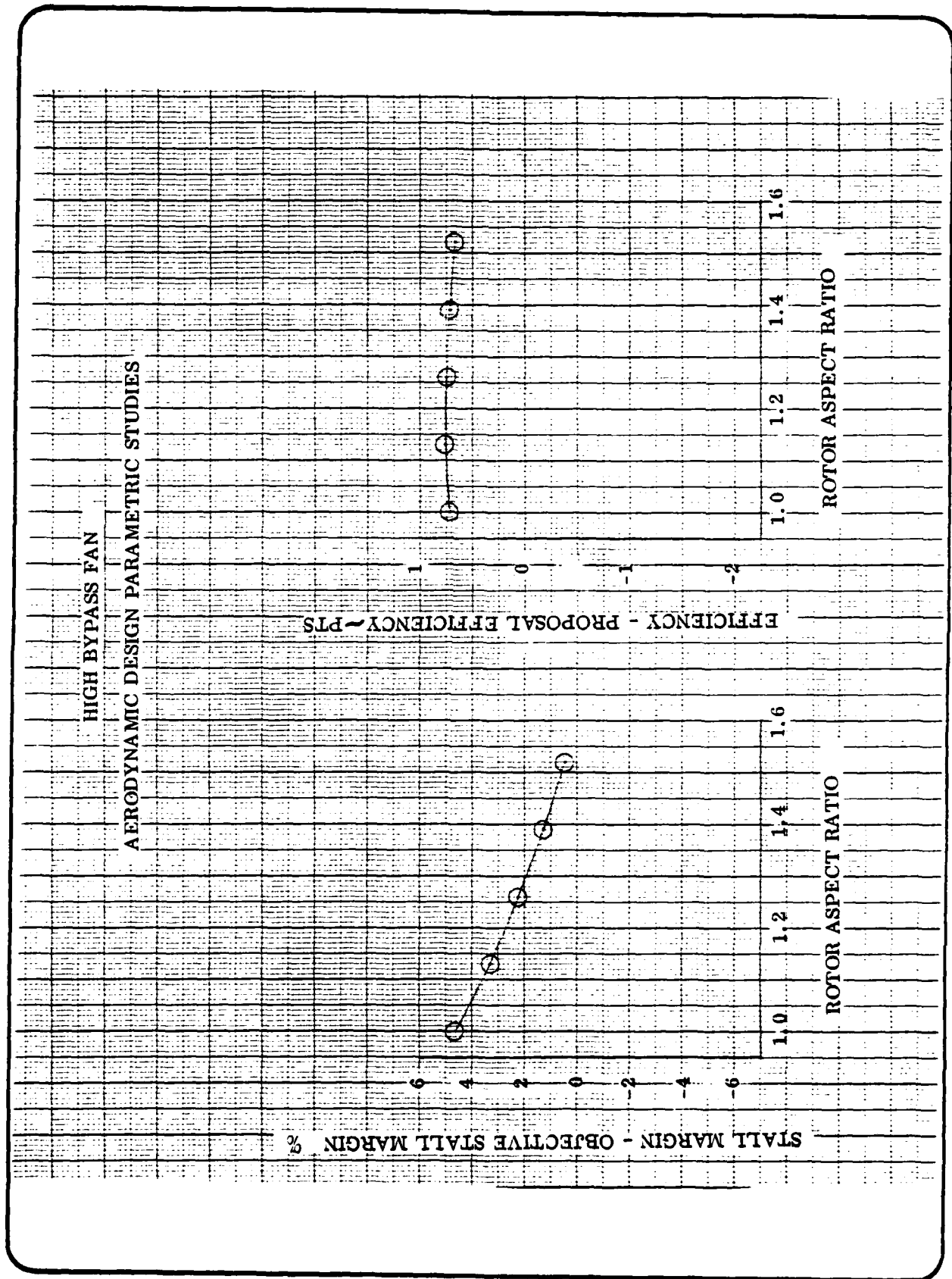


Figure 6. Rotor Aspect Ratio

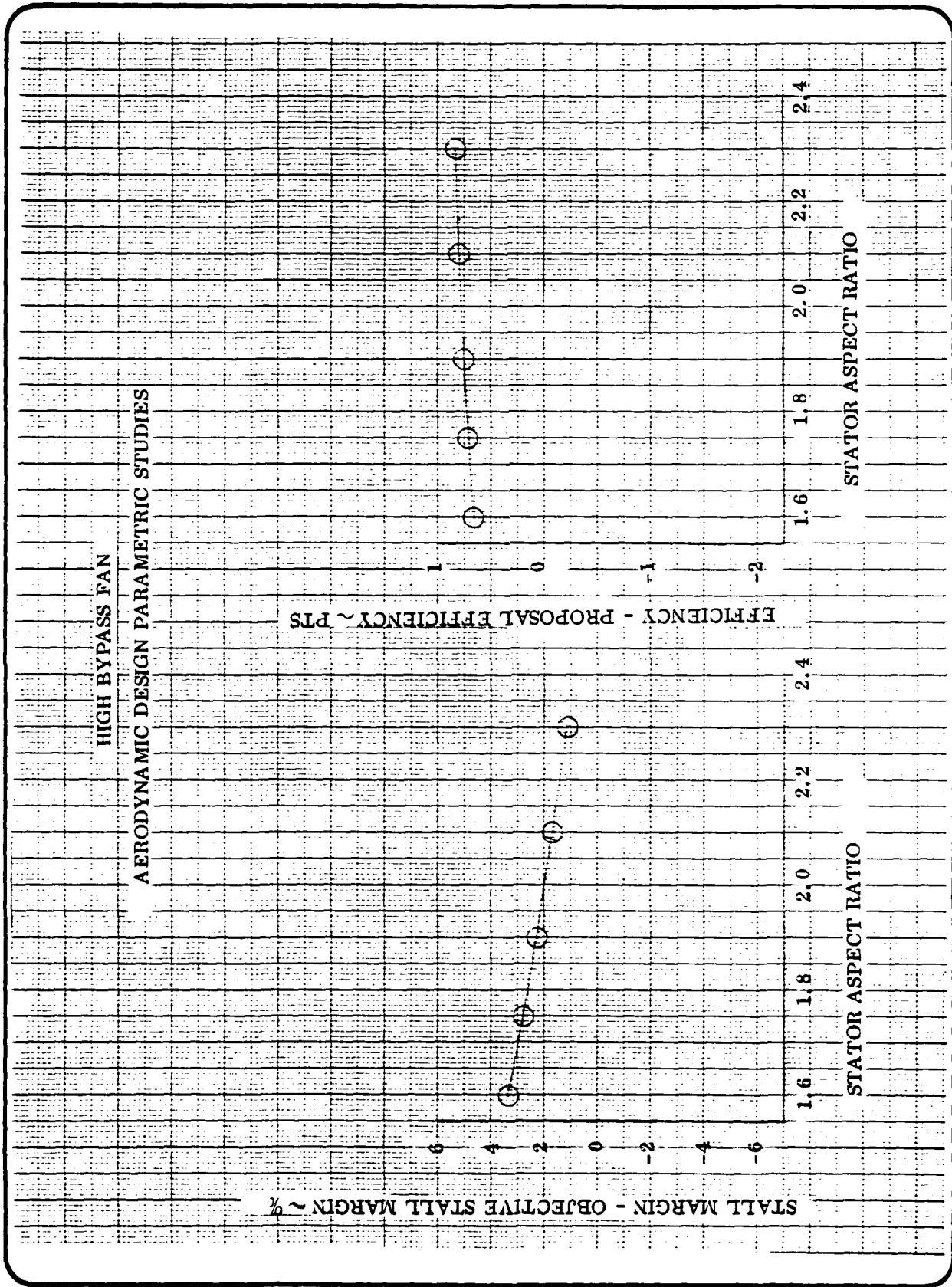


Figure 7. Stator Aspect Ratio

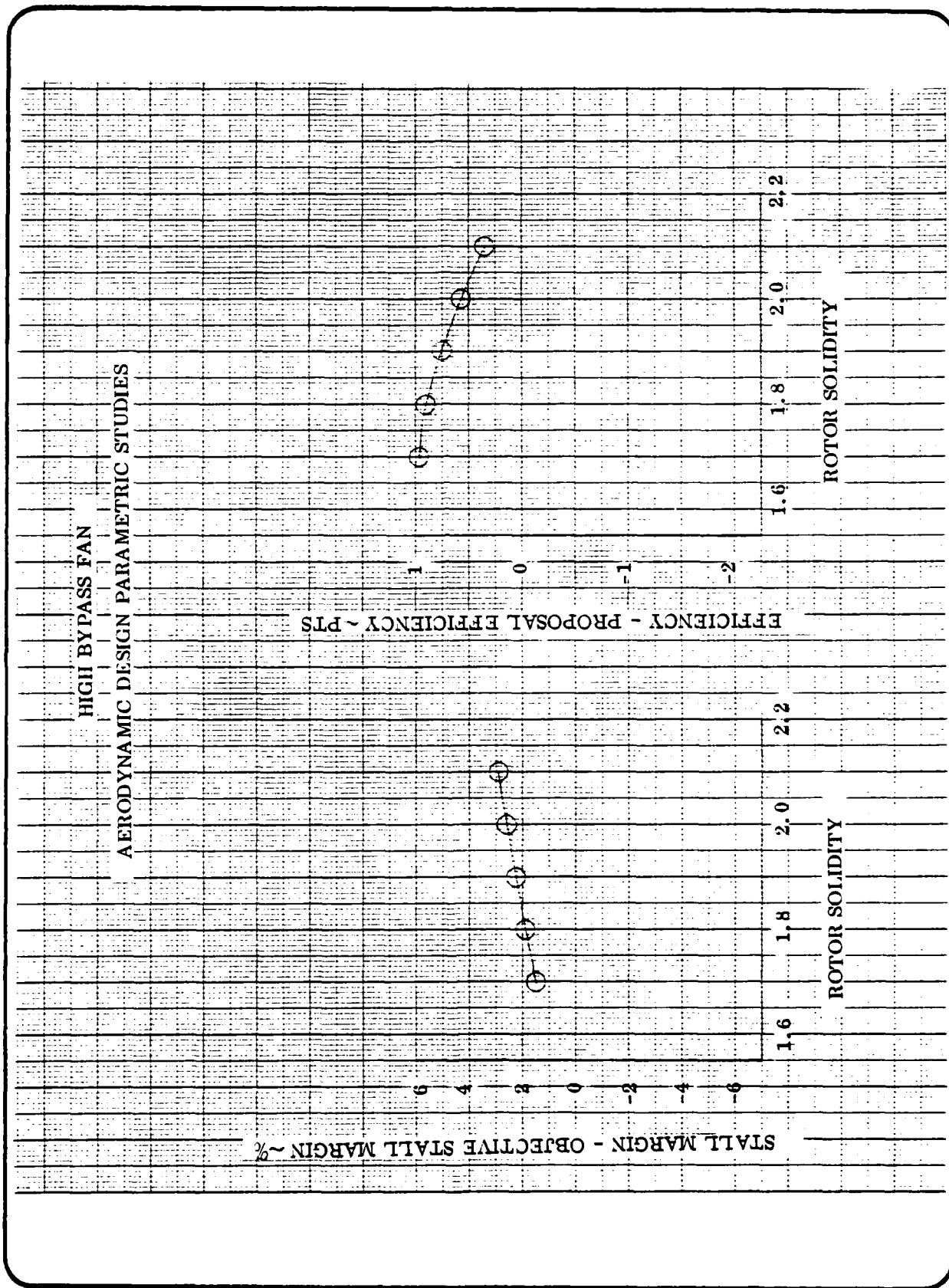


Figure 8. Rotor Solidity

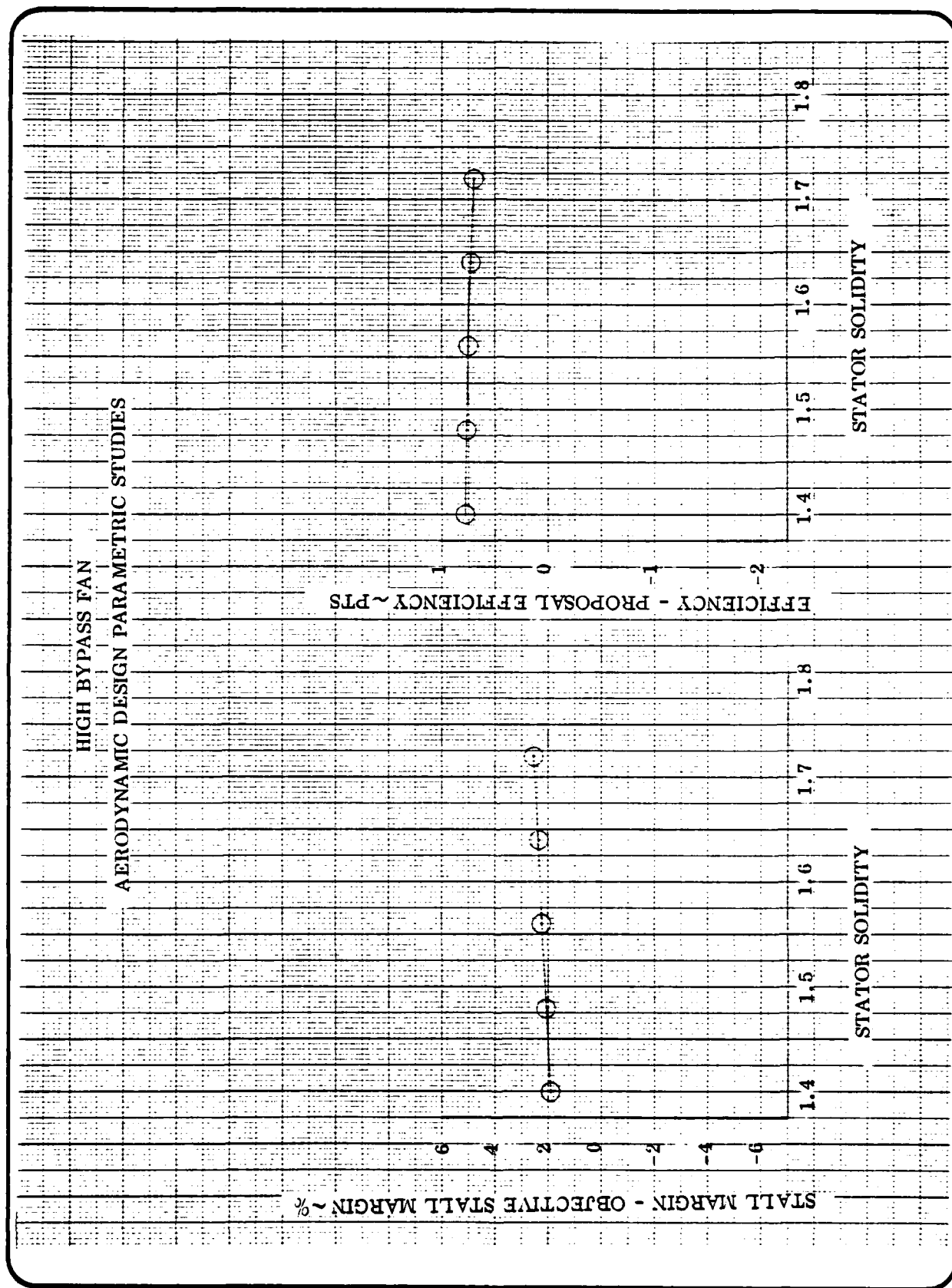


Figure 9. Stator Solidity

TABLE 6. EFFECTS OF PARAMETRIC ON STALL MARGIN AND EFFICIENCY

HIGH BYPASS FAN

AERODYNAMIC PARAMETRIC STUDY RESULTS

CHANGE IN PARAMETER FROM BASE VALUE TO OPTIMIZE PERFORMANCE

<u>Parameter</u>	<u>Stall Margin</u>	<u>Efficiency</u>
Rotor Tip Wheel speed	increase	decrease
Flow/Annulus Area	decrease	decrease
Rotor Inlet Radius Ratio	no effect	optimum
Rotor Discharge Axial Velocity	increase	decrease
Stator Discharge Mach No.	increase	optimum
Rotor Aspect Ratio	decrease	no significant effect
Stator Aspect Ratio	decrease	no significant effect
Rotor Solidity	increase	decrease
Stator Solidity	increase	no significant effect

- o Stator discharge Mach No.
- o Stator discharge Hub Radius

For the trainer fan configuration defined in Phase I, a stator hub discharge radius greater than 4.5 inches would require a longer duct or more gooseneck than previous GE fan-compressor ducts.

The effect of the fan design parameters on fan hub conditions and intercompressor duct are presented in the following figures:

<u>PARAMETER</u>	<u>FIGURE</u>
Rotor tip wheelspeed	10
Flow per annulus area	11
Rotor inlet radius ratio	12
Rotor discharge axial velocity	13
Fan discharge Mach No.	14

A summary of the effects of various fan design parameters on the fan hub flowfield and stator discharge hub radius is given in Table 7. It shows that increasing rotor tip wheelspeed and rotor inlet radius ratio or decreasing flow per annulus area help the fan hub flow conditions. Increasing flow per annulus area or decreasing rotor inlet radius ratio and stator discharge Mach No. reduce fan discharge hub radius.

The concept of flaring the casing over the rotor and/or stator was also explored during the parametric studies. Figure 15 illustrates the concept of flaring. The flared rotor has a higher discharge radius for a given set of through-flow velocities and so the rpm can be reduced to maintain discharge wheelspeed. Consequently, the inlet Mach No. and the associated losses are reduced.

The effect of rotor casing flaring on fan efficiency and stall margin is shown in Figure 16. Rotor casing flaring improves stall margin but fan efficiency is lower. Lowering the rotor tip wheelspeed improves the efficiency, but gives up some of the stall margin gained by flaring. The fan discharge hub radius is much higher with the flared casing.

Stator casing flaring did not alter flow field parameters and so it is not shown. The fan discharge radius is higher with stator casing flaring.

The parametric study indicated that rotor casing flaring improves stator hub inlet Mach Number and stator hub diffuser factor (Figure 17). But lowering the rotor tip wheelspeed gives up some of the gains due to flaring. Considerations of curvature effects not accounted for in parametric model would raise stator hub

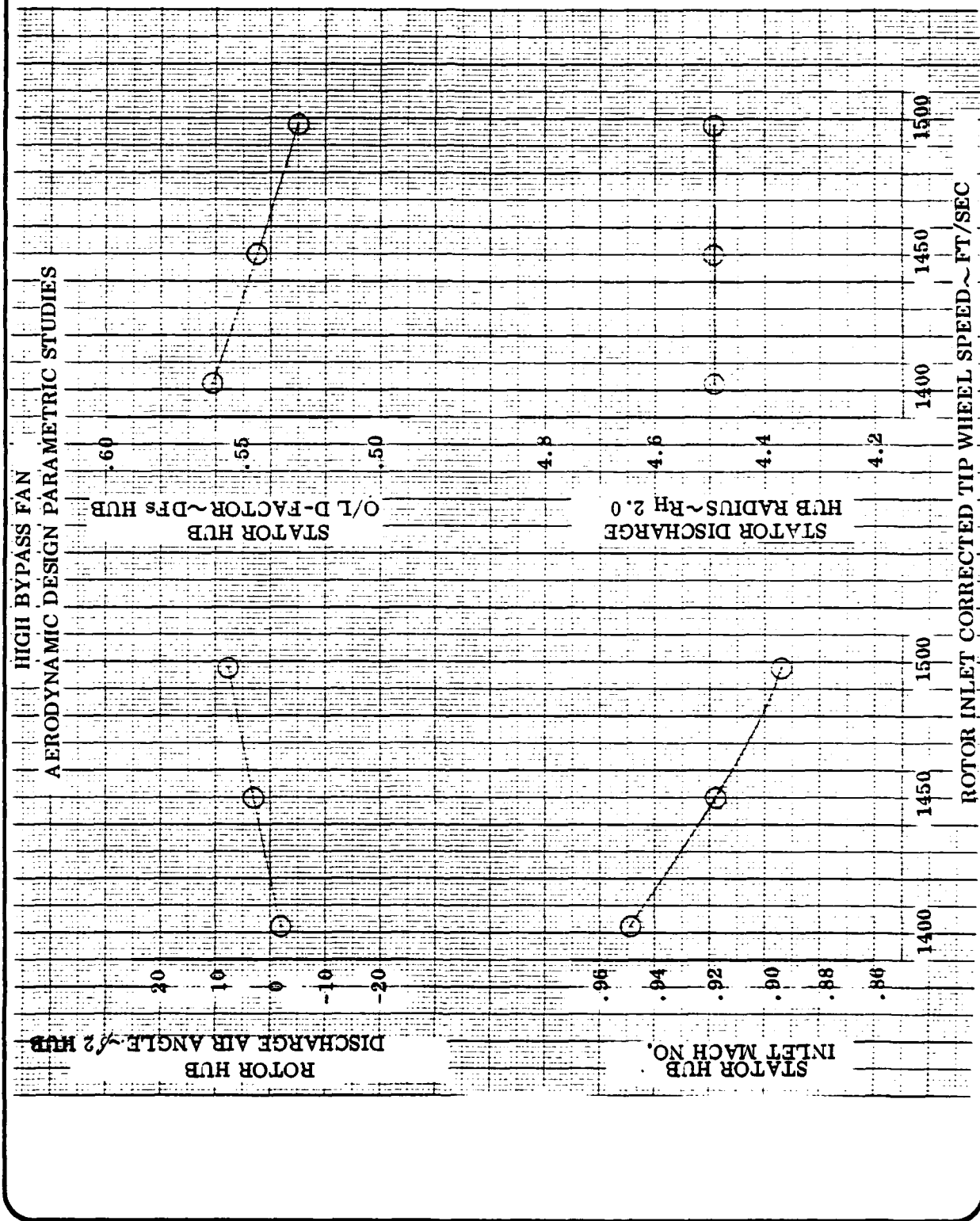
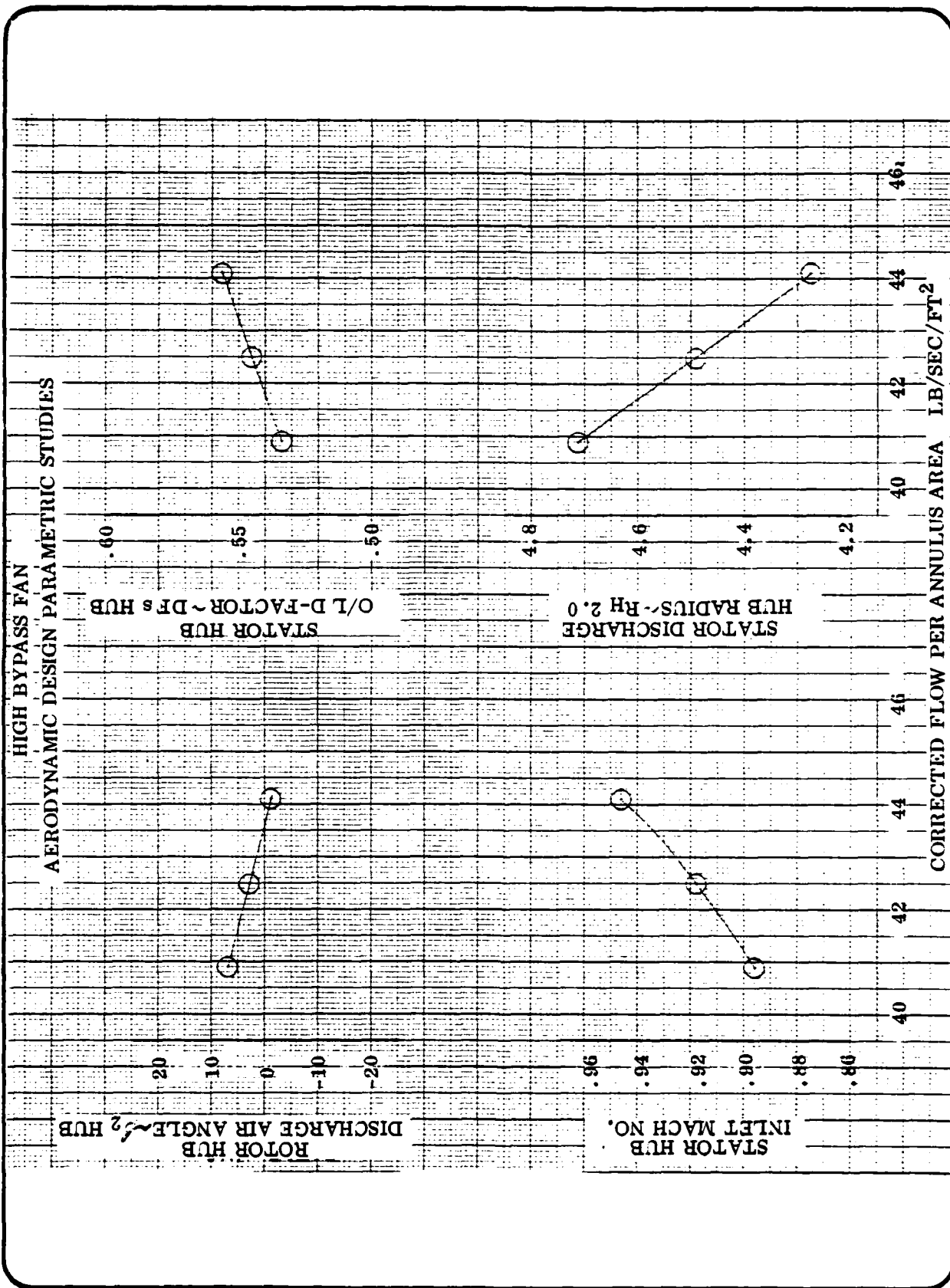


Figure 10. Rotor Tip Wheel speed



GENERAL ELECTRIC COMPANY
AIRCRAFT ENGINE GROUP

Figure 11. Flow Per Annulus Area

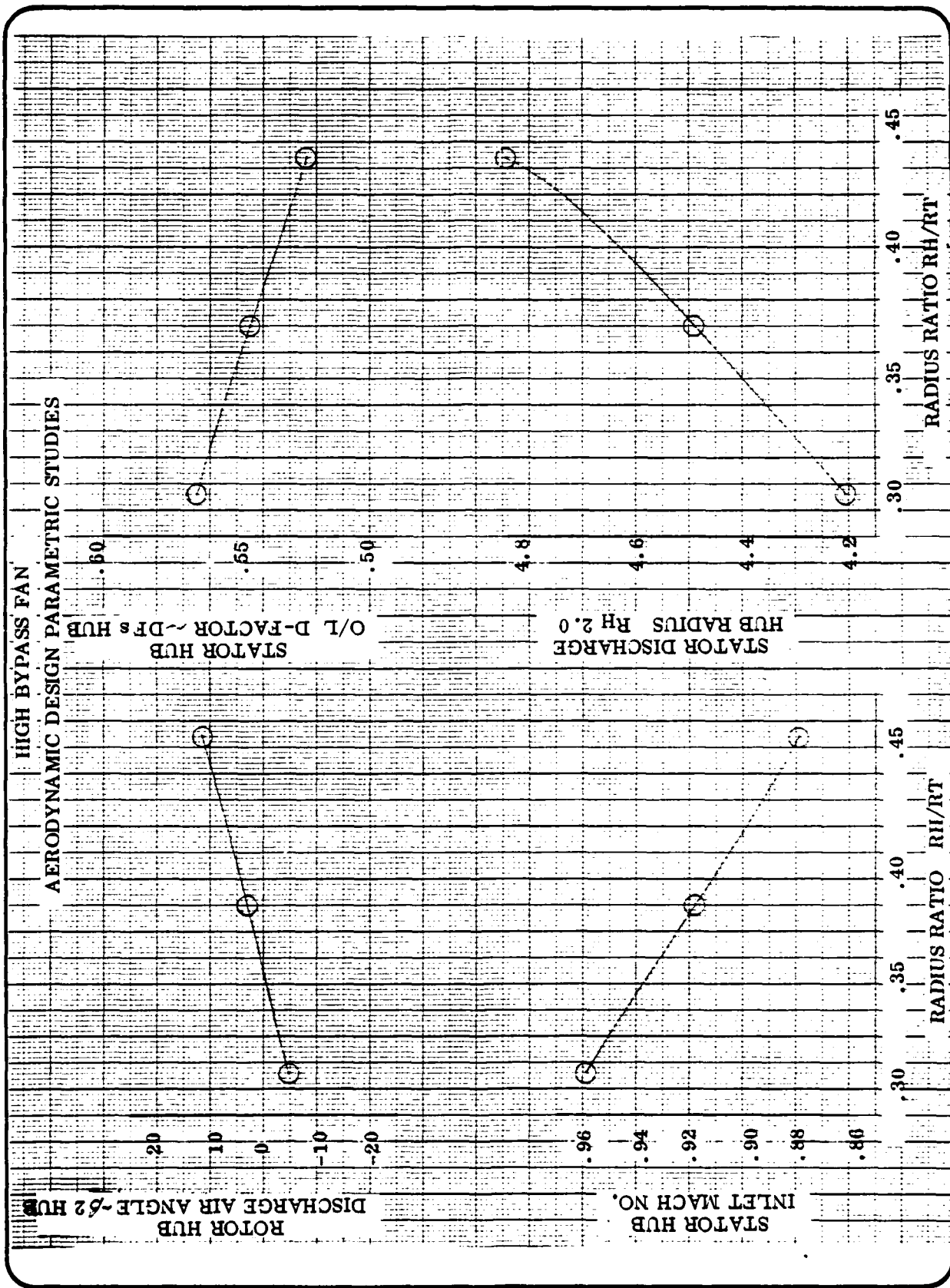
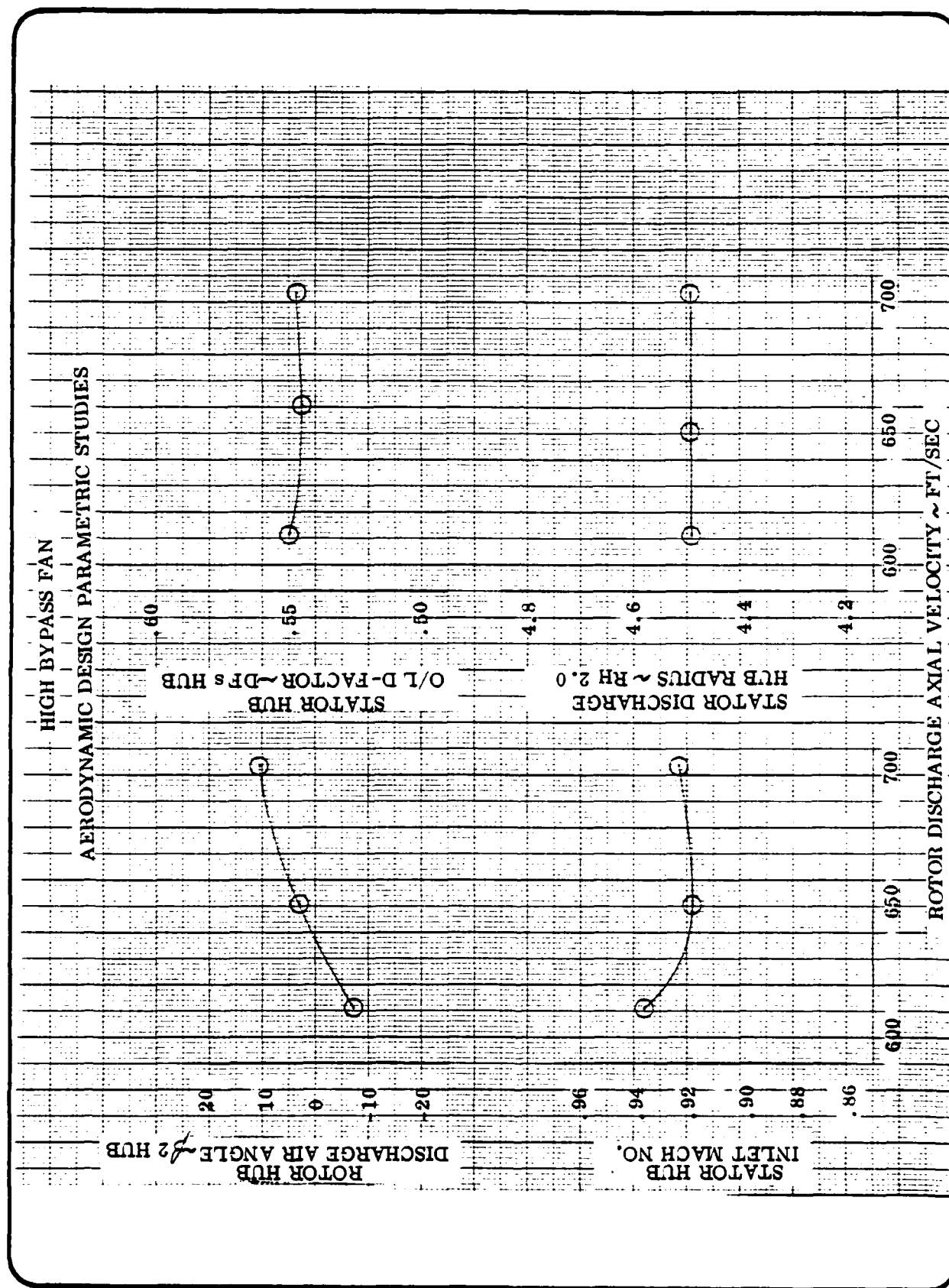


Figure 12. Rotor Inlet Radius Ratio

Figure 13. Fan Rotor Discharge Axial Velocity



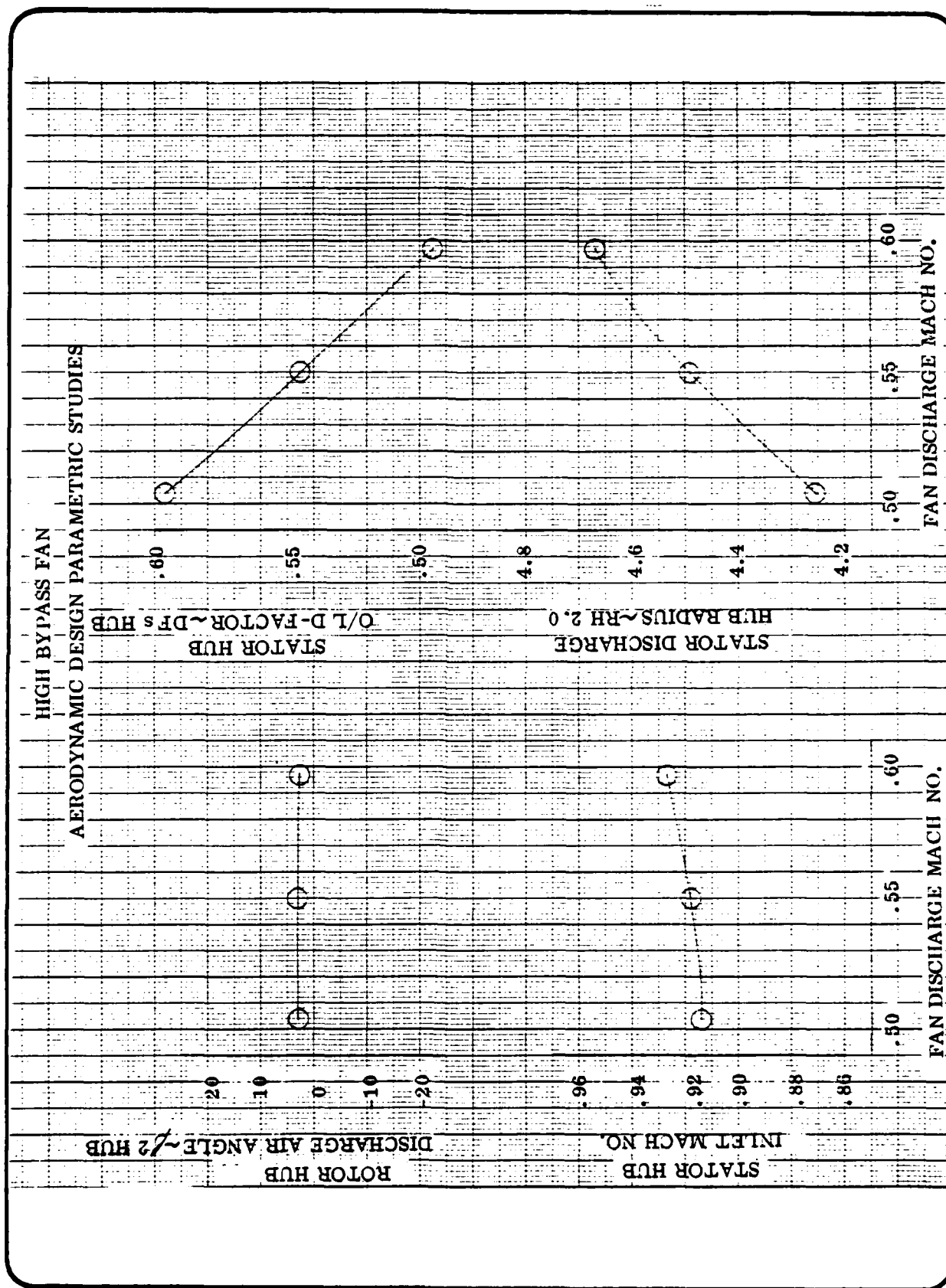


Figure 14. Fan Discharge Mach No.

TABLE 7. SUMMARY OF FAN PARAMETRIC EFFECTS

HIGH BYPASS FANAERODYNAMIC PARAMETRIC STUDY RESULTS

CHANGE REQUIRED TO IMPROVE CRITICAL HUB CONDITIONS AND TO IMPROVE INNER DUCT PERFORMANCE

Parameter	Rotor Hub Discharge Air Angle	Stator Hub Inlet Mach No.	Stator Hub D-Factor	Stator Discharge Hub Radius
Rotor Tip Wheel speed	Increase	Increase	Increase	No Effect
Flow/Annulus Area	Decrease	Decrease	Decrease	Increase
Rotor Inlet Radius Ratio	Increase	Increase	Increase	Decrease
Rotor Discharge Axial Velocity	Increase	Optimum	Optimum	No Effect
Stator Discharge Mach No.	No Effect	Decrease	Increase	Decrease

HIGH BYPASS FAN

SCHEMATIC OF FLARED CASING CONFIGURATION

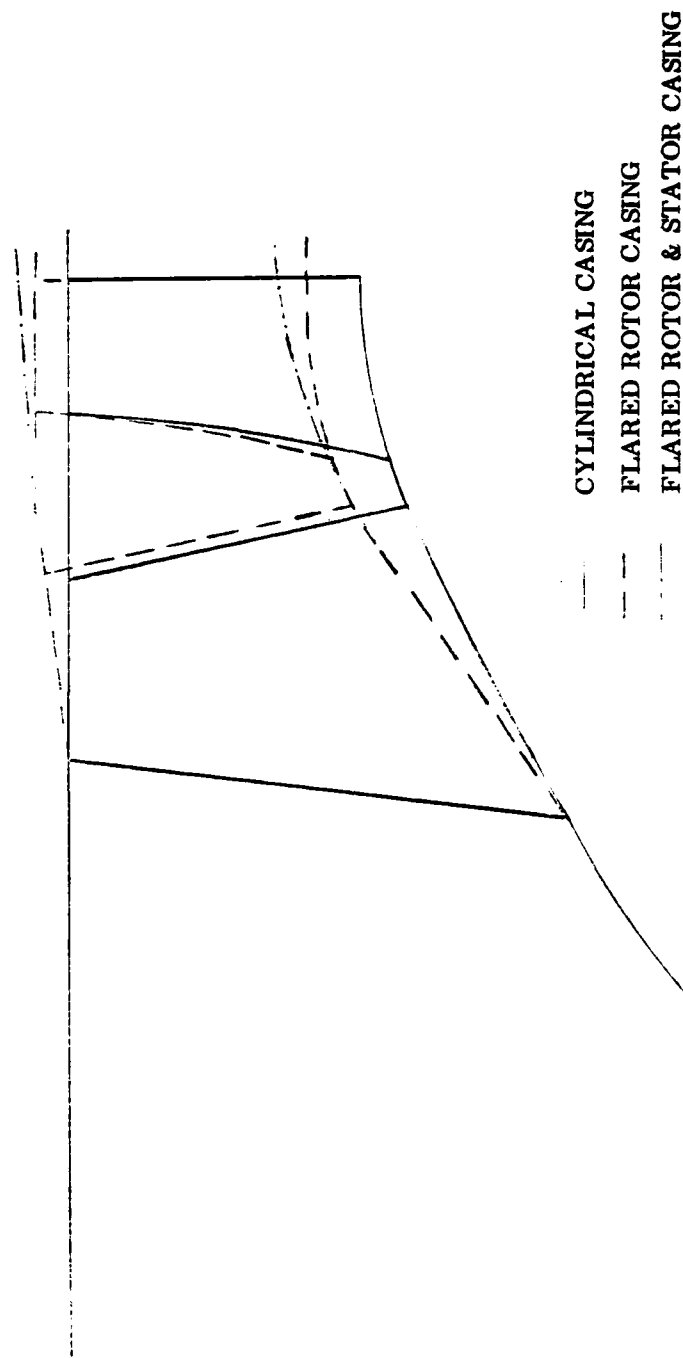
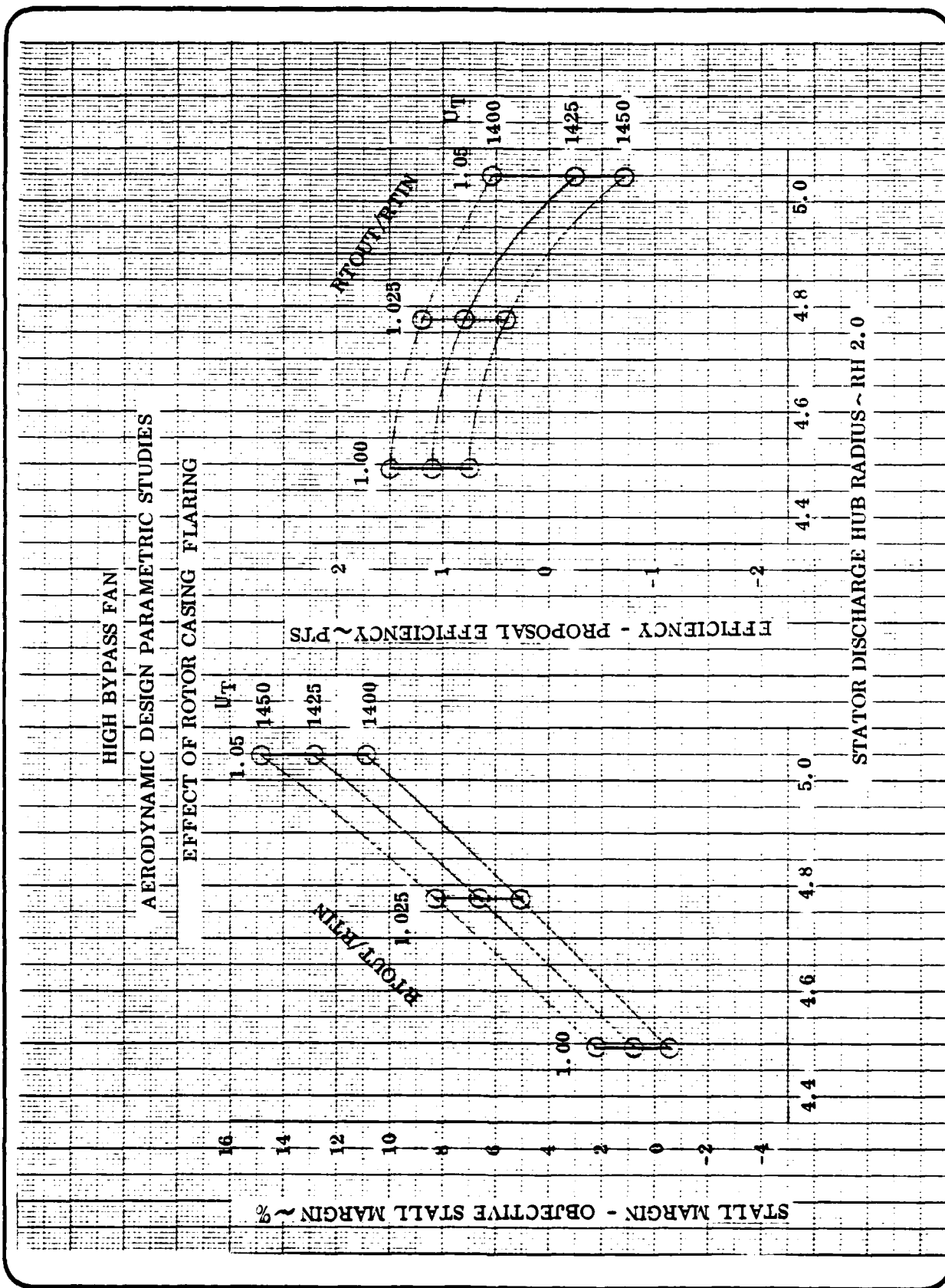
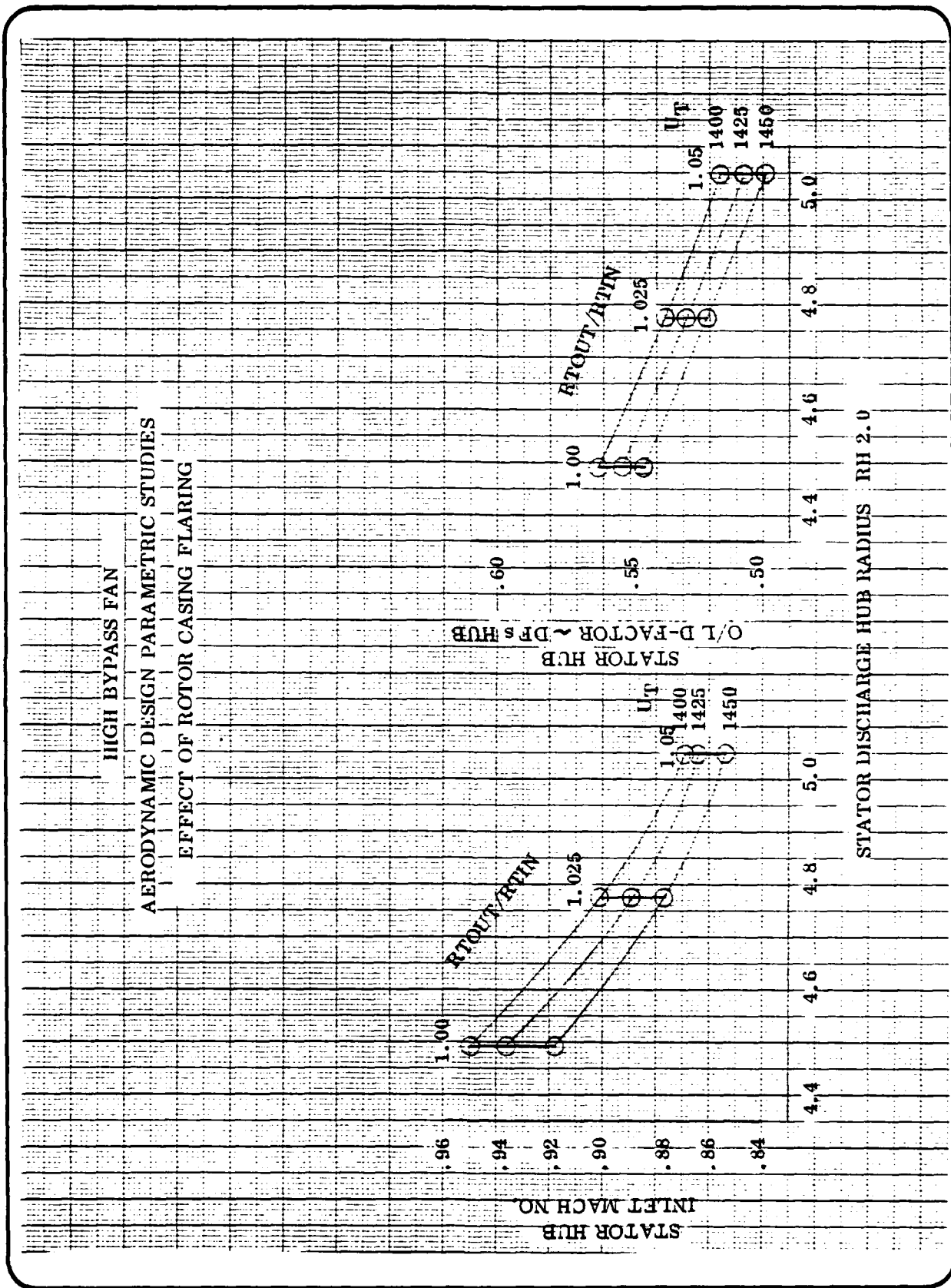


Figure 15. Flowpath Flaring Concept



GENERAL ELECTRIC COMPANY
AIRCRAFT ENGINE GROUP

Figure 16. Effects of Flaring on Efficiency and Stall Margin



GENERAL ELECTRIC COMPANY
AIRCRAFT ENGINE GROUP

Figure 17. Rotor Casing Flaring Effects

inlet Mach Number for the case of rotor casing flaring, reducing the improvement predicted by the model.

The effect of rotor casing flaring is summarized in Table 8. Flaring did improve fan performance, but the resultant penalties in other components offset the gains for this engine cycle.

TABLE 8. ROTOR CASING FLARING EFFECTS SUMMARY

ROTOR CASING FLARING

- o FLARING COMBINED WITH LOWER TIP SPEED, IMPROVES FAN EFFICIENCY
- o FLARING RAISES DISCHARGE HUB RADIUS
 - MORE SEVERE DUCT
- o LOWER TIP SPEED (RPM) HURTS LP TURBINE PERFORMANCE AND COULD REQUIRE OGV
- o PENALTIES OFFSET GAINS FOR THIS ENGINE CYCLE

3.2 FAN AERO-MECHANICAL PARAMETRIC STUDIES

This subsection describes the aeromechanical parametric studies necessary to serve as a basis for selecting a fan design mutually compatible with aerodynamic/aeromechanical/mechanical program design objectives. Parametric study results for the selected fan configuration are presented and evaluated.

3.2.1 Fan Aeromechanical Design Objectives

Advanced turbofan technology tends toward higher performance, lighter weight and lower cost. The resulting aerodynamic design trends impose greater challenges for both the aerodynamic and aeromechanical design analysis areas. Furthermore, optimization to improve, or provide for, certain mechanical design features - e.g., airfoil resistance to ingestion/FOD damage - can be in direct opposition to optimization for aerodynamic considerations. Therefore, it is necessary that the fan design be carefully derived and all design parameters fully exercised in order to achieve a balance between both aerodynamic and aeromechanical objectives. The requirements relative to mechanical performance and the criteria established to insure achieving these performance goals are identified in Tables 9 and 10 respectively.

3.2.2 Parametric Studies

The design of the fan blade and vane airfoils is derived from an iterative process. The basic performance requirements and program goals establish a preferred selection (or preferred range) of radius ratio, tip speed, aspect ratio and solidity. The aeromechanical rationale for choosing amongst these parameters is embodied in the influence that each has in contributing to the attainment of the goals/criteria established for the design. Values for the design parameters mentioned previously are chosen to give the most favorable mechanical results of frequency, stress, stability. The blade geometry, to include area, camber and stagger distribution is then utilized to obtain the desired mechanical design objectives. For example, Figure 18 shows in parametric fashion the method used to size airfoils for 2/rev avoidance and what the attendant stability (reduced velocity parameter) implications are. Note that the parameters of tip speed (UT), root aspect ratio, average radius ratio and blade geometry all can be manipulated to identify mutually acceptable values for attaining both the aerodynamic and mechanical design goals. In like fashion, Figure 19 employs the same parametric philosophy to select airfoil design parameters consistent with achieving objectives with respect to high cycle fatigue capability. Advantage can be taken of relative geometric size relationships between rotor and stator designs, as shown in Figure 20, to obtain optimum panel mode resonant placement characteristics. This might have constituted the bulk of the design problem were it not for the requirement to satisfy the MIL spec bird ingestion criteria. In addressing to the MIL spec, Table 11 outlines the requirements and identifies the related general considerations/concerns. Because the GE26/F4 frontal area is 165 in.², only 4 oz. and 2 lb. bird sizes are relevant.

TABLE 9. MECHANICAL PERFORMANCE REQUIREMENTS

AERODYNAMIC/AEROMECHANIC DESIGN TRENDS

HIGH PERFORMANCE FAN DESIGN REQUIRED AERODYNAMIC GOALS:

- HIGH SPECIFIC FLOW (I.E., FLOW/ANNULUS AREA), GENERALLY REQUIRING HIGH TIP SPEED AND RELATIVE MACH NO., WITHOUT SACRIFICING EFFICIENCY.
- HIGH AVERAGE PRESSURE RATIO
- ADEQUATE STALL MARGIN
- MORE, ACTIVE CLEARANCE CONTROL

RESULT: THIN, HIGHLY TWISTED, LOW RADIUS RATIO, LOW ASPECT RATIO, HIGHLY LOADED, FAN STAGE

- RECOGNIZING AERODYNAMIC INTENT/CONSTRAINTS, MECHANICAL PERFORMANCE MUST:
 - Avoid Forced Vibration Problems Through Frequency and/or Stimulus Control.
 - Provide Suitable Aeroelastic Stability Margin for Unrestricted Fan Mapping.
 - Satisfy MIL-E-5007D FOD/Ingestion Requirements.
 - Assure Adequate Airfoil HCF Capability By Controlling Induced Steady-State Stresses.
- TRADEOFF STUDIES/ITERATIONS REQUIRED TO ACHIEVE A BALANCED AERODYNAMIC/AEROMECHANICAL DESIGN

TABLE 10. AEROMECHANICAL CRITERIA

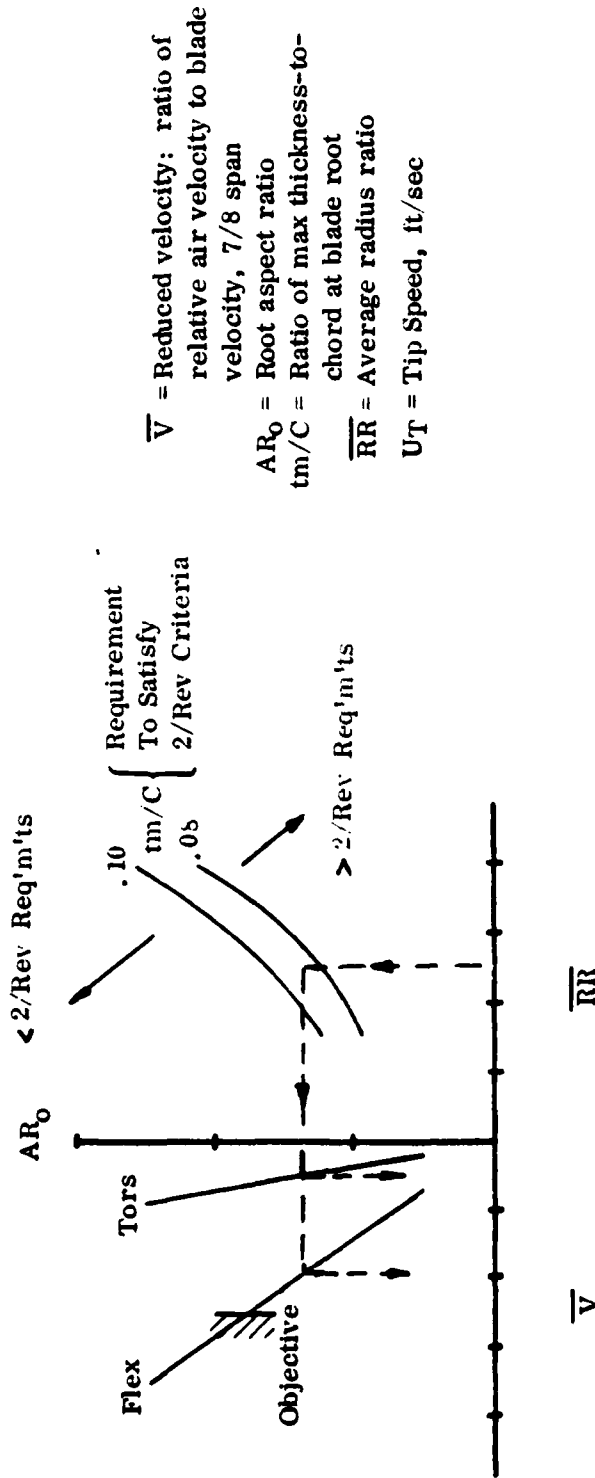
AEROMECHANICAL OBJECTIVES/CRITERIA

THE AEROMECHANICAL OBJECTIVES INCORPORATED INTO THE DESIGN ARE:

- **FORCED VIBRATION . . . FREQUENCY/STIMULUS CONTROL**
 - First Fundamental Mode of Vibration Avoidance of 2/Rev Excitation
 - Fundamental Mode Vibration (Flex, Torsion) Avoidance of Integral Order Excitation (3/Rev, 4/Rev, etc.) at the Design Speed
 - Fundamental Panel Mode Passing Stimulus Resonance Below Idle Speed (Rotor) and Above Design Speed (Stator)
 - Attenuate Wake Strength Potential by Setting Adequate Axial Spacing Between Rotor and Stator
- **FORCED VIBRATION . . . HCF CAPABILITY**
 - Airfoil Steady Stress Levels Consistent with Previous Experience on Production Parts
- **AEROELASTIC STABILITY (SUBSONIC AND SUPERSONIC)**
 - Stable Operation Over the Range of Anticipated Operating Conditions to Include Operational Extremes and Inlet Pressure Distortion Characteristics
- **MIL SPEC FOD/INGESTION**
 - Bird Ingestion Capability Will Be an Integral Part of Design Selection Procedure
 - Minimize Leading Edge Steady State Stresses

PARAMETRIC FOR 2/REV AND STABILITY . . . GE26/F4 FAN BLADE

ASSUMES: $U_T = 1450$ fps



\bar{V} = Reduced velocity: ratio of relative air velocity to blade velocity, $7/8$ span

AR_0 = Root aspect ratio

tm/C = Ratio of max thickness-to-chord at blade root

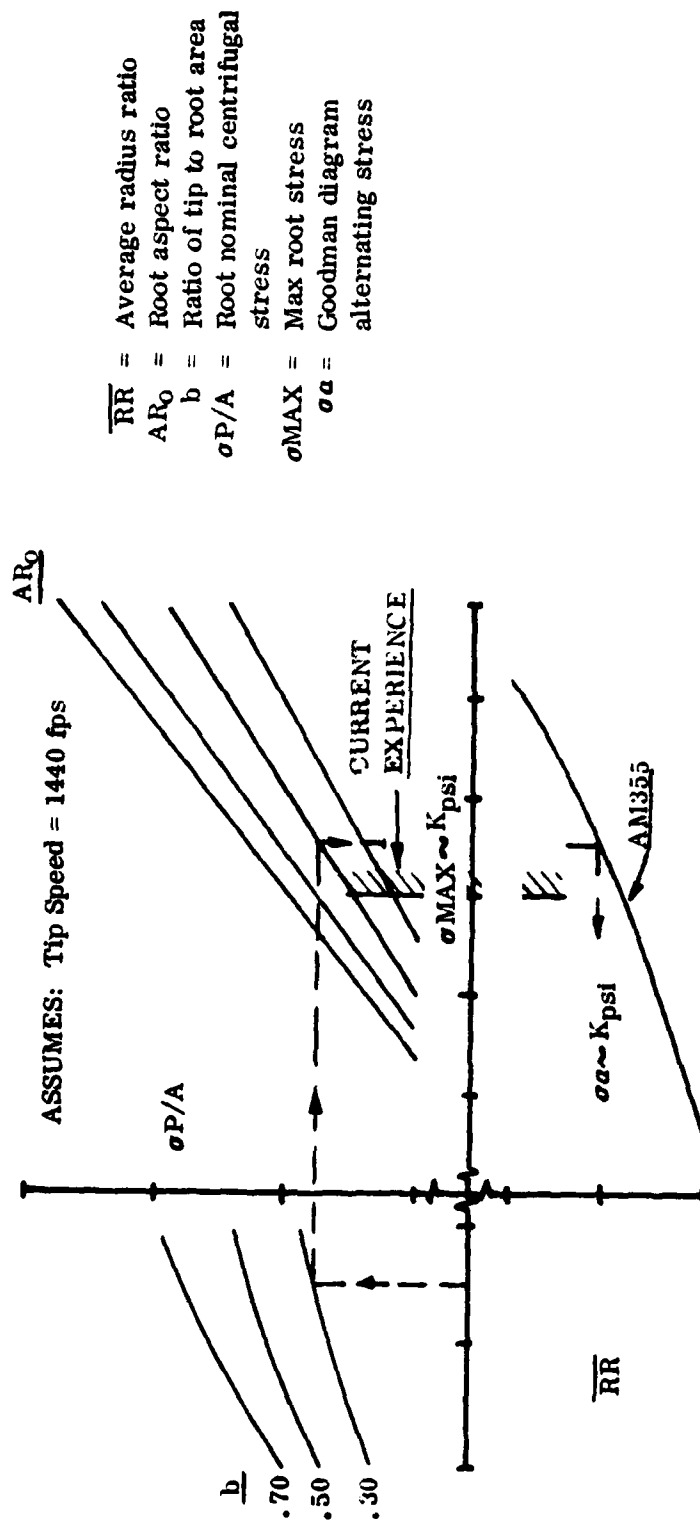
\bar{RR} = Average radius ratio

U_T = Tip Speed, ft/sec

- SIGNIFICANCE:**
- Size Blading (Aspect Ratio, Radius Ratio) for Best Possible Frequency/Stability Combination, within Design Constraints
 - Utilize Blade Geometry (Area Distribution to get Desired Frequency/Stability Results

Figure 18. Method for Airfoil 2/Rev Avoidance

PARAMETRIC FOR SELECTING AIRFOIL PARAMETERS CONSISTENT WITH ACHIEVING
STRESS OBJECTIVES

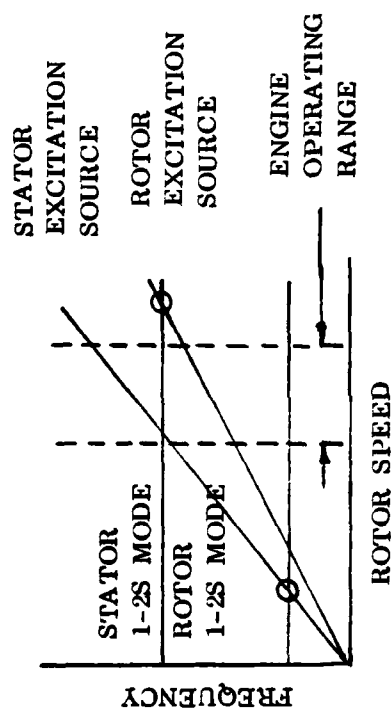


- SIGNIFICANCE:**
- HIGHLY TWISTED AIRFOILS INDUCE SIGNIFICANT ROOT STRESS ---- CAN BE MEASURED AS A MULTIPLIER ON NOMINAL CENTRIFUGAL STRESS
 - PROBLEM BECOMES AGGRAVATED BY LOW ASPECT RATIO BLADING
 - CAREFUL SELECTION OF AR , RR , TAPER AND DISTRIBUTION OF TWIST ANGLE (STAGGER) IS REQUIRED TO KEEP AIRFOIL ROOT STRESSES AT ACCEPTABLE LEVELS.

Figure 19. Method for Airfoil HCF Optimization

METHOD FOR FREQUENCY TUNING PANEL MODES

- RELATIVE ROTOR/STATOR ASPECT RATIO SELECTION



SIGNIFICANCE:

- LOW ASPECT RATIO ROTOR (FEW BLADES, LOW 1-2S MODE FREQUENCY) AND HIGH ASPECT RATIO STATOR (MANY VANES, HIGH 1-2S MODE FREQUENCY) COMBINE FOR OPTIMUM 1-2S MODE PLACEMENT FOR BOTH

Figure 20. Method for Airfoil Frequency Control

TABLE 11. BIRD INGESTION TOLERANCE DESIGN CRITERIA

BIRD INGESTION CRITERIA

MIL-E-5007D

- NUMBER AND SIZE OF BIRD BASED ON FRONTAL AREA:
 - One 2 or 4 oz Bird for Each 50 in² or Fraction > 50% thereof
 - One 2 lb Bird for Each 275 in² or Fraction > 50% Thereof
 - One 4 lb Bird for Each 400 in² or Fraction > 50% Thereof
- NO FAILURES RESULTING IN ENGINE SHUTDOWN AT CONDITIONS OF TAKEOFF, CRUISE, DESCENT
 - Engine Shall Promptly Recover to Pre-Ingestion Operating Point

CONSIDERATIONS IN ADDRESSING TO MIL-E-5007D

- AIRFOIL DAMAGE . . . FRAGMENTATION, FRACTURE, TEARING, BULGING, FOLDING
- STRUCTURAL DAMAGE . . . SPINNER, CASING, ROTOR UNBALANCE, VANE DISENGAGEMENT
- CONTAINMENT
- SECONDARY DAMAGE

CONCERNS

- MAJOR DISADVANTAGES INHERENT IN SMALL ENGINES
 - Bird Size (Weight) Which Can Be Safely Ingested is Proportional to (Scale Factor)³
 - Number of Blades Impacted Is Proportional to (Scale Factor)⁻¹
 - Bird Footprint is Proportional to (Scale Factor)⁻¹
- POTENTIAL FOR GREATER DAMAGE REQUIRES HIGHER FACTORS OF SAFETY . . .
MORE SEVERE AERO/WEIGHT PENALTIES

Related to Table 11 is a graphical presentation of the criteria requirements, Figure 21 showing quite distinctly the penalty that the requirement imposes on the smaller engine. For instance, a 6" diameter fan blade would be expected to have a 4 oz. bird reside over 90% of the blade span, whereas, the same size bird resides over only 10% of the blade span for a 28" diameter fan blade. Similar examples can be constructed for the larger bird sizes. This implies that smaller engines have higher risks of suffering severe gross blade deformation. The consideration discussed in this section, and which the design analysis procedure addresses to is airfoil separation under impact loading, specifically, fracture and fragmentation. The rationale is to avoid the spectre of creating potential severe secondary damage/non-containment due to airfoils exiting the fan, thus, decreasing the potential damage attributed to bird ingestion and improving the ability of the fan to recover power.

The elements in the analytical formulation of the bird impact problem are developed by considering, in order, Figures 22-24 and Table 12. The most important elements contained in this approach are the bird approach angle and footprint shown in Figure 22. The "slicing" action which occurs during bird impact is shown schematically in Figure 23. As the bird velocity is increased relative to the blade velocity, the bird is sliced into fewer pieces, i.e., fewer blades impacted. One final observation based on Figures 22 and 23 is that if the bird velocity were equal to the air velocity, no footprint would result since the bird approach angle is essentially equal to the leading edge metal angle. Obviously, the smaller the bird footprint, the smaller the pressure load exerted on the airfoil; translating to an increased airfoil tolerance to bird impact. Throughout the discussion on bird impact, the structural parameter used to identify/compare impact tolerance is material shear strength. As identified in Figure 24 and Table 12, the bird impact load is theorized to be resisted in shear. Comparison of this developed shear stress under impact to the material shear capability is the governing factor in identifying the acceptability of a given design.

A very basic ingredient of the bird impact problem is a determination of the impact conditions which are to be imposed upon the airfoil. Considerations such as bird size, bird velocity, impact location all must be evaluated, and appropriate decisions arrived at using the MIL spec input. In general, impact at the blade tip location during aircraft takeoff or descent represents the most severe impact condition as depicted in Figure 25.

The culmination of this analytical procedure is embodied in the parametric shown in Figure 26 depicting the iterative method utilized to insure that the fan blade design incorporated sufficient thickness (at the extremities of the bird footprint) to prevent fragmentation. This figure is derived using the assumptions rationalized by Figure 25, i.e., bird velocity of 150 fps and impact at blade tip region. Based on a given bird velocity, choosing a blade speed at the reference (or impact) location produces a bird approach angle. Combining a leading edge metal angle with the bird approach angle, recognizing the bird size (bird diameter),

GRAPHICAL REPRESENTATION OF MIL-SPEC WITH PERSPECTIVE
ON EXTENT OF AIRFOIL PRESSURIZATION ZONE

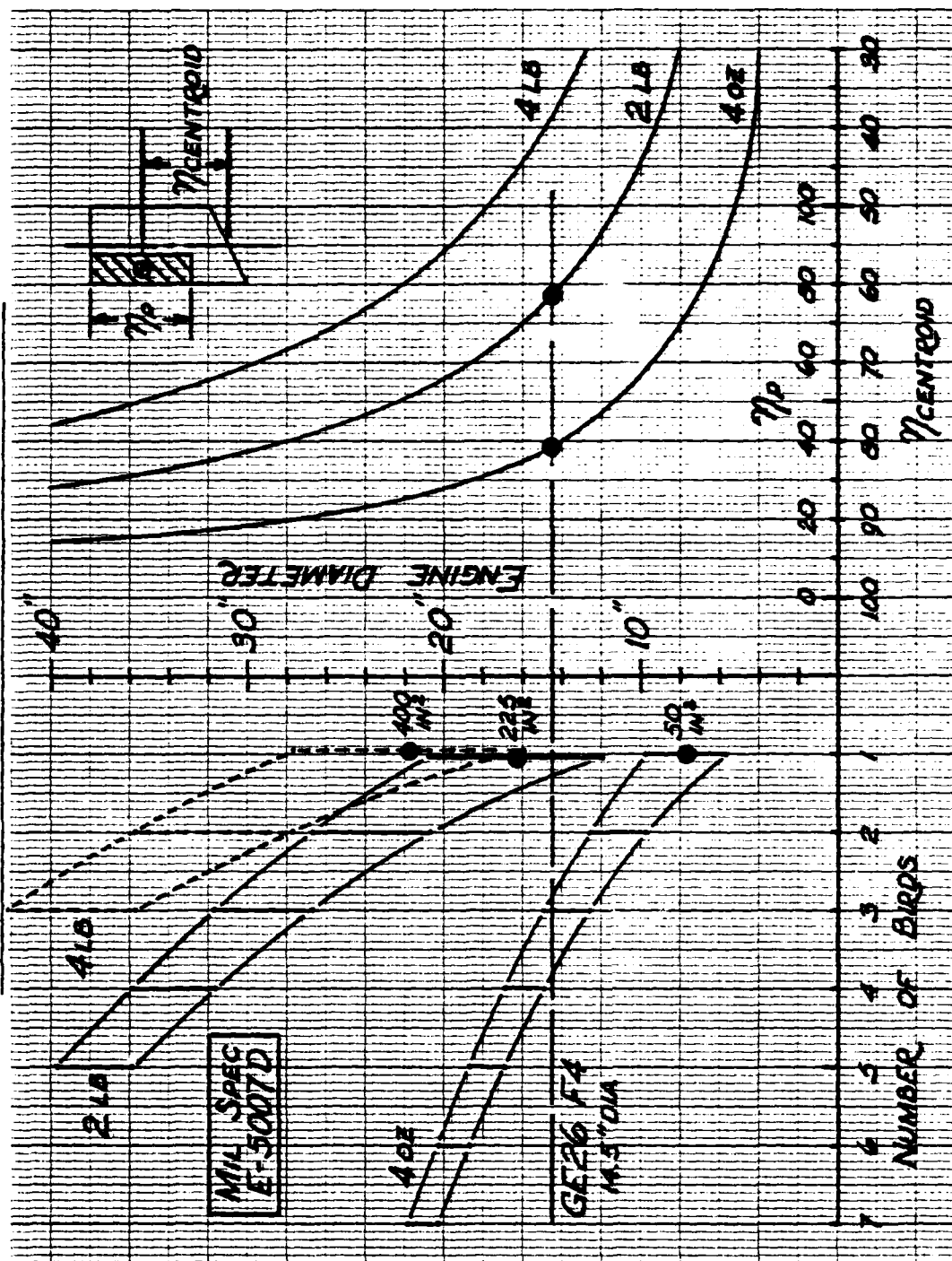


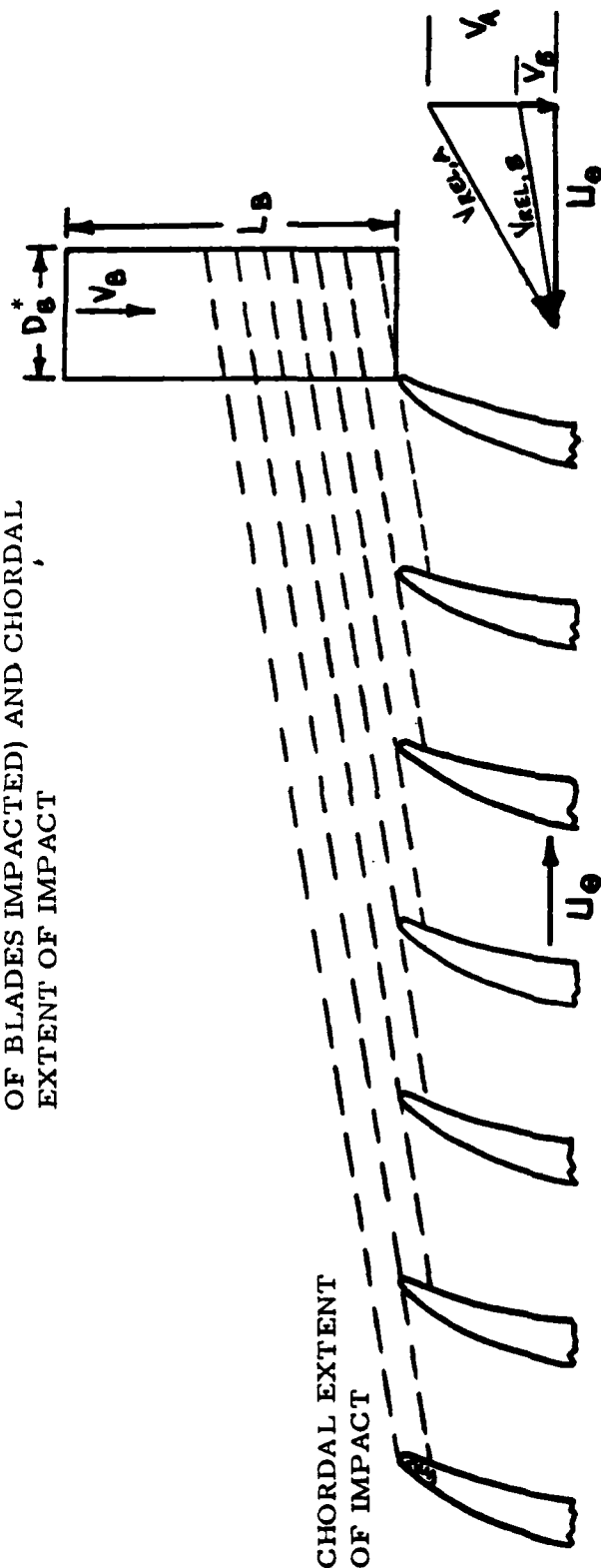
Figure 21. Airfoil Pressurization Due To Bird Strike

B_{-} —Leading edge metal angle
 θ_{-} —Bird approach angle = $\tan^{-1}\left(\frac{V_B}{U_\theta}\right)$
 i_B —Bird incidence angle = $B - \theta$
 Cp —Chordal extent of impact
 DB_{-} —Bird diameter (related to bird weight)
 V_B —Bird velocity
 U_θ —Tangential wheel speed
 V_{REL} —Bird relative velocity
 $Pressurized\ Zone_{-}$ —Bird footprint = $Cp \times DB$

Figure 22. Bird Approach Angle and "Footprint"

BIRD/BLADE IMPACT SCHEMATIC

- VELOCITY TRIANGLE IMPLICATIONS ON CASCADE INVOLVEMENT (I.E., NUMBER OF BLADES IMPACTED) AND CHORDAL EXTENT OF IMPACT



LEADING EDGE
AIRFOIL REGION

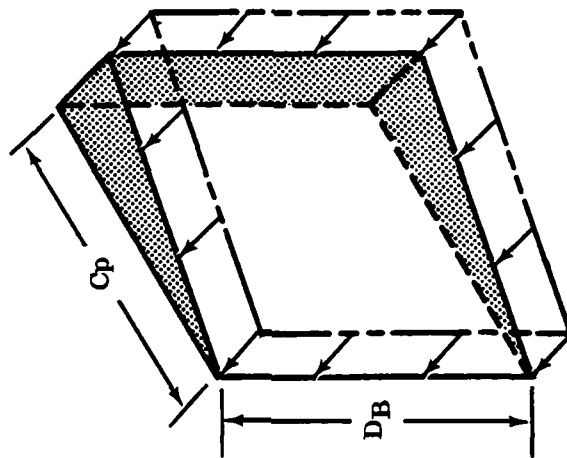
DB ...	BIRD DIAMETER
LB ...	BIRD LENGTH
U_{θ} ...	BLADE VELOCITY
V_B ...	BIRD VELOCITY
$V_{REL, B}$...	BIRD RELATIVE VELOCITY
V_A ...	AIR VELOCITY
$V_{REL, A}$...	AIR RELATIVE VELOCITY

* D_B IS PROPORTIONAL TO $\sqrt[3]{W_B}$
SINCE L/D IS ASSUMED CONSTANT

Figure 23. Slicing Action During Bird Impact

BIRD STRIKE ANALYSIS . . . PROBLEM FORMAT FOR FRAGMENTATION

OBJECTIVE: Prevent Separation and Loss of Airfoil Fragments During Inadvertent Bird Ingestion Encounters



Distributed load which exists in the pressurized zone must be resisted in shear, and not cause bird footprint to be "punched out" of the airfoil

Cross hatched region represents shear area available to resist distributed load.

- Define Threshold Shear Stress (τ_{CRIT}) which Causes Separation of the Footprint Fragment from the Airfoil
- Define a Shear Area which will Cause Max Developed Shear Stress (τ_{MAX}) below (τ_{CRIT})

Figure 24. Bird Impact Load/Stress Mode

TABLE 12. BIRD STRIKE PROBLEM/SOLUTION FORMAT

BIRD STRIKE ANALYSIS --- PROBLEM FORMAT FOR FRACTURE

OBJECTIVE

- PREVENT GROSS DAMAGE FROM OCCURRING TO FAN BLADES, WITH RESULTING SEVERE SECONDARY DAMAGE / CONTAINMENT

PROBLEM

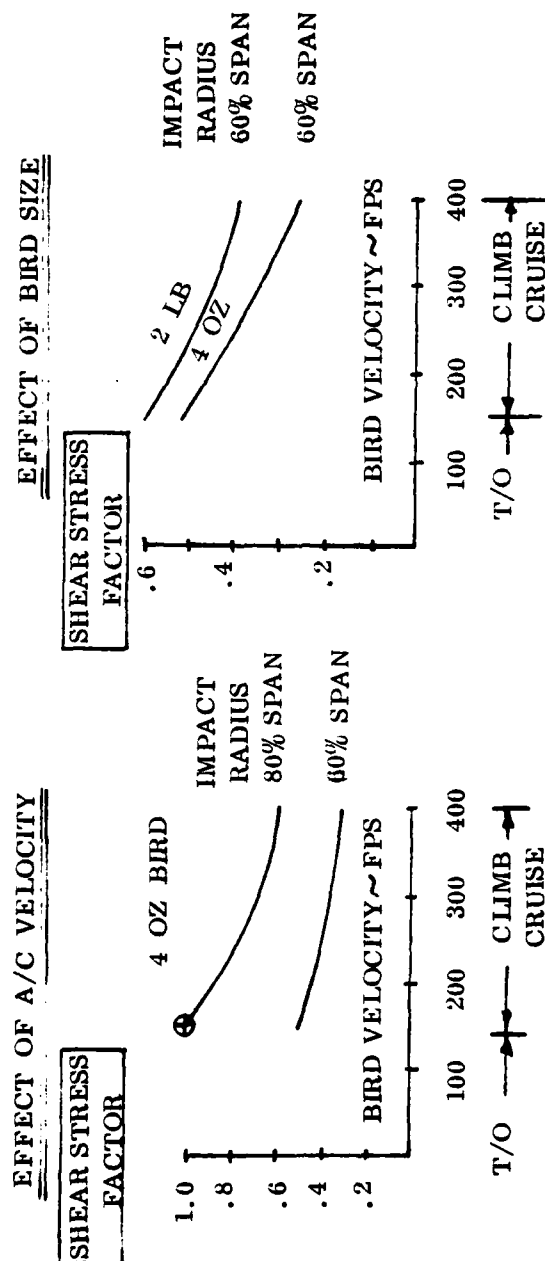
- AVOID SEPARATION (VIA ROOT FRACTURE) AND LOSS OF ROTOR AIRFOIL DURING INADVERTENT BIRD INGESTION ENCOUNTERS
- WANT TO UTILIZE FULL CAPABILITY OF MATERIAL AND AVOID PREMATURE CONTACT BETWEEN ROTOR AND STATOR

SOLUTION

- SUDDENLY APPLIED TRANSIENT DISTRIBUTED LOAD EXISTING ON THE AIRFOIL MUST BE RESISTED IN THE ROOT REGION BY SECTION SHEAR
- ASSUME LOAD EXISTS OVER A MAJORITY OF THE AIRFOIL SPAN
- DEFINE THRESHOLD SHEAR STRESS (τ_{ult}) WHICH CAUSES FRACTURE
- DEFINE SHEAR AREA WHICH WILL YIELD MAXIMUM DEVELOPED SHEAR STRESS (τ_{max}) BELOW τ_{ult}

BIRD INGESTION CAPABILITY/EVALUATION

FRAGMENTATION



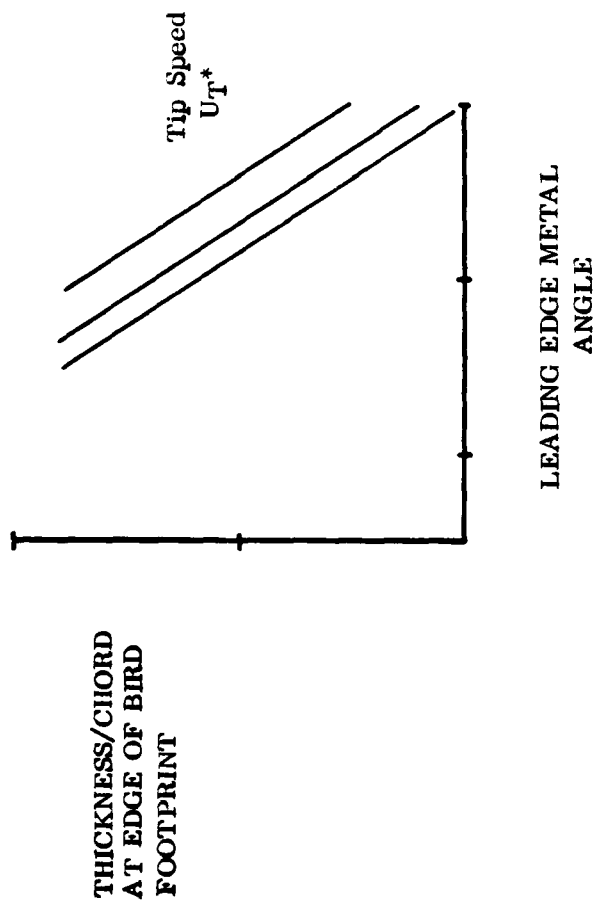
SIGNIFICANCE:

- BIRD IMPACT PROBLEM IS MOST SEVERE AT THE TAKEOFF(T/O) CONDITION
- SMALL BIRD (4 OZ) IMPACT AT BLADE TIP DURING TAKEOFF IS MOST SEVERE CONDITION

GE26/F4 FAN DESIGNED FOR BIRD INGESTION AT T/O SPEED ASSUMING IMPACT AT BLADE TIP.

BIRD INGESTION PARAMETRIC STUDY FOR FRAGMENTATION PREVENTION

- Define Bird Size, Velocity
- Define Reference Section
- Calculate Pressure Load
- Define Required Airfoil Thickness
 - Max Shear Stress Less Than Fragmentation Threshold Stress Level



- SIGNIFICANCE:
- Utilize Parametric Concept for Integration with Aero Objectives and Quick Convergence to a Realistic Preliminary Design
 - Select Appropriate Parameter Values, Conduct Detailed Analysis

produces a footprint. This derived footprint then implies an impact pressure load which then sets a shear area such that the developed shear stress does not exceed the material shear strength capability.

Another aspect of the parametric study is the airfoil material selection process. The information contained in Table 13 depicts the rationale for choosing among the available material options based on identified aeromechanical considerations. Both the shear strength capability and the modulus of toughness (ability to absorb energy in the plastic range) pertain to the bird impact problem, and as such, are weighted very heavily given equivalent high cycle fatigue (HCF) capability. The overstress capability is of importance as it addresses airfoil stall capability and was not considered on the same level of significance as the other parameters especially for a product design.

The final aspect of the design evolution procedure involved the rotor blade airfoil attachment. Having arrived at a reasonable airfoil design, an airfoil load and radial position are now available. The problem then addresses to whether sufficient area exists in which to design a dovetail form capable of supporting the airfoil load. As suggested by the data depicted in Figure 27, the GE26/F4 airfoil and flowpath constraints result in a nominal blade dovetail neck stress of 50 Kpsi due to centrifugal effects. This is considered an undesirably high level since dovetail axial position, airfoil bending loads and stress concentration effects could easily double that value. The blisk (integral blade disc) design was utilized in order to alleviate this attachment stress problem. A side benefit of the blisk construction is that it allows a lighter airfoil weight. Satisfying the forced vibration objectives, namely first flex 2/rev margin, tends to set the airfoil area distribution. With a low airfoil inlet radius ratio, conventional dovetails have long shanks thus providing significant bending flexibility. This flexibility acts to reduce the blade design frequency and must be compensated for by increasing the airfoil frequency, i. e., more area thus more weight.

TABLE 13. RATIONALE FOR BLADE MATERIAL SELECTION

AIRFOIL MATERIAL SELECTION

• AEROMECHANICAL CONSIDERATIONS

- TOUGHNESS -- BIRD INGESTION / FOD
- HIGH CYCLE FATIGUE -- FORCED VIBRATION
- OVERSTRESS -- STALL, RUB
- SHEAR STRENGTH -- BIRD INGESTION

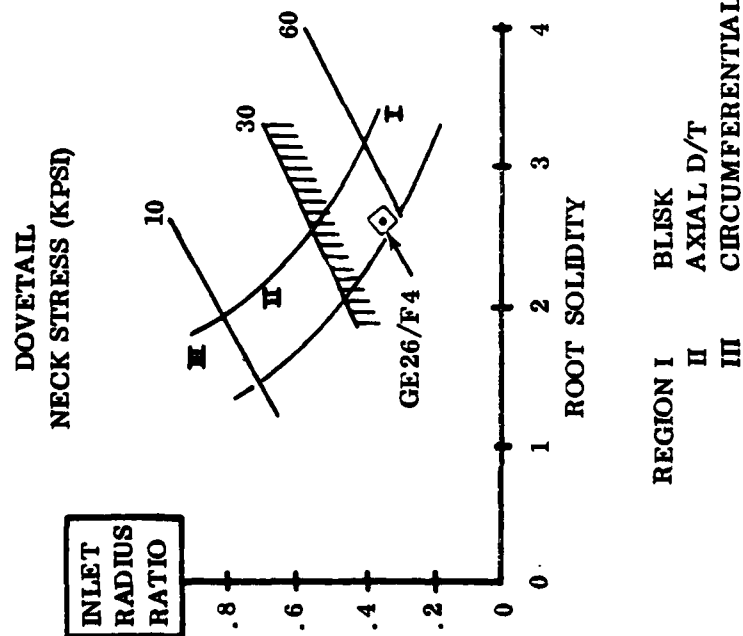
• FOR BIRD INGESTION REQUIREMENTS, TOUGHNESS AND SHEAR STRENGTH CAPACITY BECOME MAJOR CONSIDERATIONS

MATERIAL	RANKING			
	SHEAR STRENGTH	MODULUS OF TOUGHNESS	HCF	OVERSTRESS
AM355	2	2	1	4
TI-6-4	4	4	2	5
IN 718	1	1	3	1
17-4PH (CAST)	5	4	5	3
A286	3	3	3	2

• BEST CHOICES, CONSIDERING AEROMECHANICAL CONSIDERATIONS ONLY, ARE AM355 AND IN718

• CONSIDERATIONS OF COST, WEIGHT, MANUFACTURABILITY GIVE AM355 THE ADVANTAGE

BLADE AIRFOIL ATTACHMENT



SIGNIFICANCE: • Low radius ratio, high root solidity do not allow sufficient material to satisfy both airfoil and disc dovetail stress objectives.

- Blisk design utilized
 - Avoids shank flexibility . . . lower weight airfoil.

Designing An Airfoil Attachment

- Dovetail neck width is sized by airfoil load.
 - Length determined by airfoil chord.
- Tang contact area is sized by crush stress criteria.
- Once the airfoil attachment is sized, the available disc post neck thickness falls out.
 - Disc neck width must be capable of supporting $\sim 1.5 \times$ airfoil load.
- Blade and disc dovetail stresses should be equivalent for optimum design.

Figure 27. Method for Selecting Blade Airfoil Attachment

3.3 FAN AERODYNAMIC DESIGN

This subsection describes the approaches and execution of the detailed fan aerodynamic design based upon the combination of the preceding Fan Aerodynamic and Fan Aeromechanical Parametric Studies.

3.3.1 Effect of Birdstrike Requirement on Fan Performance

The requirement that the fan be able to withstand bird ingestion per MIL Spec 5007D leads to thicker rotor airfoils than one would normally design. It is then desirable to select fan design parameters such that the thickness increase is minimized.

The velocity vector diagram in Figure 28 shows the velocity and direction of a bird striking the rotor and compares that to the air velocity/direction and to the blade metal angle. CZ air is primarily a function of flow per annulus area. The diagram is used to determine the velocity component normal to the airfoil, and hence the force on the airfoil, and to study ways to reduce that force. Design parameters available to reduce the force are the wheelspeed U, flow/annulus area (determines CZair) and blade incidence.

The velocity triangles in Figure 28 were used to determine the blade thickness required to meet bird strike requirements as a function of rotor wheelspeed and rotor inlet metal angle. Then aerodynamic parametric study results were used to determine lines of constant flow per annulus area for a specified incidence (Figure 29). The curve shows that flow per annulus area is the most important parameter to reduce blade thickness for bird strike. The final selection of design parameters requires less thickness than the proposal configuration would have required.

The resultant axial thickness distribution of the high bypass fan blade is shown in Figure 30.

In order to understand the impact of the thickened blade on fan design/performance, it is necessary to review the blade-to-blade design parameters.

The blade passage design parameters are defined in Figure 31. The region forward of the first covered wave (FCW) determines the maximum airflow. It is desirable to keep AM as small as possible to minimize total blade passage diffusion. The internal area contraction from the mouth to the throat must be minimized to assure that the shock structure is "started." The discharge area must be large enough to achieve the desired work input.

The suction surface incidence, defined in Figure 32 is used to set the blade forward of the first covered wave to assure adequate flow capability.

HIGH BYPASS FAN VELOCITY VECTOR DIAGRAM FOR FAN ROTOR INLET

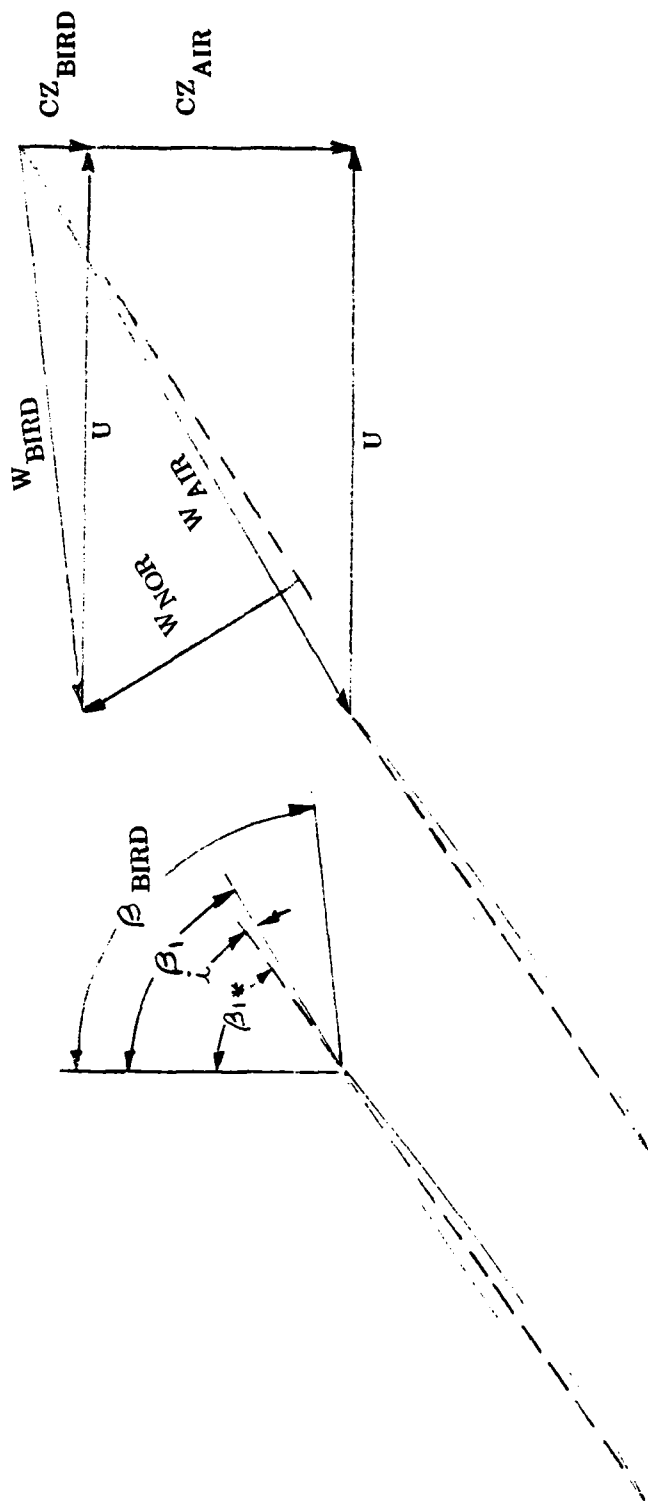


Diagram Utilized to Reduce Impact Force Due to Birdstrike
Velocity Components to Scale

Figure 28. Velocity Vector Diagram Including Bird Path

HIGH BYPASS FAN

THICKNESS REQUIRED TO MEET BIRDSTRIKE REQUIREMENTS
AS FUNCTION OF ROTOR TIP SPEED AND FLOW/ANNULUS AREA

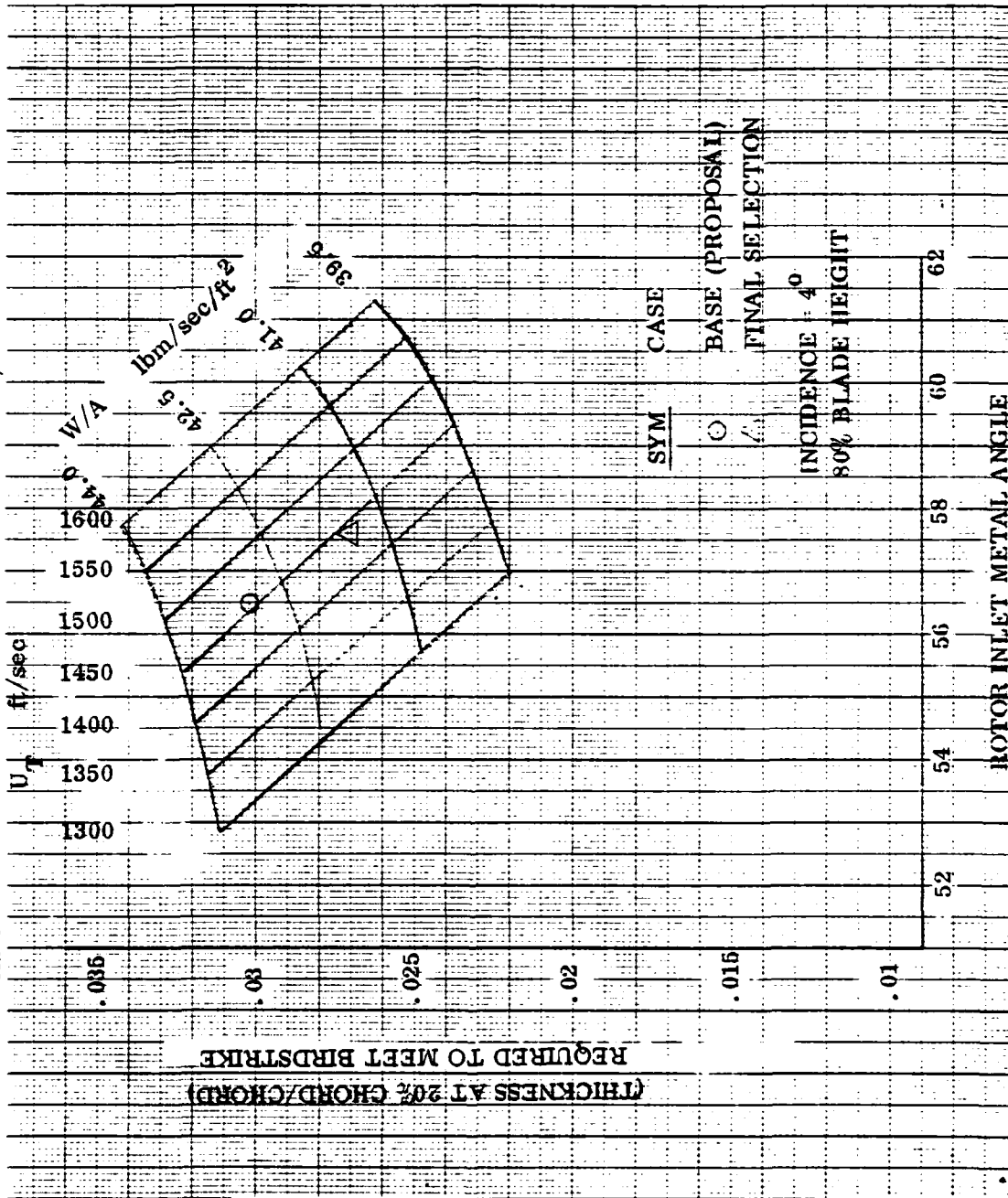


Figure 29. Airfoil Thickness Requirements to Satisfy Bird Strike Conditions

GENERAL ELECTRIC COMPANY /
AIRCRAFT ENGINE GROUP

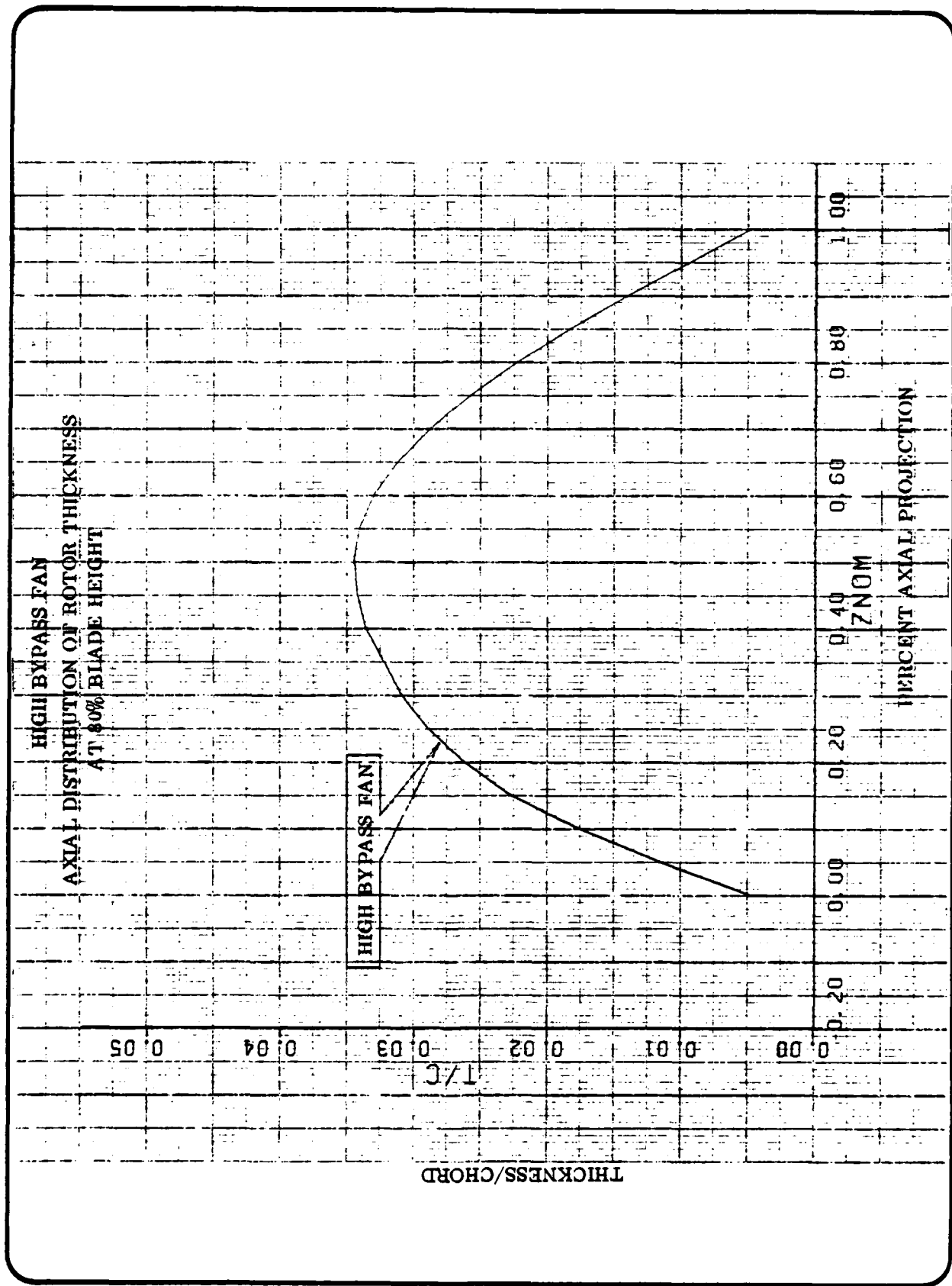
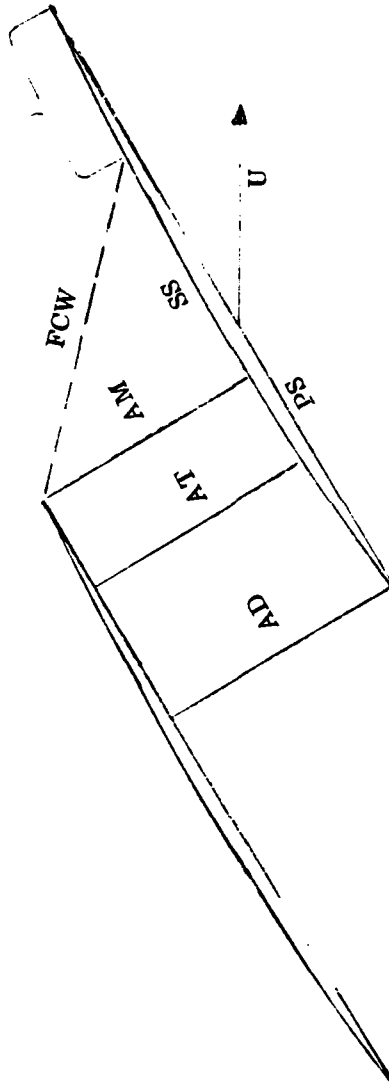


Figure 30. Rotor Airfoil Thickness Axial Distribution

HIGH BYPASS FAN BLADE PASSAGE DESIGN PARAMETERS

Region where suction surface
shape determines max. airflow



FCW First Covered Wave
AM Mouth Area
AT Throat Area
AD Discharge Area
SS Suction Surface
PS Pressure Surface
U Wheel speed

FCW
AM
AT
AD
SS
PS
U

Figure 31. Blade Passage Design Parameters

DEFINITION OF SUCTION SURFACE INCIDENCE

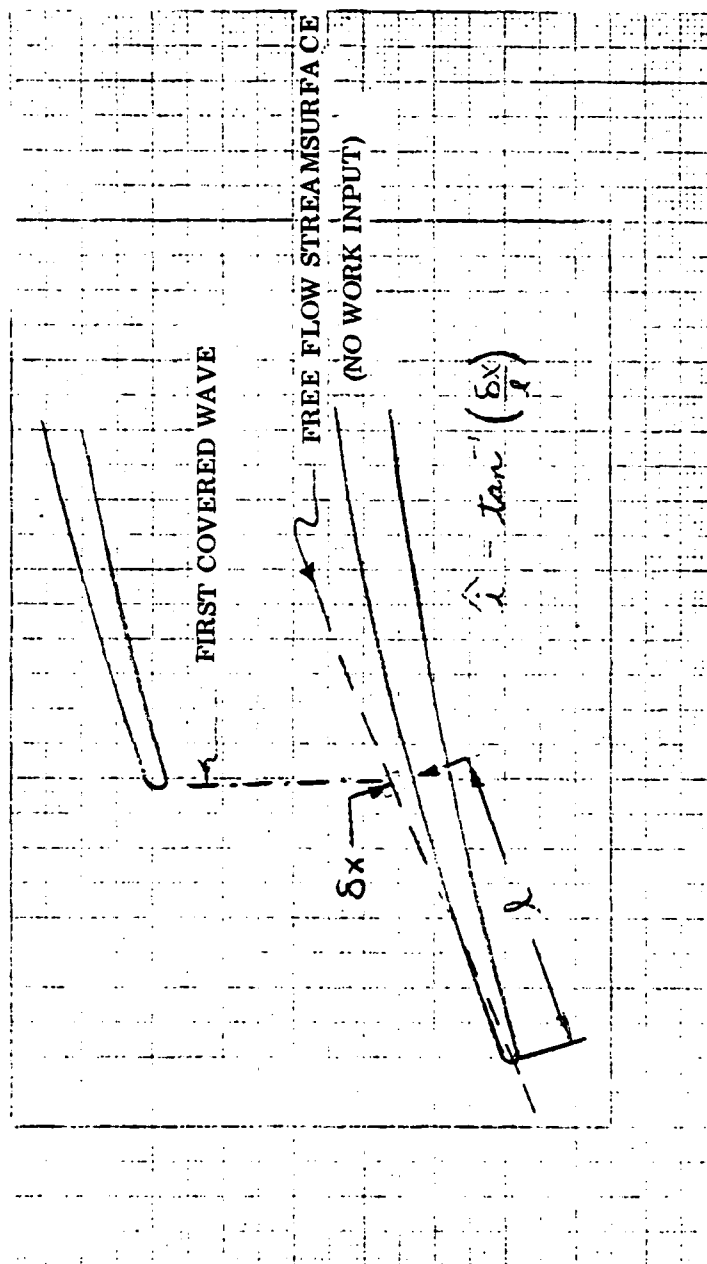


Figure 32. Suction Surface Incidence Considerations

The effect of the birdstrike requirement on blade passage design is illustrated in Figure 33 by superimposing a blade designed to meet bird strike over a blade with conventional thickness distribution. The meanline angle must be lowered forward of the first covered wave to maintain the suction surface and flow capacity. The rapid increase in thickness aft of the leading edge closes the pressure surface and hence it is more difficult to maintain low internal area contraction and to keep the throat forward. The blade angle must be opened more rapidly aft of the mouth to control blade passage area.

The leading edge wedge angle is larger for the high bypass fan thickness distribution than for a typical fan thickness distribution. The leading edge bow shock is pushed forward when the wedge angle exceeds the maximum wedge angle for attached shock, creating higher losses (Figure 34).

The effects of meeting the bird strike requirement are summarized in Table 14.

3.3.2 Selected Configuration

The final selection of fan aerodynamic design parameters is tabulated in Table 15.

The principle reasons for the selection of each of the design parameters are given in Tables 16, 17, and 18.

The important design conditions of the final GE26/F4 fan are compared to the values of the proposal in Table 19. In general, the final configuration is very similar to that of the proposal. The most significant change is the reduction in flow/annulus area to reduce the thickness necessary to meet the MIL Spec 5007D bird ingestion requirement.

3.3.3 Fan Axisymmetric Flowfield Specification

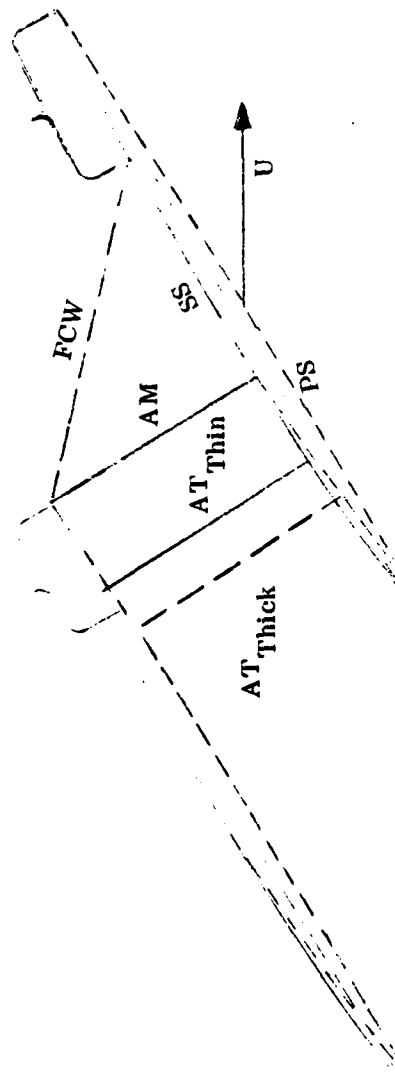
The final selection of fan aerodynamic parameters were used to generate an axisymmetric flow model of the fan. The axisymmetric model was then used to study the radial and axial distribution of the various design parameters to obtain a well balanced fan design.

The final flowpath of the high bypass fan is given in Figure 35. The forward portion of the rotor hub is scalloped to provide more throat margin. The hub flow-path near the rotor discharge through the stator was contoured to control the hub Mach No. The conical spinner prevents ice buildup on the spinner. The leading edge of the stator is swept at the ID to help control losses due to the high stator hub inlet Mach No.

HIGH BYPASS FAN EFFECT OF BIRDSTRIKE REQUIREMENT ON BLADE PASSAGE DESIGN

Region where Bird
Strikes Airfoil

Region where suction surface
shape determines max. airflow



FCW First Covered Wave
AM Mouth Area
AT Thin Throat Area Typical Blade Tip Section
AT Thick Throat Area Blade Thickened for Birdstrike
SS Suction Surface
PS Pressure Surface
U Wheelspeed

Figure 33. Effect of Birdstrike Requirement on Blade Passage Design

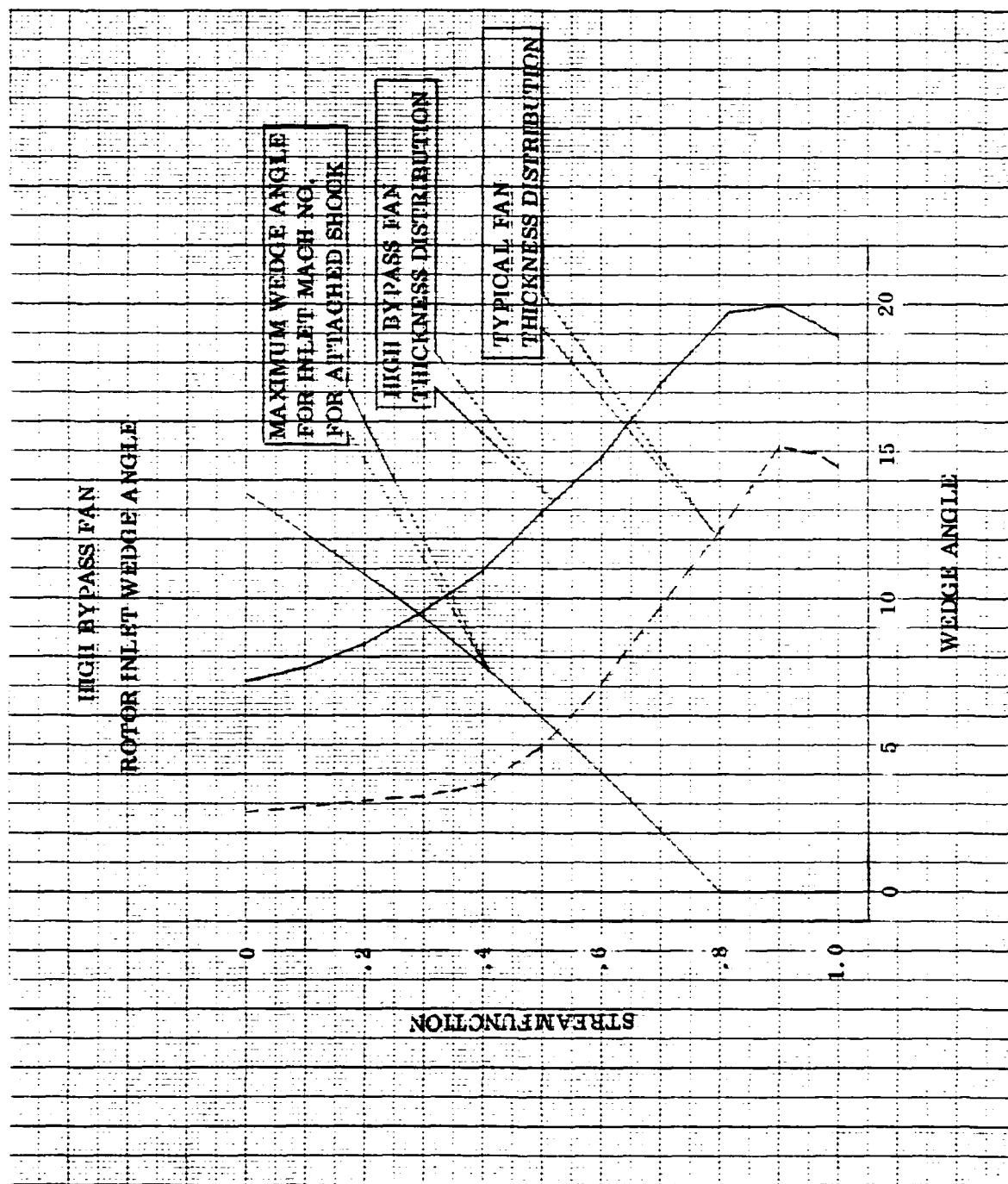


Figure 34. Wedge Angle for Various Fan Blade Shapes vs. Maximum Wedge Angle

GENERAL ELECTRIC COMPANY
AIRCRAFT ENGINE GROUP

TABLE 14. IMPACT OF MEETING BIRD STRIKE REQUIREMENT

HIGH BYPASS FAN

BIRDSTRIKE REQUIREMENT: IMPACT ON PERFORMANCE

- o Thicken Blade Rapidly After Leading Edge
 - Larger wedge angle pushes shock forward in pitch region, increasing bow shock losses
- o Rapid Increase in Thickness Makes
 - Blade passage design more difficult
 - LE suction surface set by flow requirements
 - Pressure surface angle tends to
 - . Force throat aft
 - . More difficult to minimize internal contraction
 - . Blade must be opened more abruptly aft of mouth

TABLE 15. FINAL SELECTION OF AERODYNAMIC DESIGN PARAMETERS

HIGH BYPASS FAN

AERODYNAMIC DESIGN PARAMETERS

FINAL SELECTION

ROTOR TIP SPEED	1440 ft/sec
FLOW/ANNULUS AREA	41.5 lbm/sec/ft ²
INLET RADIUS RATIO	.36
STATOR DISCHARGE MACH NO.	.54
RATIO OF ROTOR ANNULUS AREA CONVERGENCE TO STAGE ANNULUS AREA CONVERGENCE	.70
ROTOR PITCH SOLIDITY	1.87
STATOR PITCH SOLIDITY	1.60
ROTOR ASPECT RATIO	1.26
STATOR ASPECT RATIO	1.94
ROTOR TIP FLARING	1.0
STATOR TIP FLARING	1.0

TABLE 16. REASONS FOR FINAL DESIGN SELECTION

HIGH BYPASS FAN

AERODYNAMIC DESIGN PARAMETERS

REASONS FOR FINAL SELECTION

41.5 lbm/sec/ft²

FLOW/ANNULUS AREA

- W/A SELECTED TO MINIMIZE BLADE THICKNESS REQUIRED TO MEET BIRD STRIKE

- OPTIMUM FLOW ANNULUS AREA IS 41.5

ROTOR TIP SPEED

1440 ft/sec

- IMPROVED EFFICIENCY BY LOWERING ROTOR INLET MACH NO.

- FURTHER REDUCTION WOULD RAISE INTERNAL LOADING, REDUCE STALL MARGIN AND RAISE LP TURBINE LOADING

INLET RADIUS RATIO

.36

- PARAMETRIC CONFIRMED ORIGINAL CHOICE

TABLE 17. REASONS FOR FINAL DESIGN SELECTION

HIGH BYPASS FAN

AERODYNAMIC DESIGN PARAMETERS

REASONS FOR FINAL SELECTION

STATOR DISCHARGE MACH NO. .54

- BALANCE BETWEEN INCREASED FAN STALL MARGIN
AND INNER DUCT PERFORMANCE

RATIO OF ROTOR ANNULUS AREA
CONVERGENCE TO STAGE ANNULUS
AREA CONVERGENCE .70

- OPTIMIZED EFFICIENCY

TABLE 18. REASONS FOR FINAL DESIGN SELECTION

HIGH BYPASS FAN

AERODYNAMIC DESIGN PARAMETERS

REASONS FOR FINAL SELECTION

1.26

o ROTOR ASPECT RATIO

- MEETS AEROMECHANICAL REQUIREMENTS
- LOW ASPECT RATIO HELPS STALL MARGIN

1.94

o STATOR ASPECT RATIO

- SATISFIES AERODYNAMIC AND AEROMECHANICAL REQUIREMENTS

1.87

o ROTOR PITCH STUDY

- GOOD BALANCE BETWEEN STALL MARGIN AND EFFICIENCY

1.60

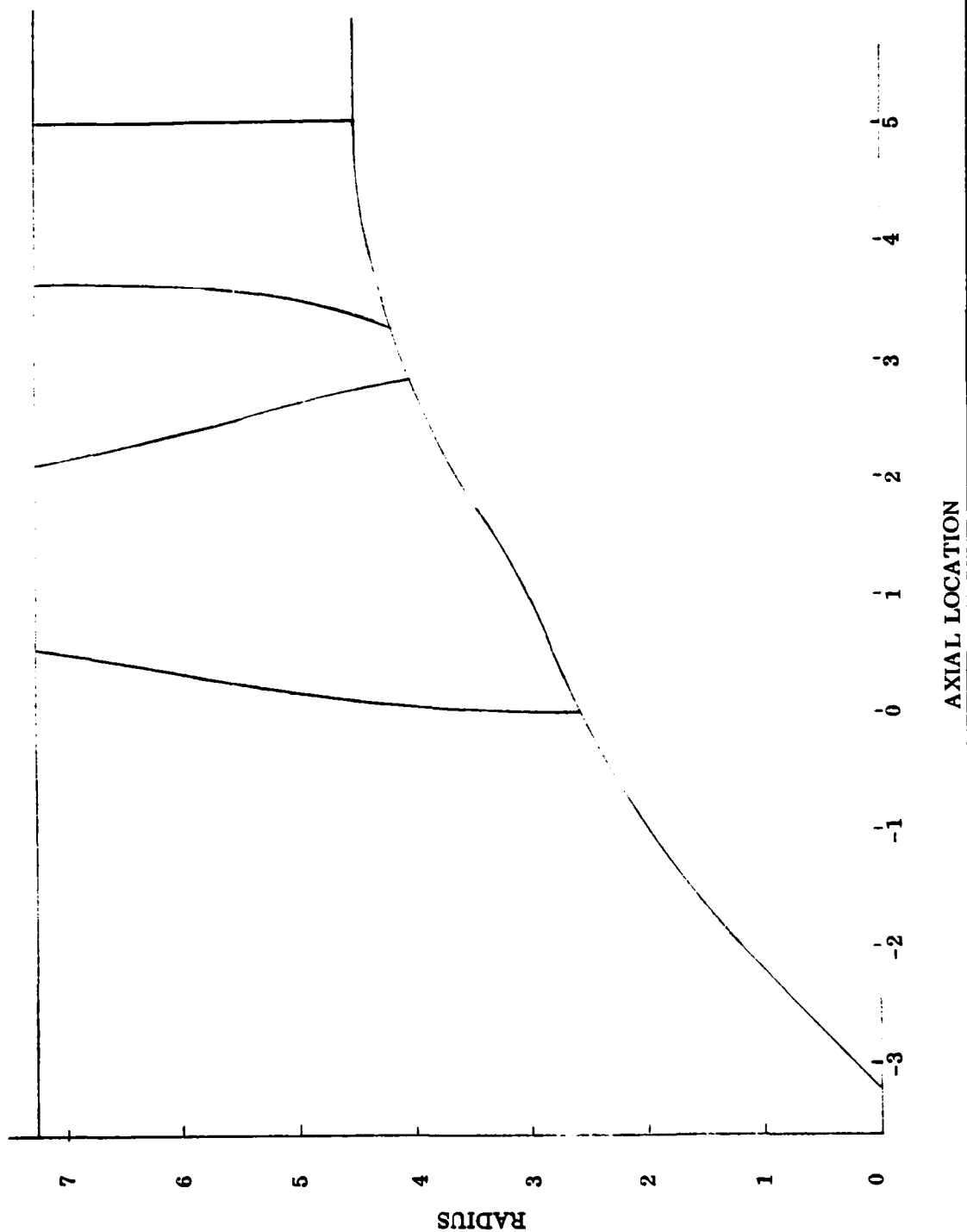
o STATOR PITCH SOLIDITY

- GOOD STALL MARGIN

TABLE 19. COMPARISON OF IMPORTANT, GE26/F4 DESIGN CONDITIONS WITH PROPOSAL

SELECTED GE26/F4 FAN DESIGN CONDITIONS COMPARED WITH ORIGINAL PROPOSAL			
PARAMETER	PROPOSAL	GE26/F4	
Flow - lbms/sec	41.57	41.6	
Flow/Annulus Area - lbm/sec/ft ²	43.0	41.5	
Tip Speed, Rotor - ft/sec	1455	1440	
Pressure Ratio, stage	1.758	1.758	
Stator Exit Mach No. ($\lambda = .95$)	.547	.54	
Inlet Hub Radius Ratio	.36	.36	
Rotor Hub Speed Ratio	$\frac{819}{524} = 1.56$	$\frac{821}{519} = 1.58$	
Rotor Hub Work Coefficient $\sim 2 g J \Delta H/U^2$	2.013	1.99	
Solidity, Rotor Avg.	2.04	1.87	
Aspect Ratio, Rotor	1.27	1.26	
Rotor Construction	Shroudless/Blisk	Shroudless/Blisk	
Number of Rotor Blades	21	20	
Number of Stator Vanes	52	42	
Max Thick/Chord - rotor tip/hub	.030/.096	.03/.093	
Tip Radius	7.134	7.263	
RPM	23368	22720	
Adiabatic Efficiency	85.5	85.5	
Stall Margin @ Constant Flow, Percent	20	20	

HIGH BYPASS FAN FINAL FLOWPATH



GENERAL ELECTRIC COMPANY
AIRCRAFT ENGINE GROUP

Figure 35. Final Aerodynamic Flow Path

The rotor and stator discharge profiles of pressure ratio and adiabatic efficiency are shown in Figure 36. The average bypass stream pressure is 1.75 and the average core stream pressure is 1.80 at the stator discharge.

The rotor total pressure loss coefficient $(PT2 - PT1)/(PT1 - PS1)$ used in the design is shown in Figure 37. The profile and level of loss coefficient reflects experience on similar GE fans, when operating at the same tip Mach No. with adjustment for differences in radial distributions of Mach No. and loading level profiles. The stator total pressure loss coefficient used in the design is shown in Figure 38.

The percent cumulative change in total temperature used to define the axisymmetric flow field within the rotor is shown in Figure 39. The temperature is imparted to the flow on the aft portion of the blade at the tip, since the blade must be kept closed forward of the mouth to control passage area and suction surface Mach No. The nearly linear rate of work input at the hub reflects the high hub slope of the rotor.

The percent cumulative change in stator air angle used to define the axisymmetric flow field within the stator is shown in Figure 40. The stator angle change follows a quarter sine wave distribution at the OD, but the turning is removed further aft at the ID to control the suction surface Mach No. at the stator inlet where the inlet Mach No. is very high.

Figure 41 shows that the rotor diffusion factor is reasonable everywhere. Rotor hub diffusion factor is very low. The stator diffusion factor is reasonable everywhere (Figure 42). Careful attention was paid to stator hub diffusion factor during parametric studies selection. Hub flowpath and axial/radial distribution of stator turning were tuned during the axisymmetric flow studies to reduce diffusion factor.

The rotor inlet and discharge relative air angles are shown in Figure 43. The rotor discharge angle at the hub is $.5^\circ$. The stator inlet and discharge angle are shown in Figure 44. The air is turned back to axial at the stator discharge.

The rotor relative inlet Mach No. is shown in Figure 45. The stator absolute inlet Mach No. is shown in Figure 46. The stator inlet Mach No. reaches .99 locally at the ID. The absolute Mach No. at the discharge of the stator is shown in Figure 47. The average discharge Mach No. is .54, but the Mach No. of the core stream is about .6.

The ratio of discharge axial velocity to inlet axial velocity across the rotor is shown in Figure 48. There is considerable streamtube contraction across the hub, due to the high value of rotor annulus area convergence required for the high hub boost pressure profile. The axial velocity is nearly constant across the stator, as shown in Figure 49.

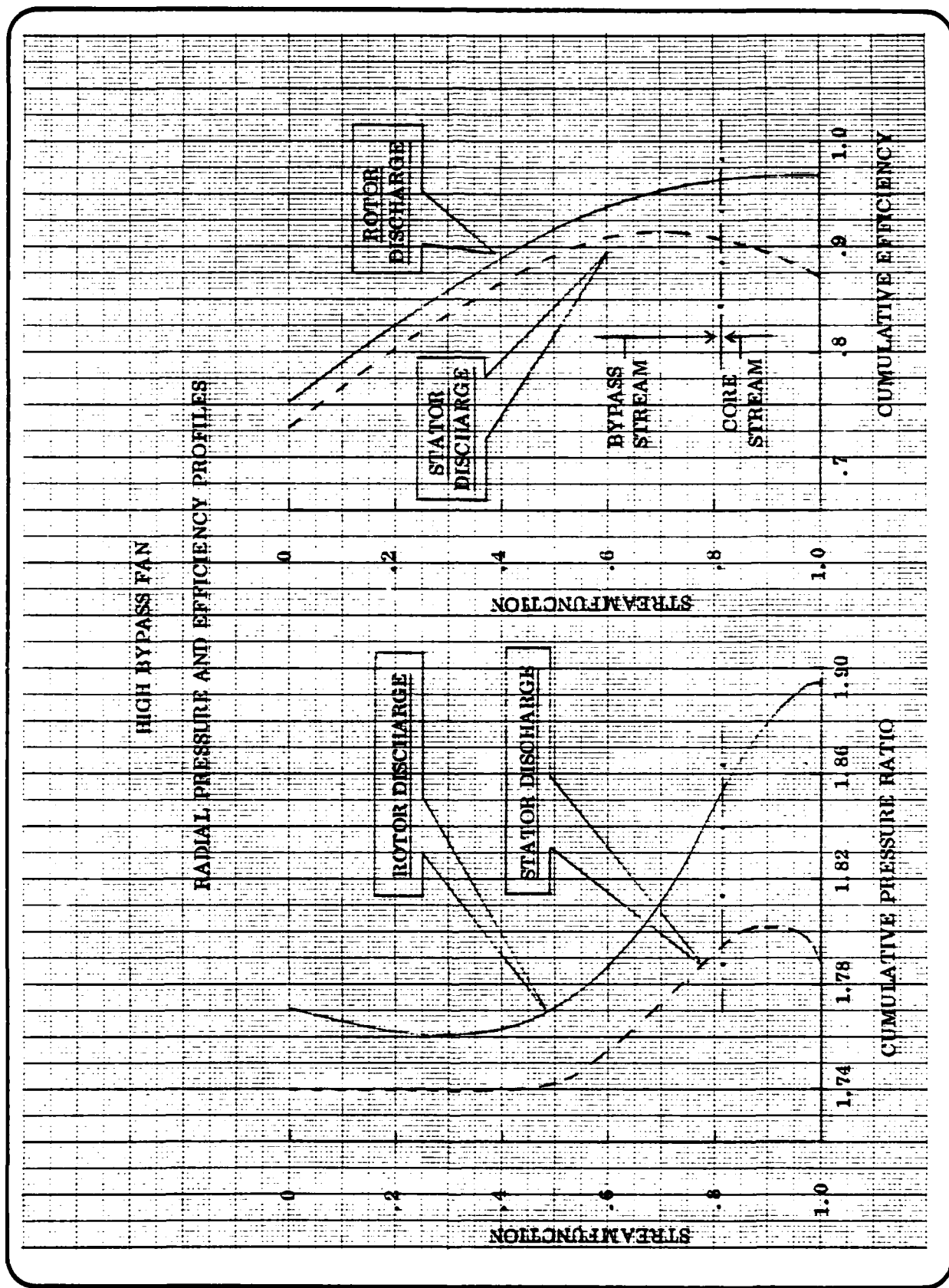


Figure 36. Rotor and Stator Discharge Profiles

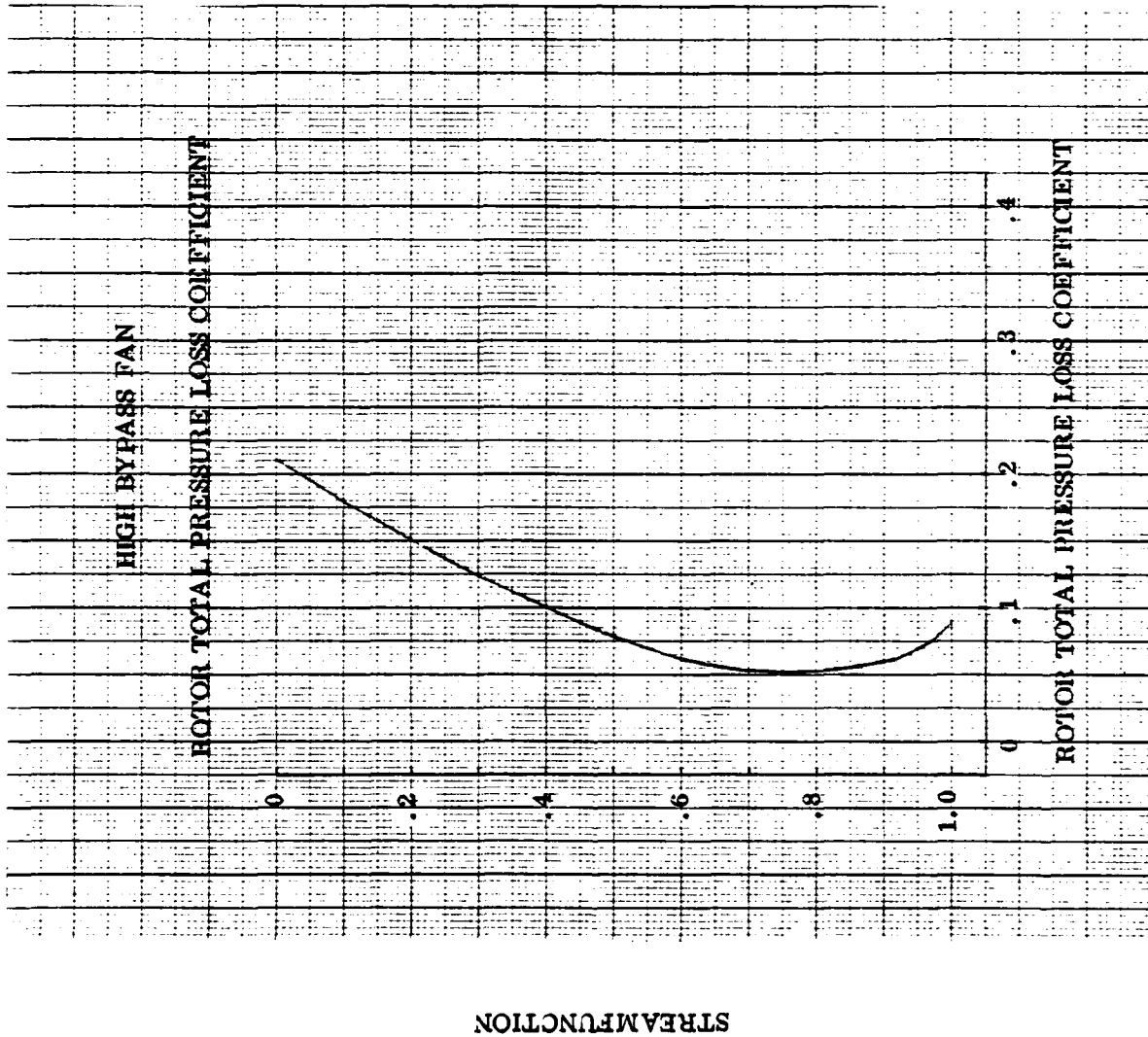


Figure 37. Rotor Total Pressure Loss Coefficients

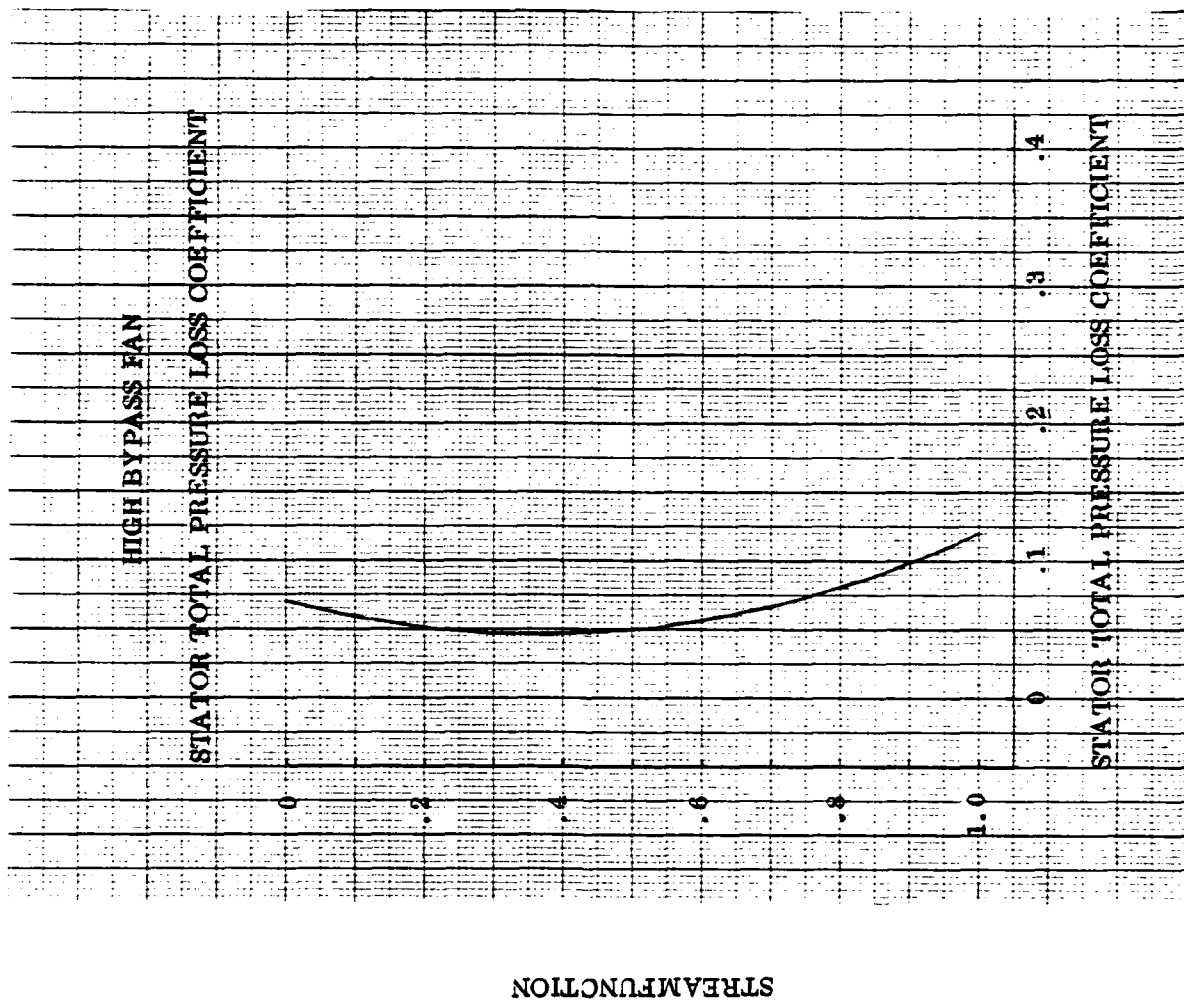


Figure 38. Stator Total Pressure Loss Coefficients

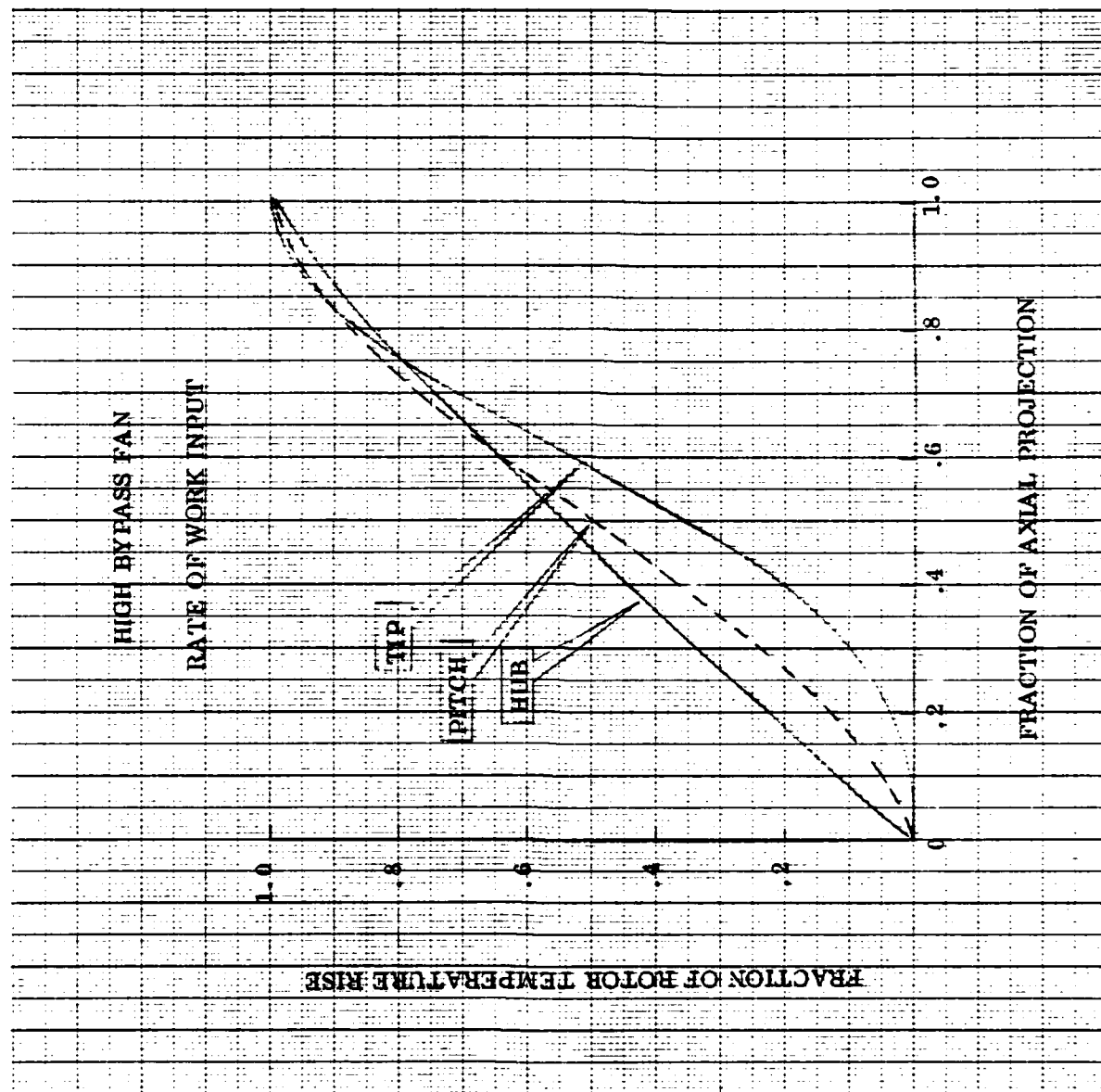


Figure 39. Percent Cumulative Change in Total Temperature

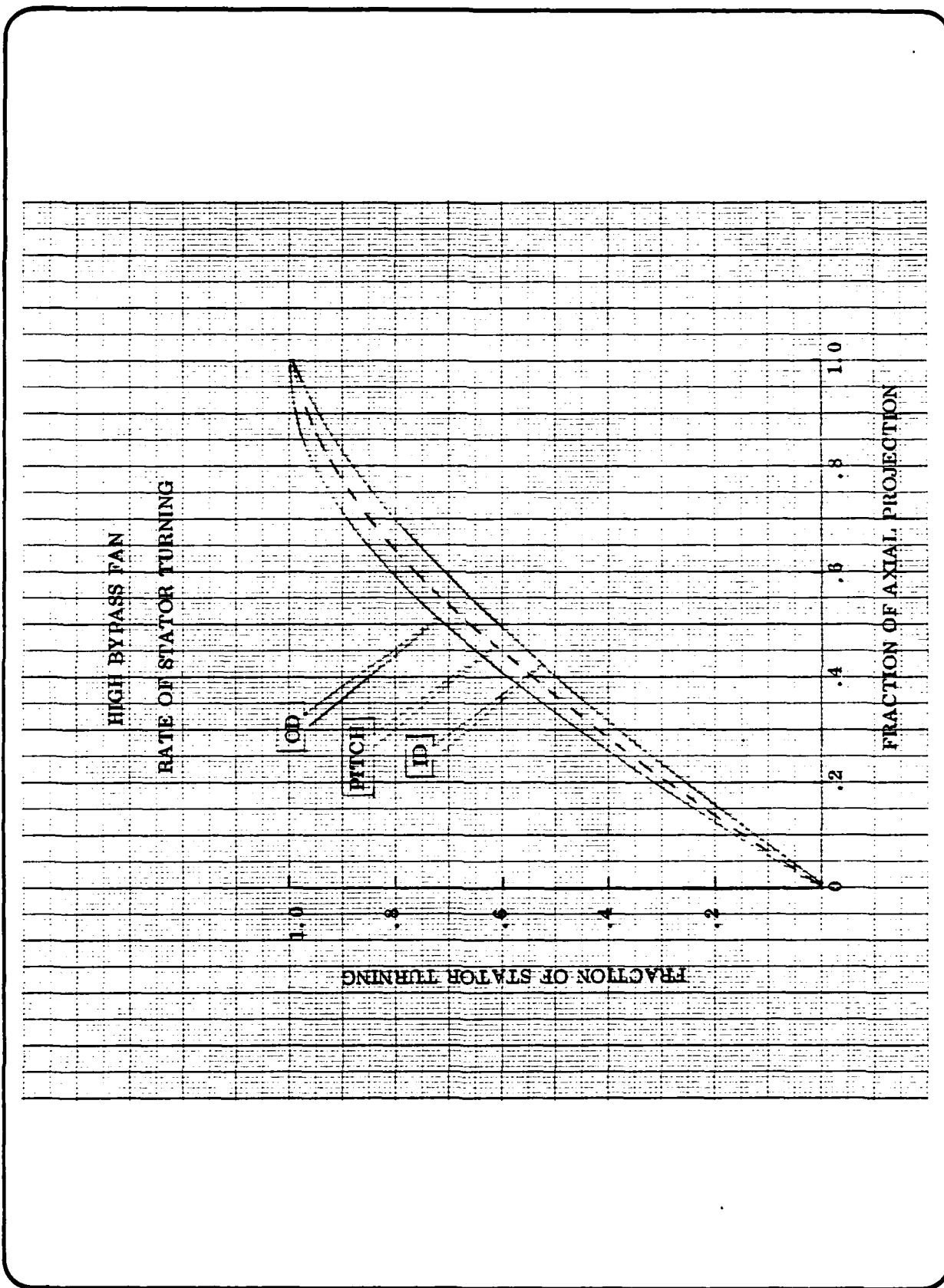


Figure 40. Percent Cumulative Change in Stator Air Angle

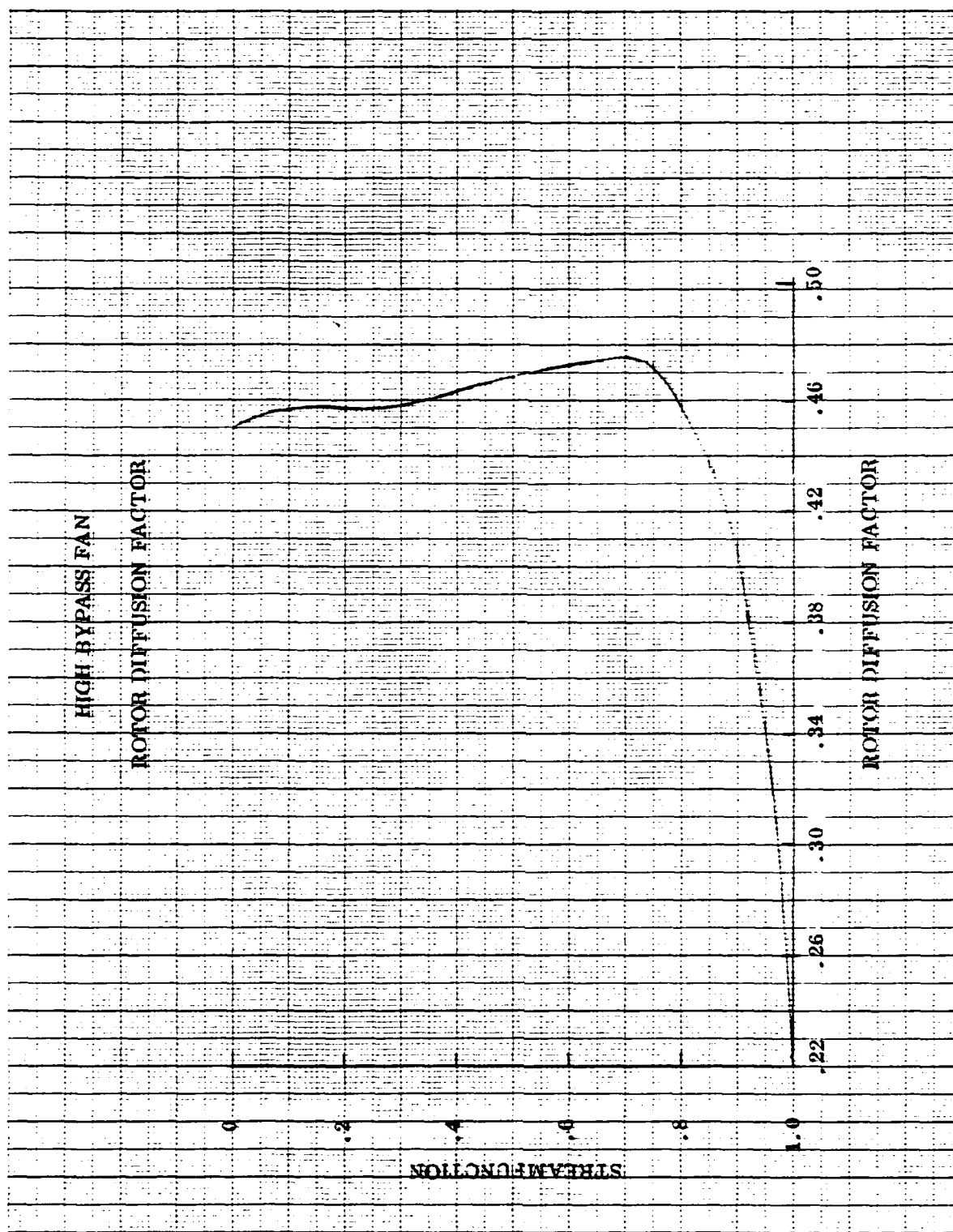


Figure 41. Rotor Diffusion Factor

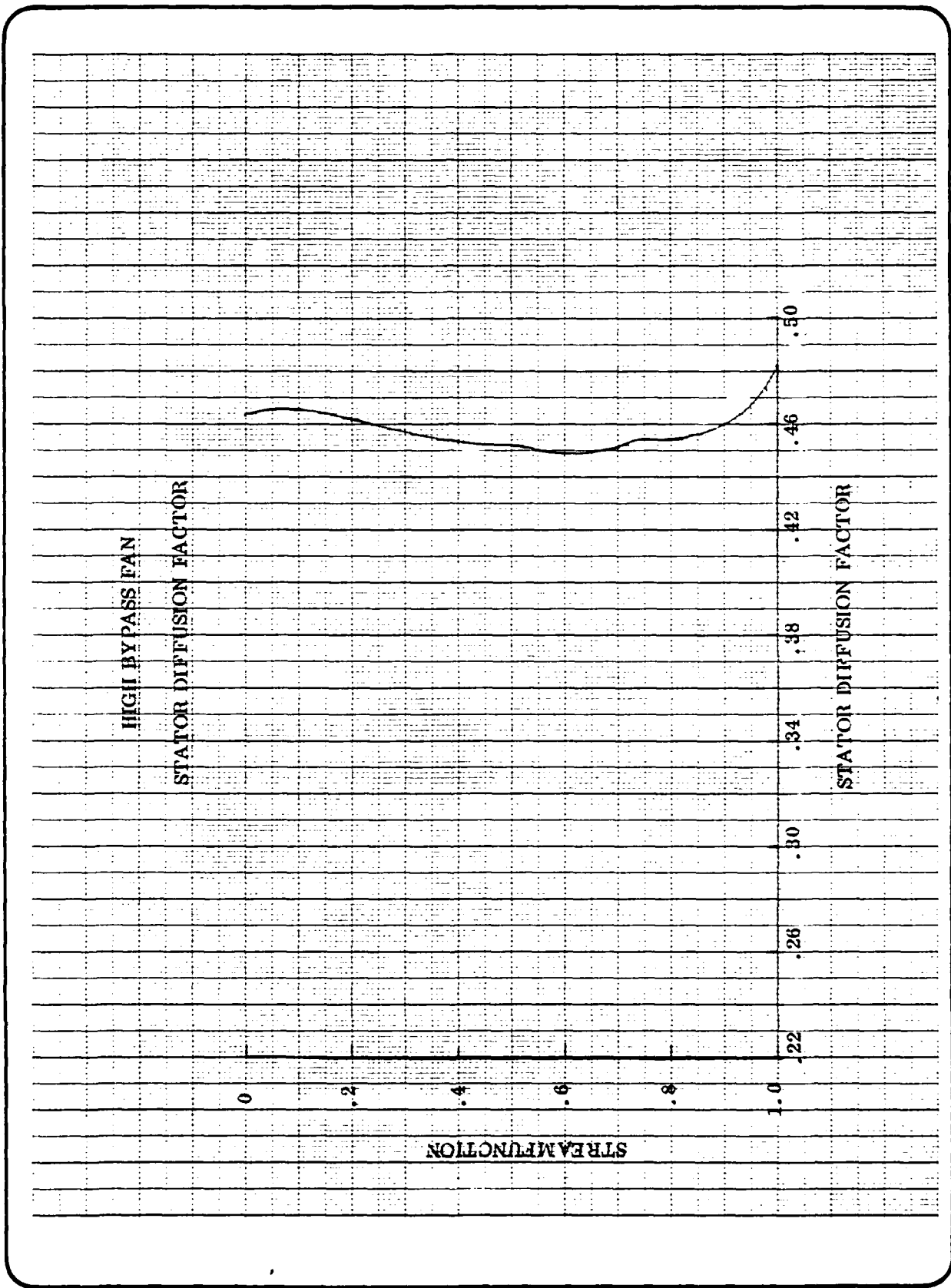


Figure 42. Stator Diffusion Factor

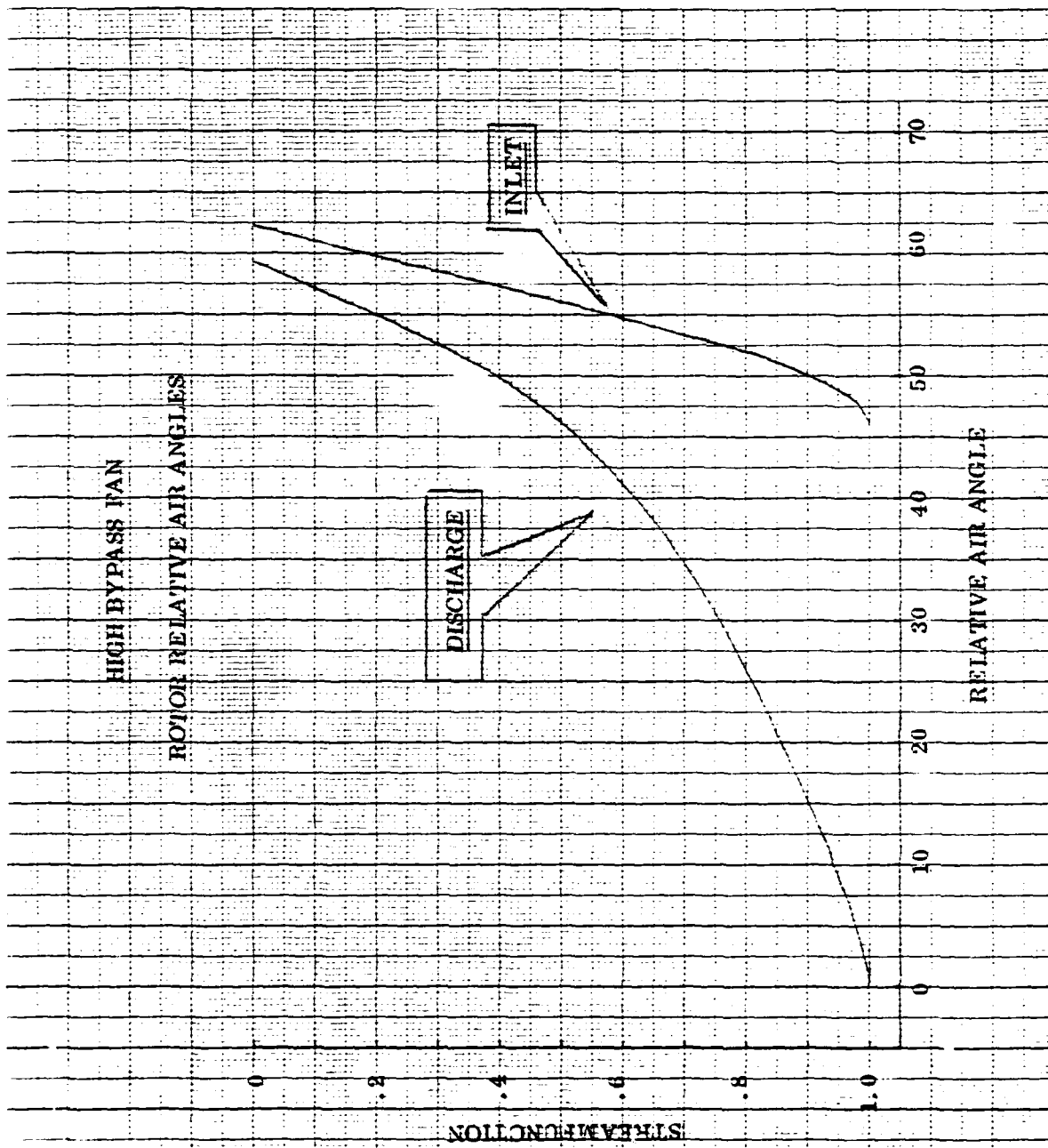


Figure 43. Rotor Inlet and Discharge Relative Air Angles

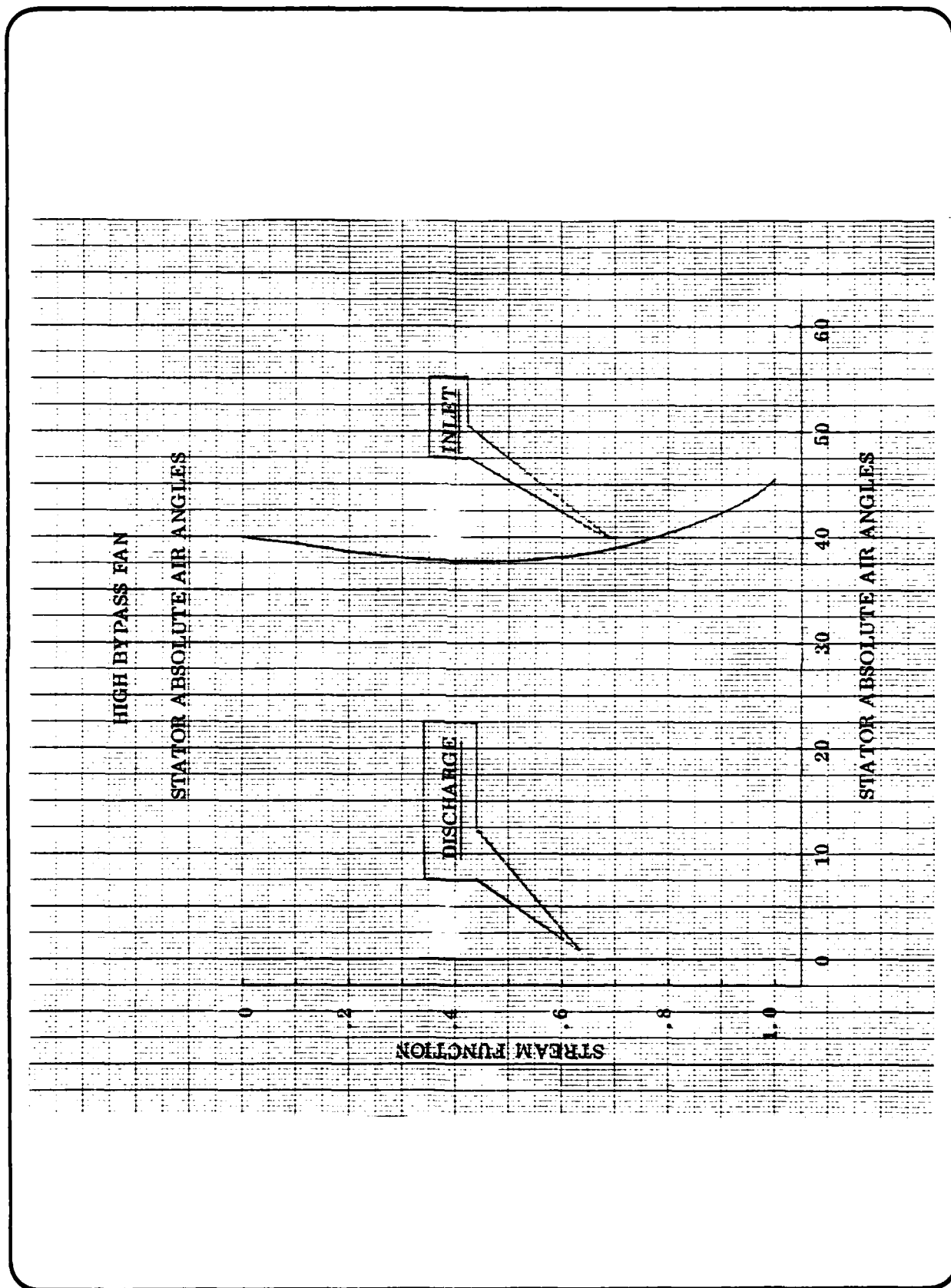
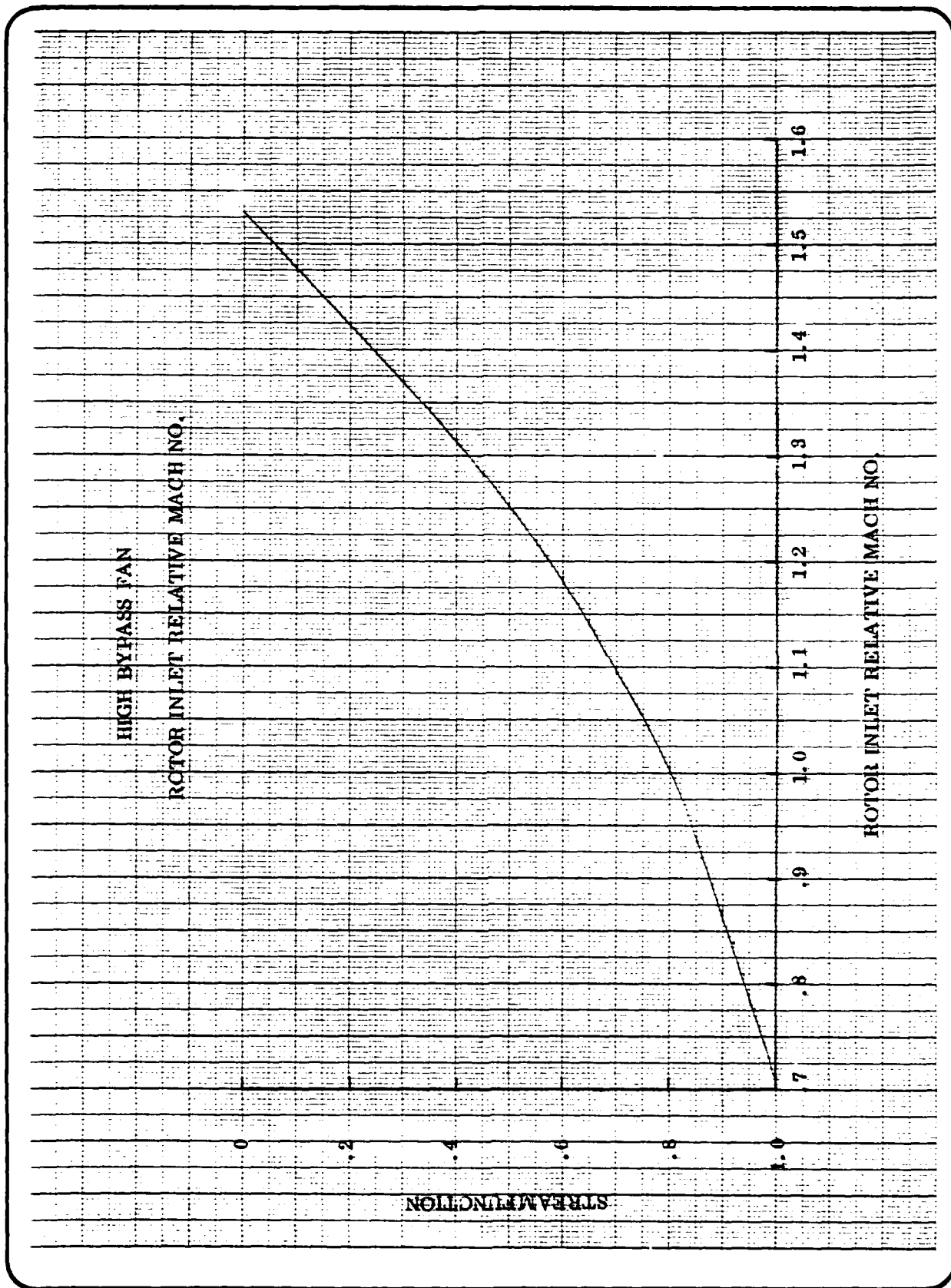


Figure 44. Stator Inlet and Discharge Angles



GENERAL ELECTRIC COMPANY
AIRCRAFT ENGINE GROUP

Figure 45. Rotor Relative Inlet Mach No.

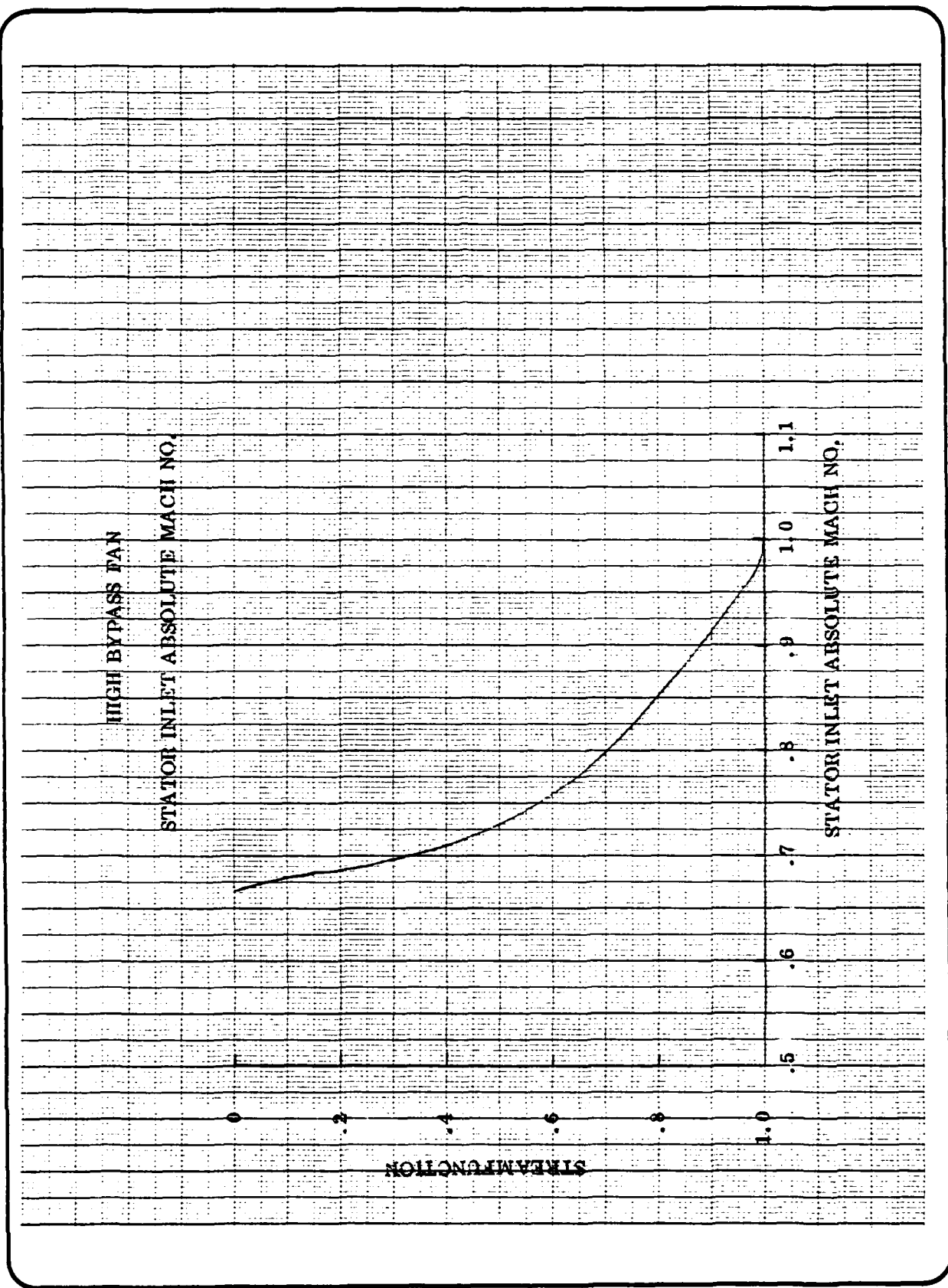
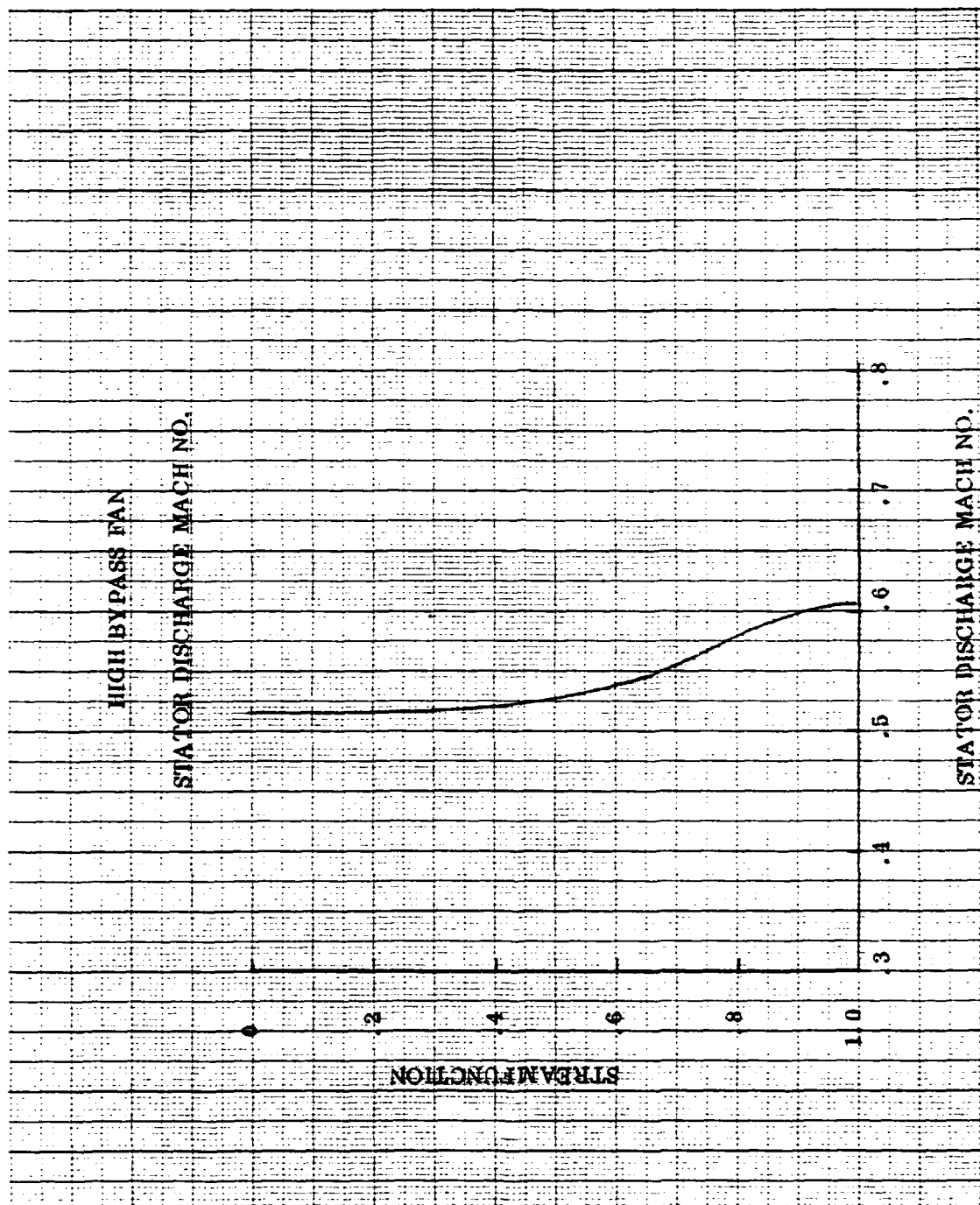


Figure 46. Stator Absolute Inlet Mach No.



GENERAL ELECTRIC COMPANY
AIRCRAFT ENGINE GROUP

Figure 47. Stator Discharge Absolute Mach No.

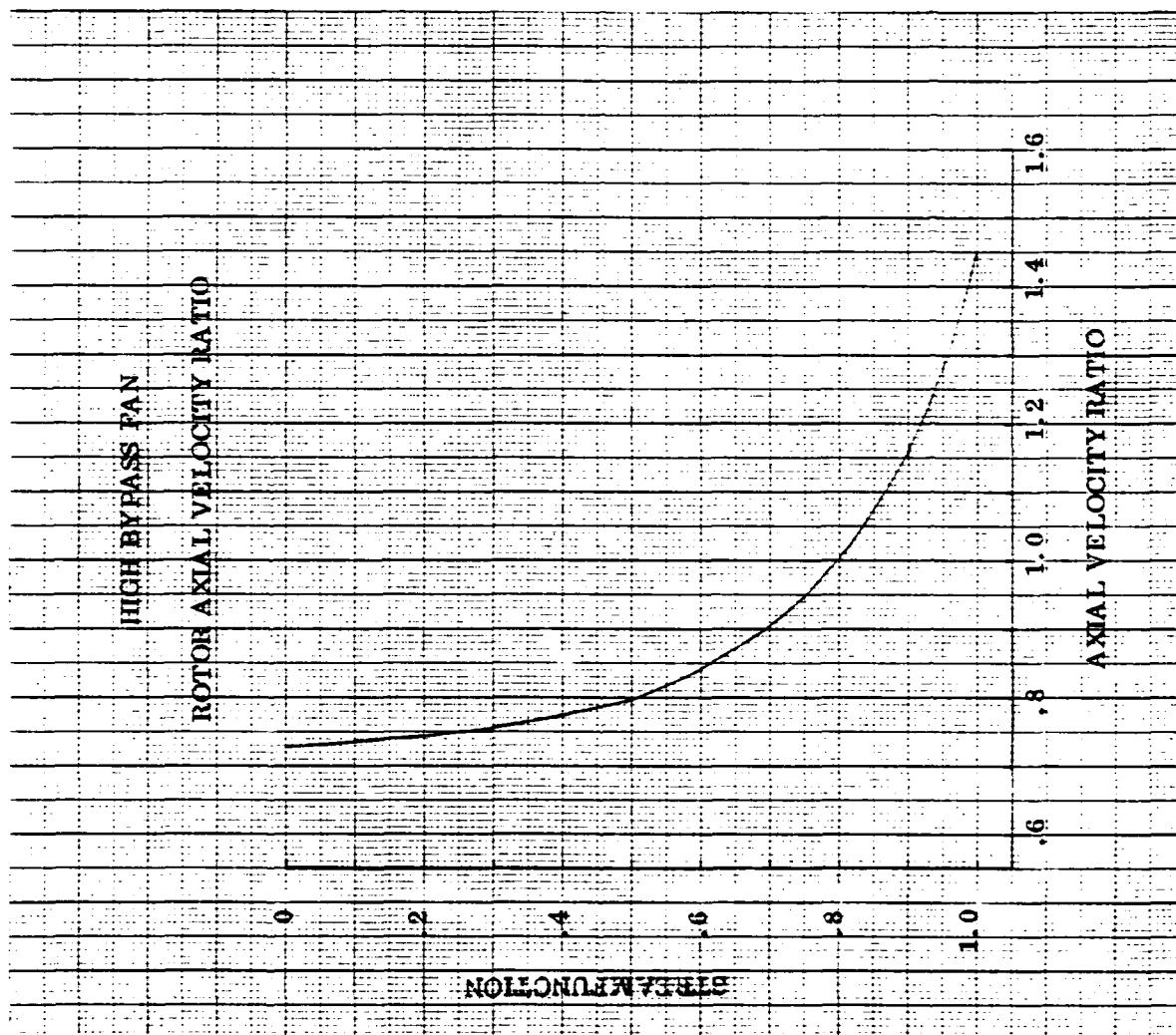
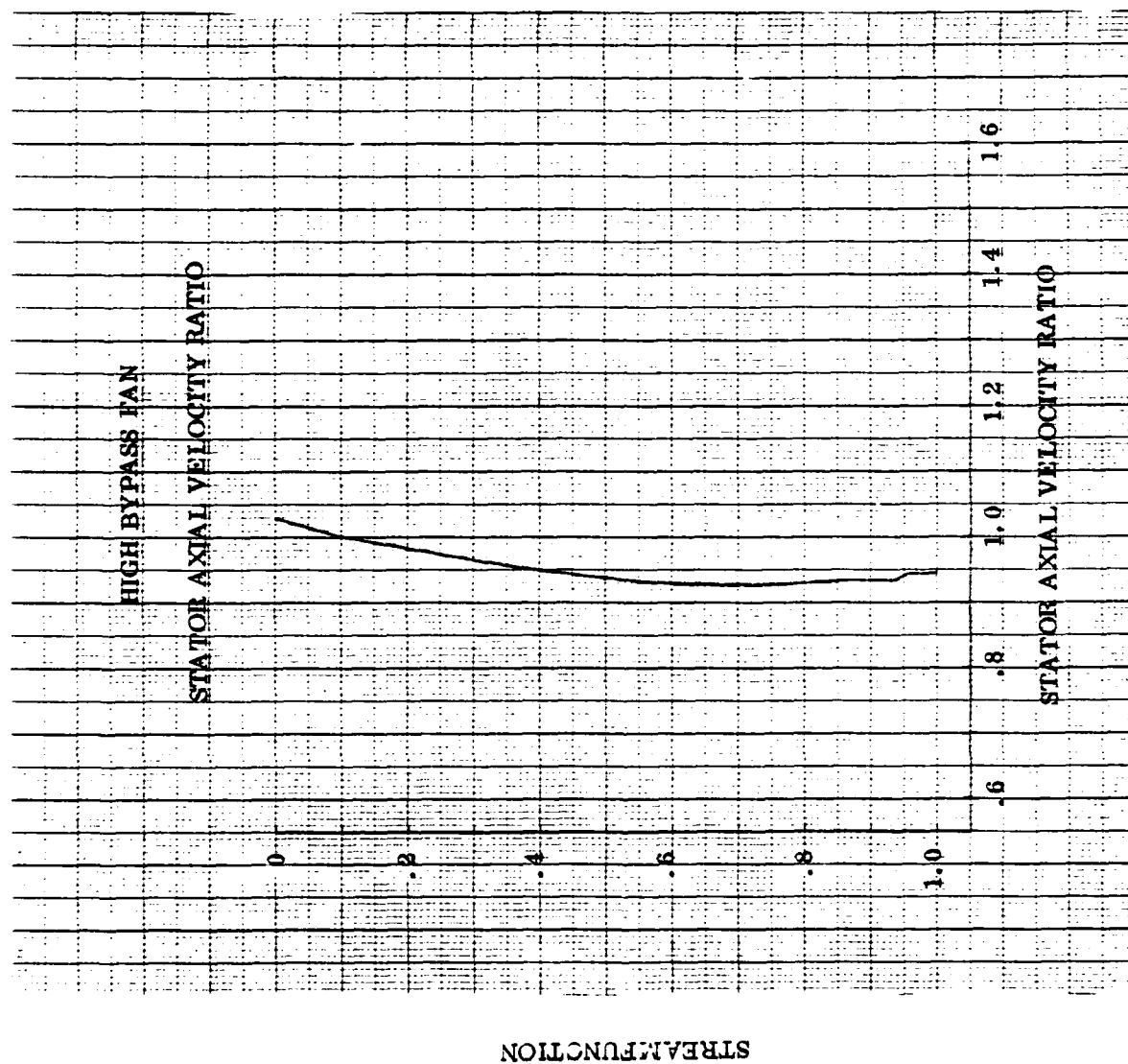


Figure 48. Ratio of Discharge to Inlet Axial Velocity Across Rotor



GENERAL ELECTRIC COMPANY
AIRCRAFT ENGINE GROUP

Figure 49. Stator Axial Velocity Ratio Profile

3.3.4 Detailed Blade Design

The detailed blade design was performed by analysis of blade passages along streamlines to determine the best blade shape to meet the fan performance objectives. Radial variations of parameters such as chord and thickness were iterated with the aeromechanical design to achieve a good balance between aerodynamic and aeromechanical design objectives.

The radial distribution of rotor chord is shown in Figure 50. The average chord was selected during the parametric studies. The radial distribution of chord was set to provide higher solidity in the tip and pitch region and to provide an adequate covered passage at the tip, but reduce the chord at the hub where the diffusion is very low. The increase in chord from tip to pitch also provides sweep which may reduce shock losses in the high Mach No. tip region. The resulting radial distribution of rotor solidity is shown in Figure 51.

The radial distribution of stator chord is shown in Figure 52. The average chord was set by the parametric studies. The hub chord is larger than the tip chord to reduce the diffusion factor and to assure adequate stall margin. The resultant radial distribution of stator solidity is shown in Figure 53.

The radial distribution of rotor maximum thickness to chord ratio is shown in Figure 54. The radial distribution of stator maximum thickness to chord ratio is shown in Figure 55. Both rotor and stator t_m/c distributions were selected to achieve satisfactory stress and vibration characteristics with the least impact on aerodynamic performance.

The radial distribution of rotor incidence is shown in Figure 56. The selection of tip incidence reflects a good balance to meet design flow capacity (desire high incidence) and birdstrike and stall margin (desire lower incidence) requirements. The pitchline incidence was selected to provide zero incidence on the suction at the leading edge. The hub incidence provides adequate throat margin.

The radial distribution of stator incidence is shown in Figure 57. The level was chosen primarily for optimum efficiency. The low tip (OD) incidence should help stall margin while the high hub (ID) incidence helps throat margin.

The radial variation of rotor deviation is shown in Figure 58. The deviation general follows Carter's rule, but is adjusted to account for secondary flow and to assure adequate discharge area for supersonic flow sections. The radial variation of stator deviation is shown in Figure 59. The deviation is based on Carter's rule.

The rotor meanline angles are shown as a function of percent axial projection for each streamline in Figure 60. Rotor streamline camber and

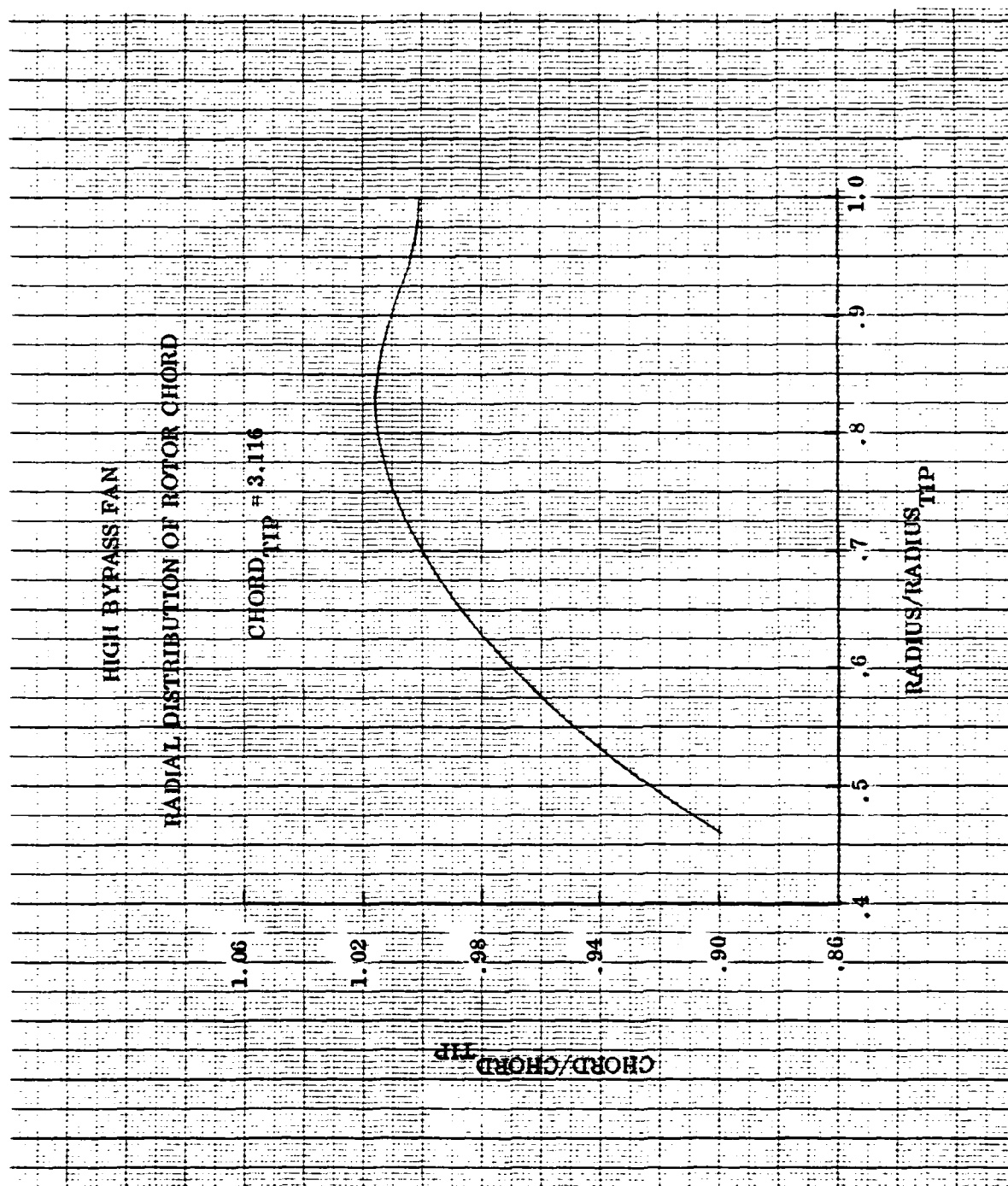


Figure 50. Radial Distribution Rotor Chord

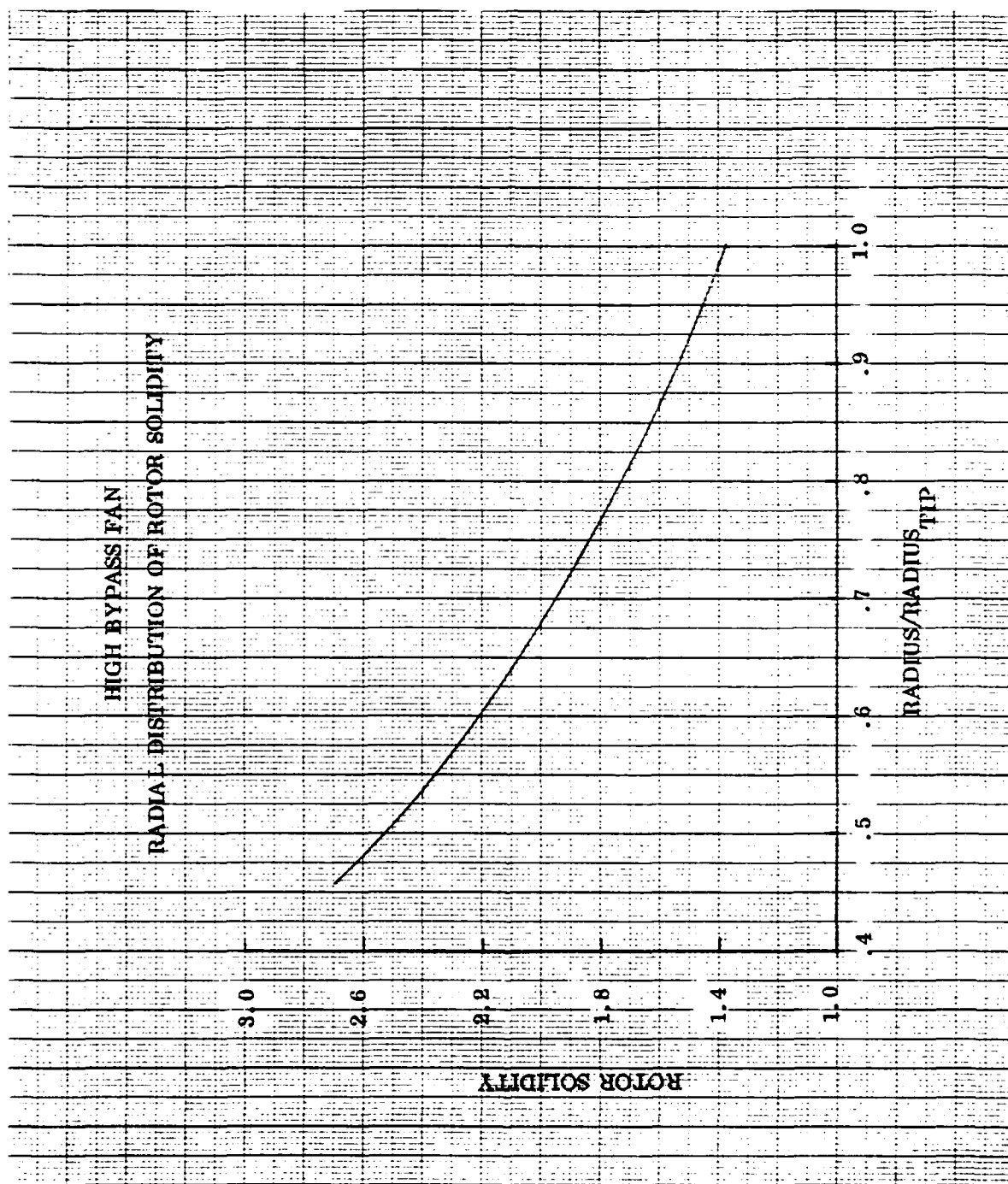


Figure 51. Rotor Solidity Radial Distribution

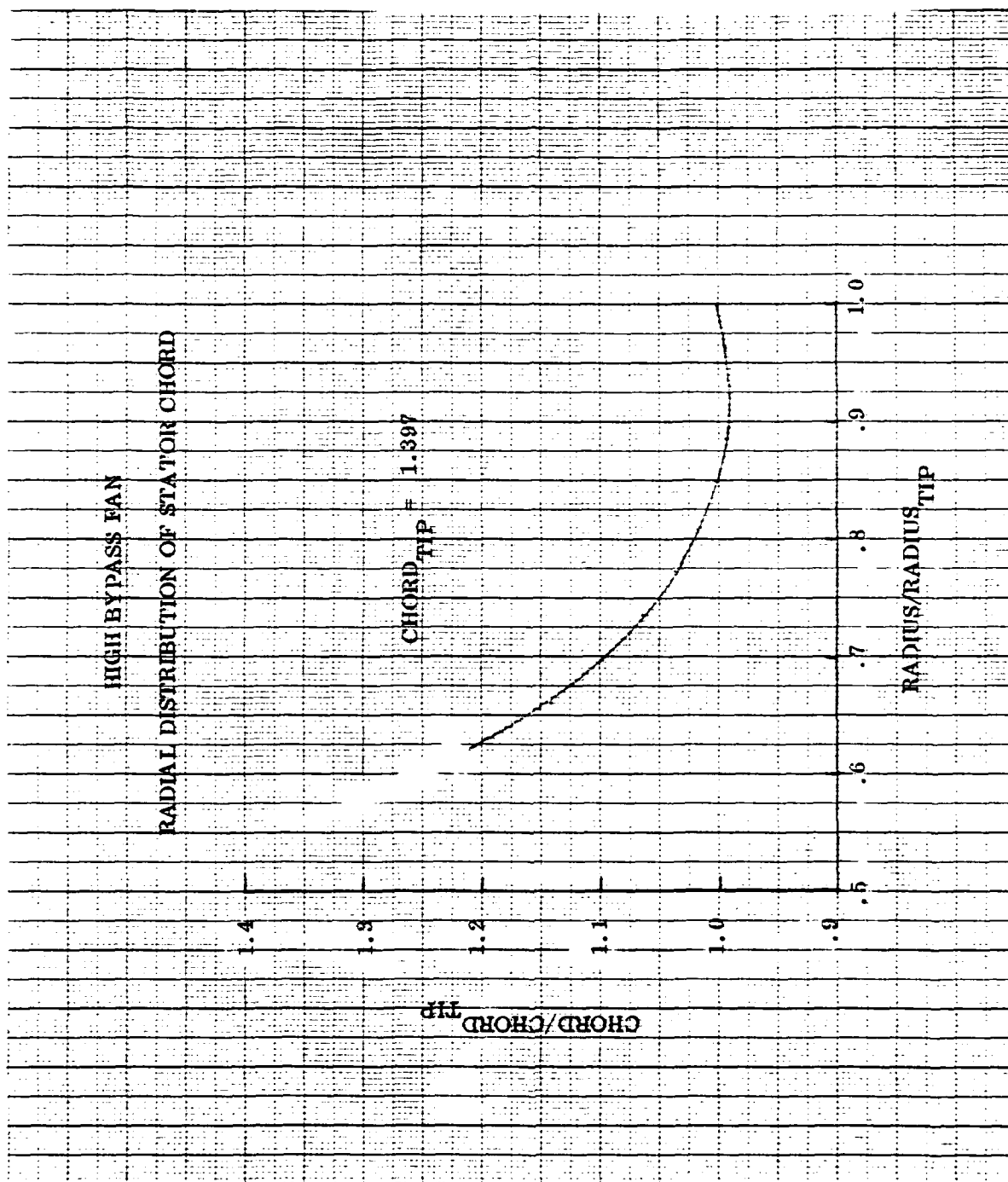


Figure 52. Stator Chord Radial Distribution

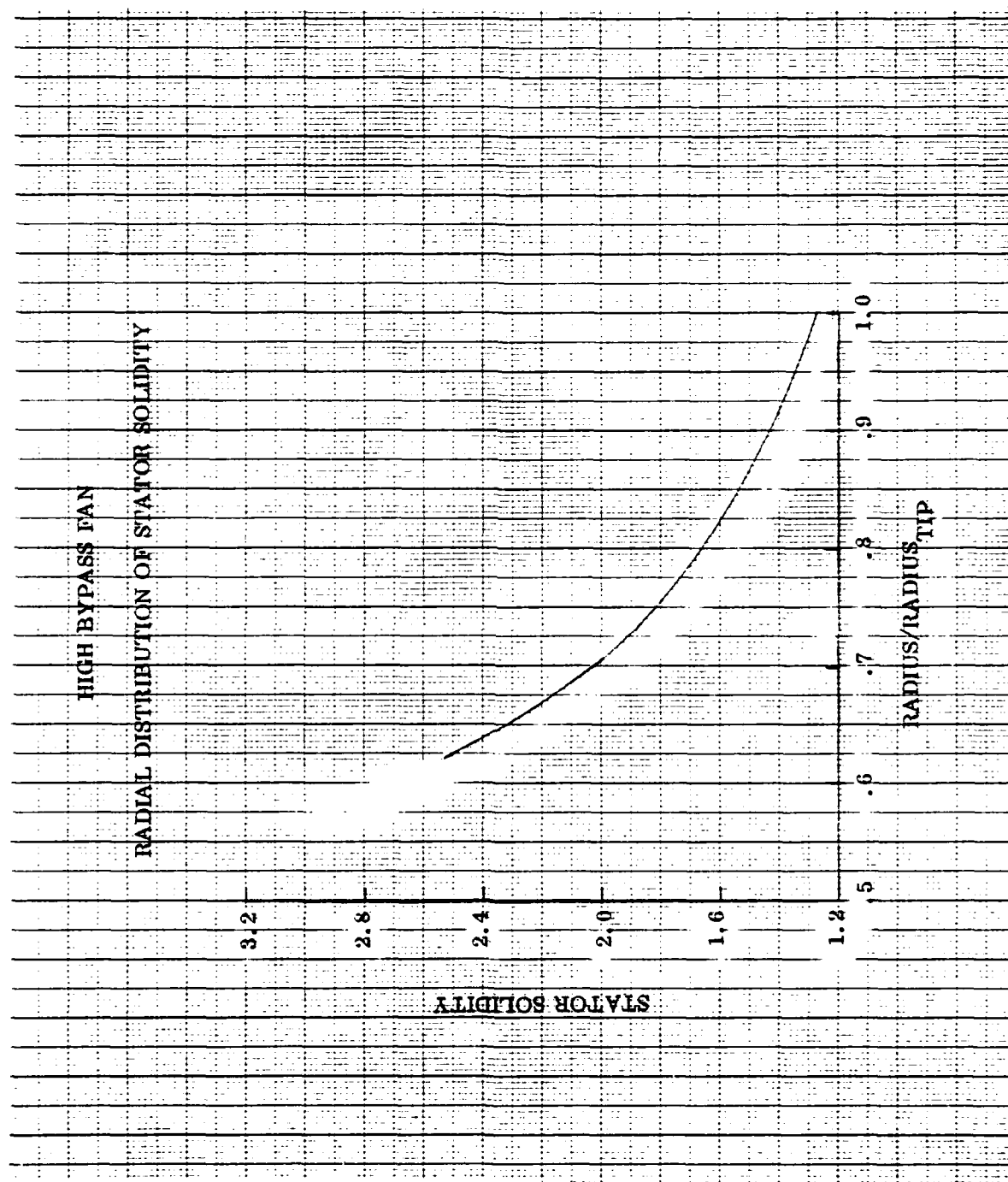
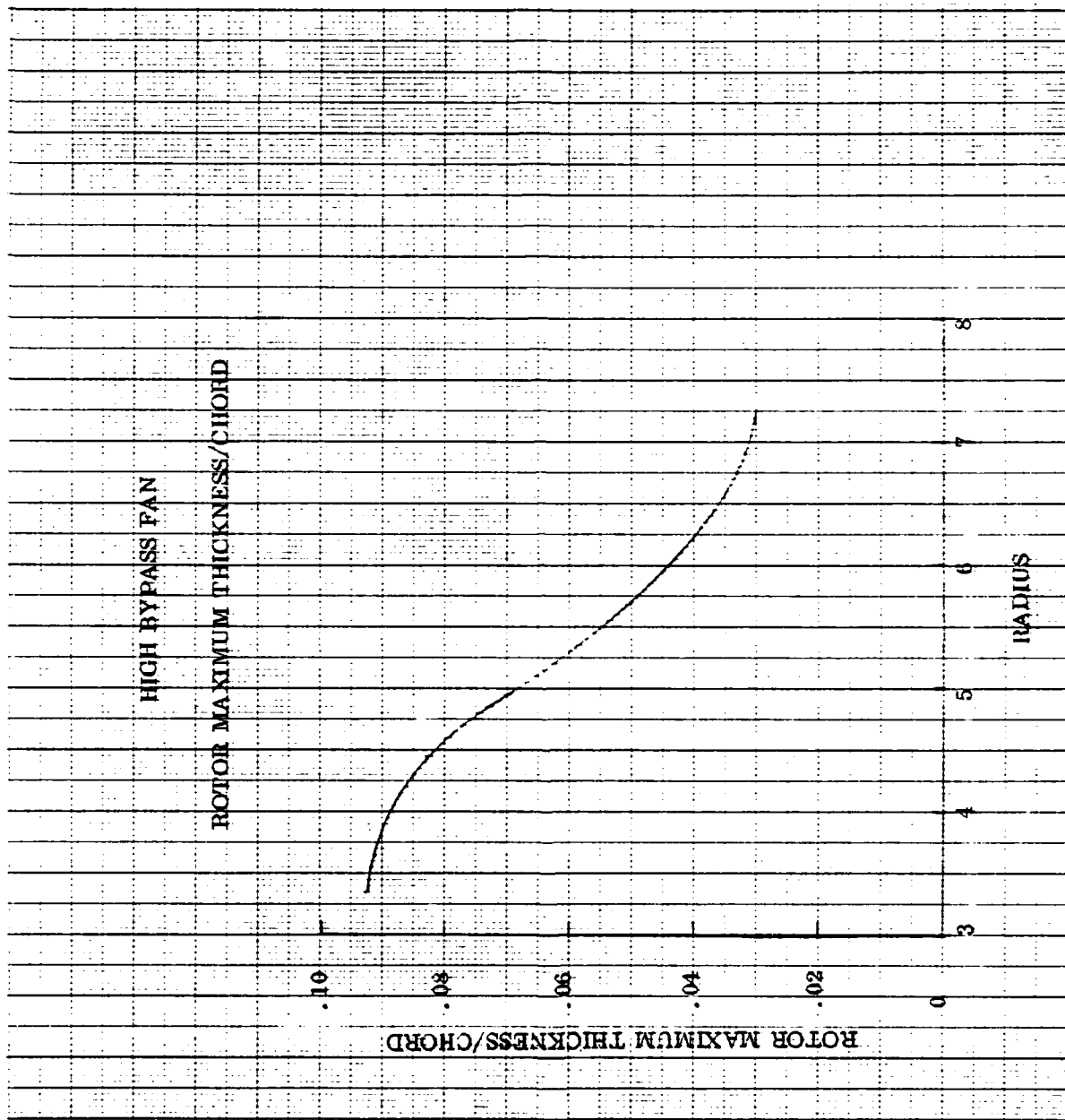


Figure 53. Stator Solidity Radial Distribution



GENERAL ELECTRIC COMPANY
AIRCRAFT ENGINE GROUP

Figure 54. Rotor Maximum Thickness/Chord Radial Distribution

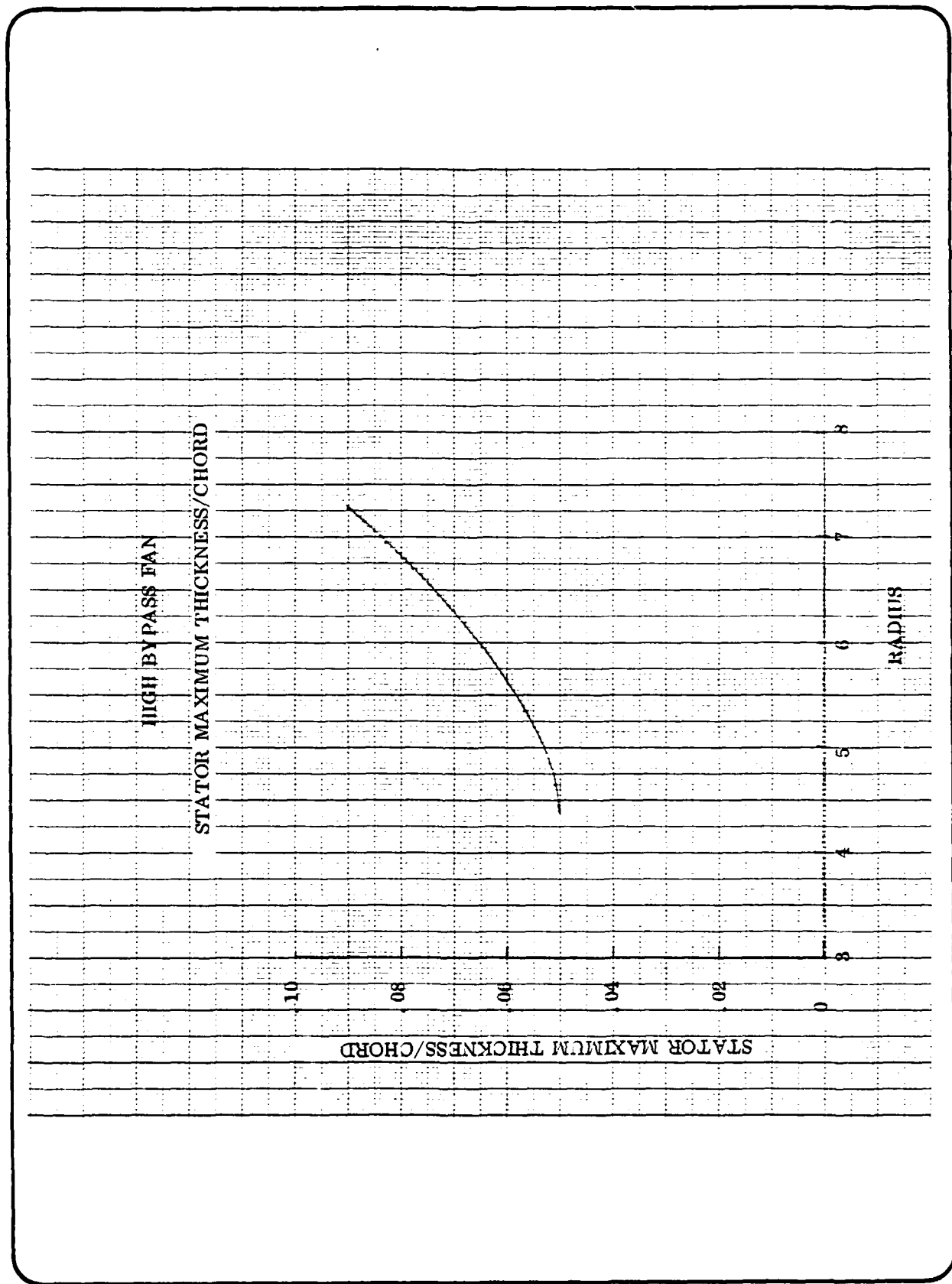


Figure 55. Stator Maximum Thickness/Chord Radial Distribution

AD-A082 753

GENERAL ELECTRIC CO LYNN MA AIRCRAFT ENGINE GROUP F/G 21/5
HIGH BYPASS TURBOFAN COMPONENT DEVELOPMENT. PHASE II. DETAILED --ETC(U)
AUG 79 H MAUCH, T OLDAKOWSKI, D WELDON F33615-78-C-2060

AFAPL-TR-79-2064

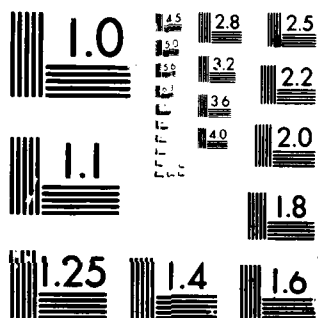
NL

UNCLASSIFIED

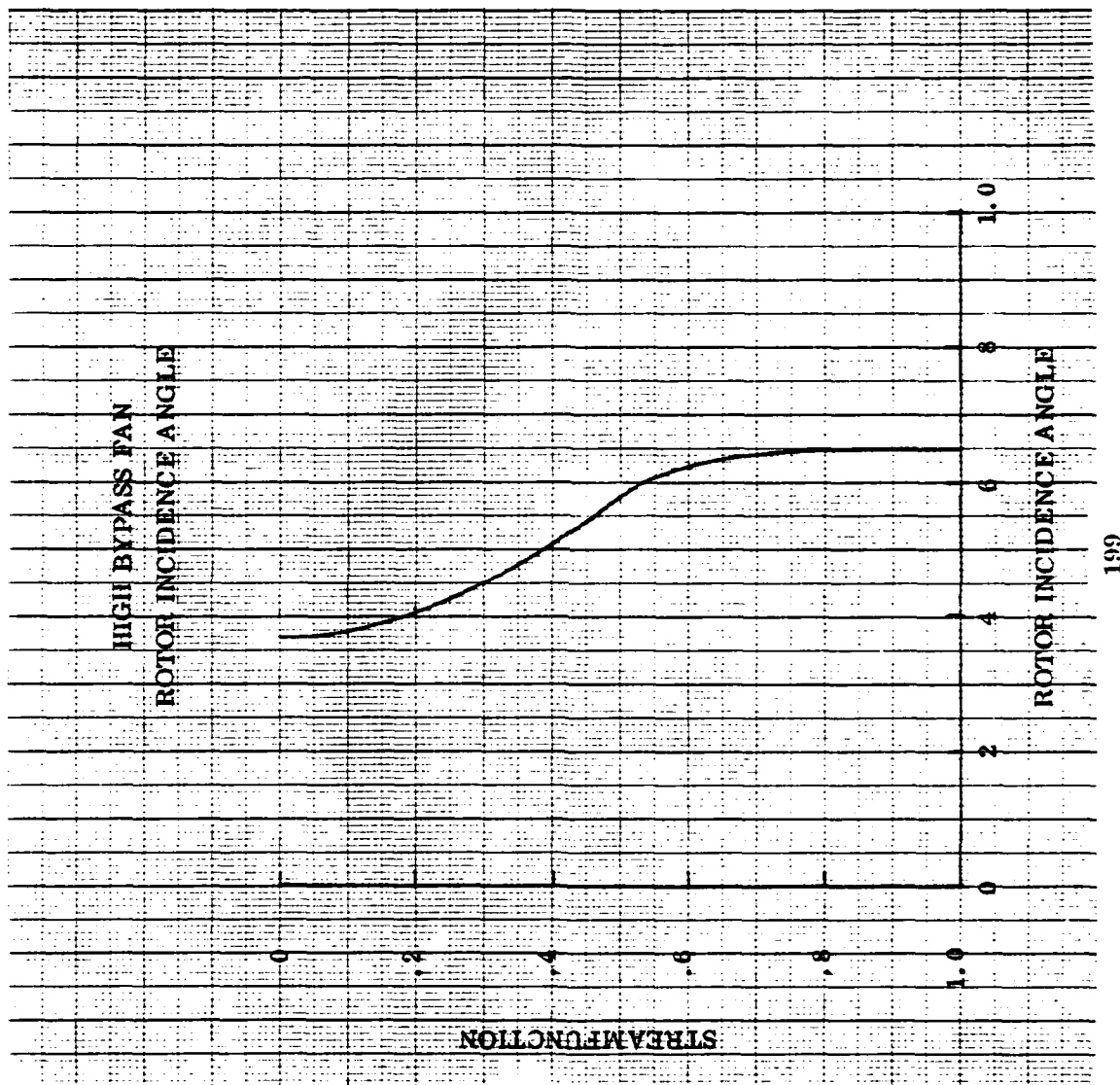
212
SII
ADP/7-1



END
DATE
FILMED
5-80
DTIC



MICROCOPY RESOLUTION TEST CHART
NATIONAL BUREAU OF STANDARDS-1963-A



199

Figure 56. Rotor Incidence Angle Radial Distribution

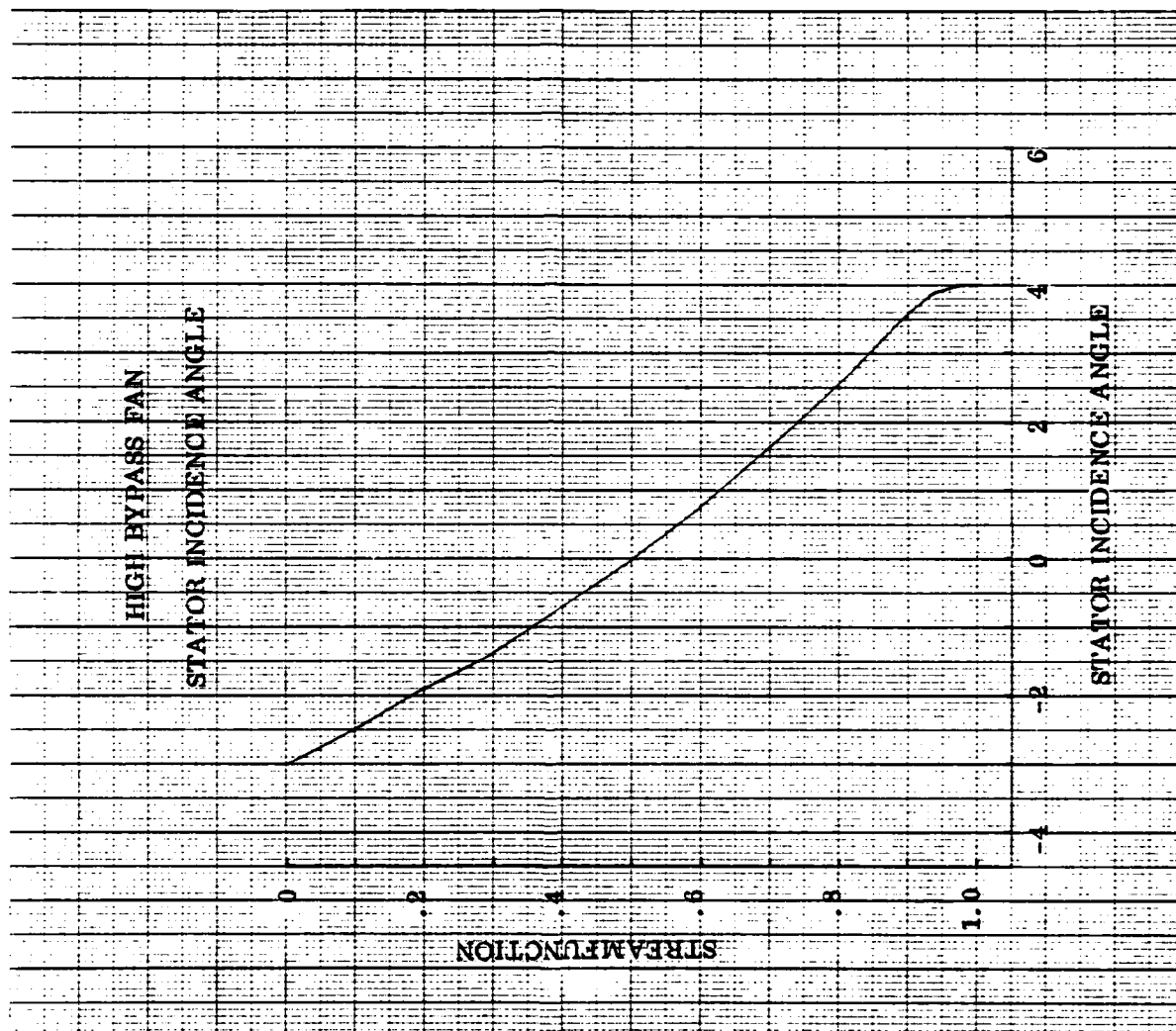


Figure 57. Stator Incidence Angle Radial Distribution

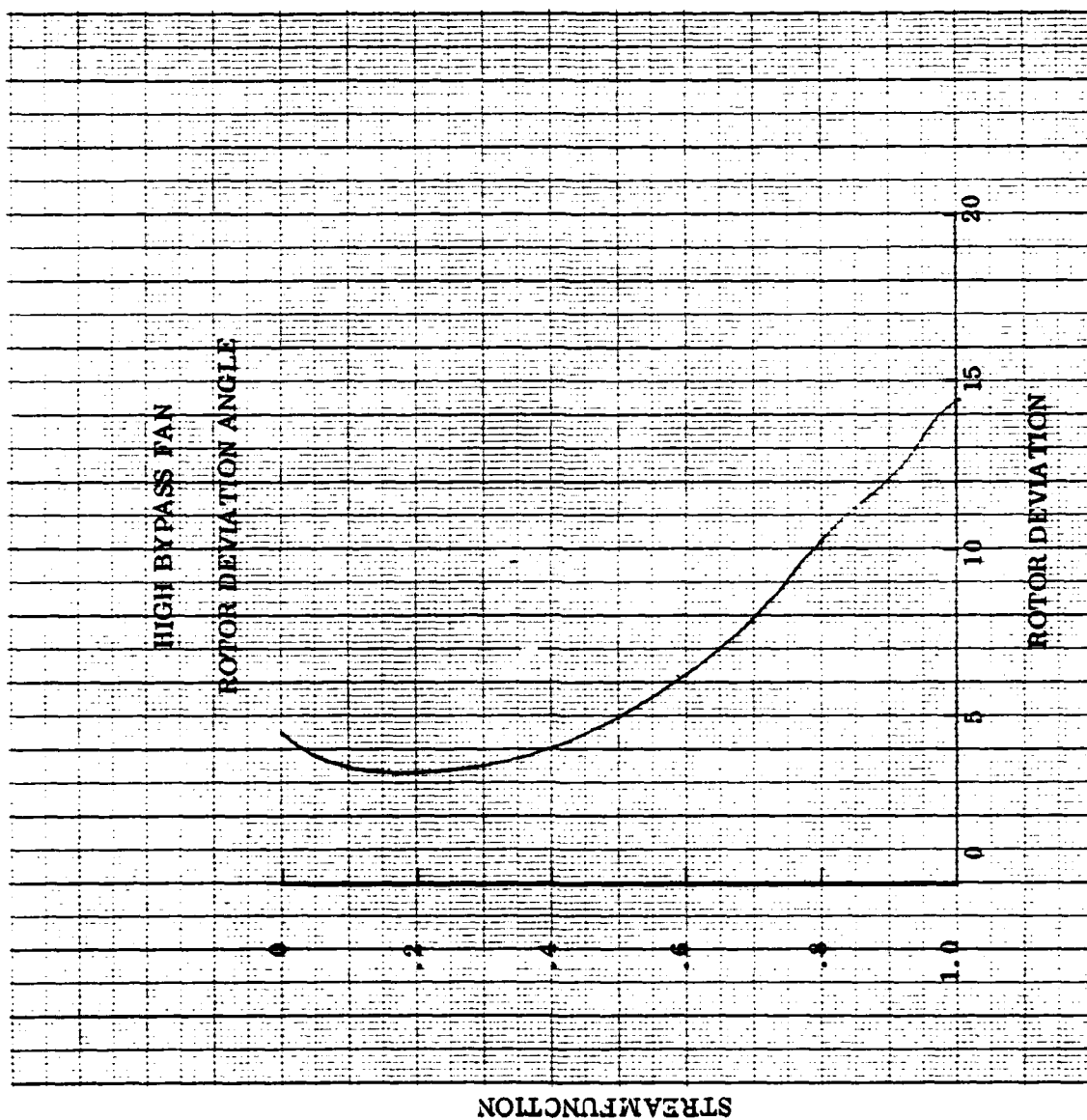


Figure 58. Rotor Deviation Angle Radial Distribution

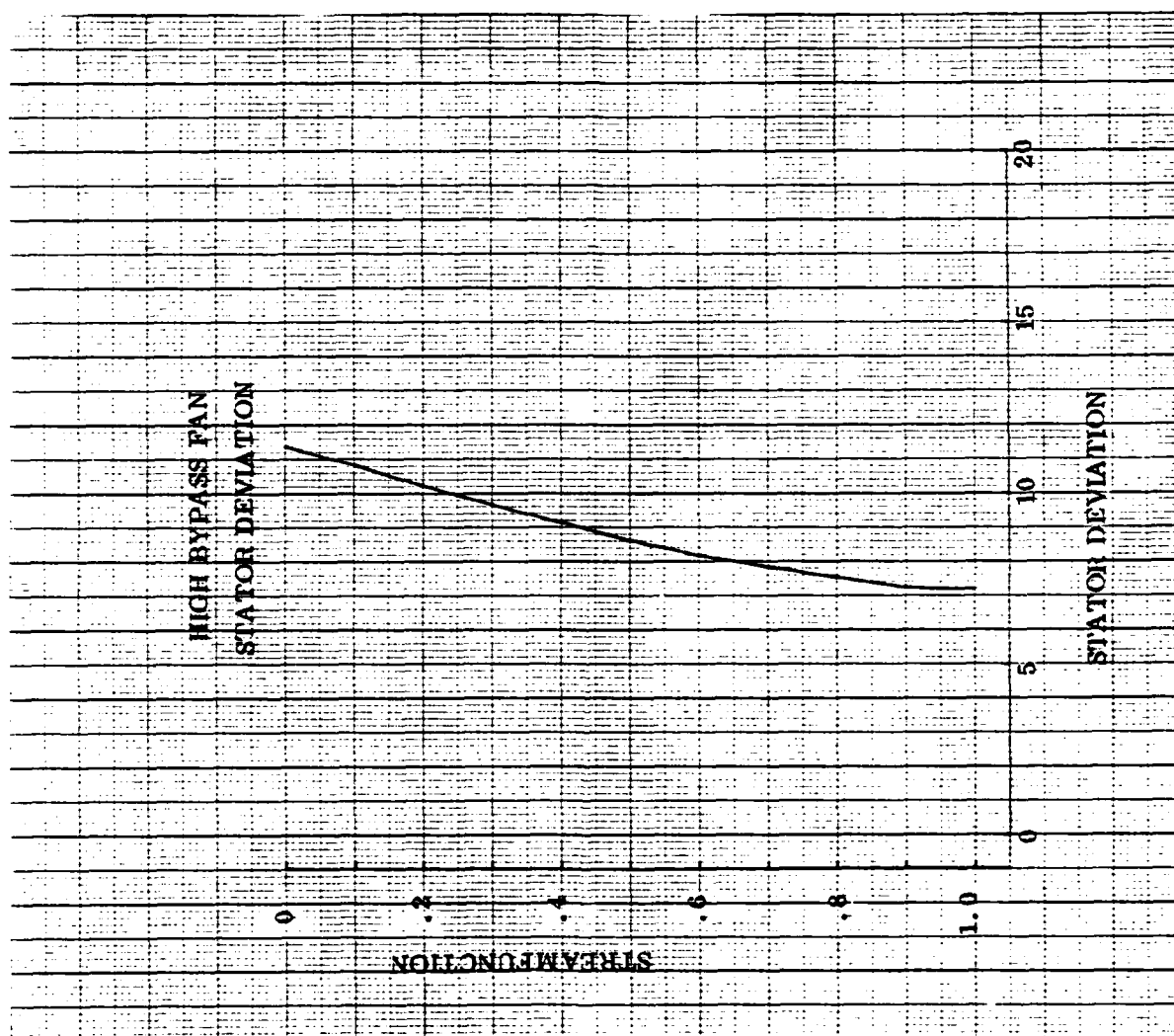


Figure 59. Stator Deviation Radial Distribution

HIGH BYPASS FAN ROTOR MEANLINE METAL ANGLES

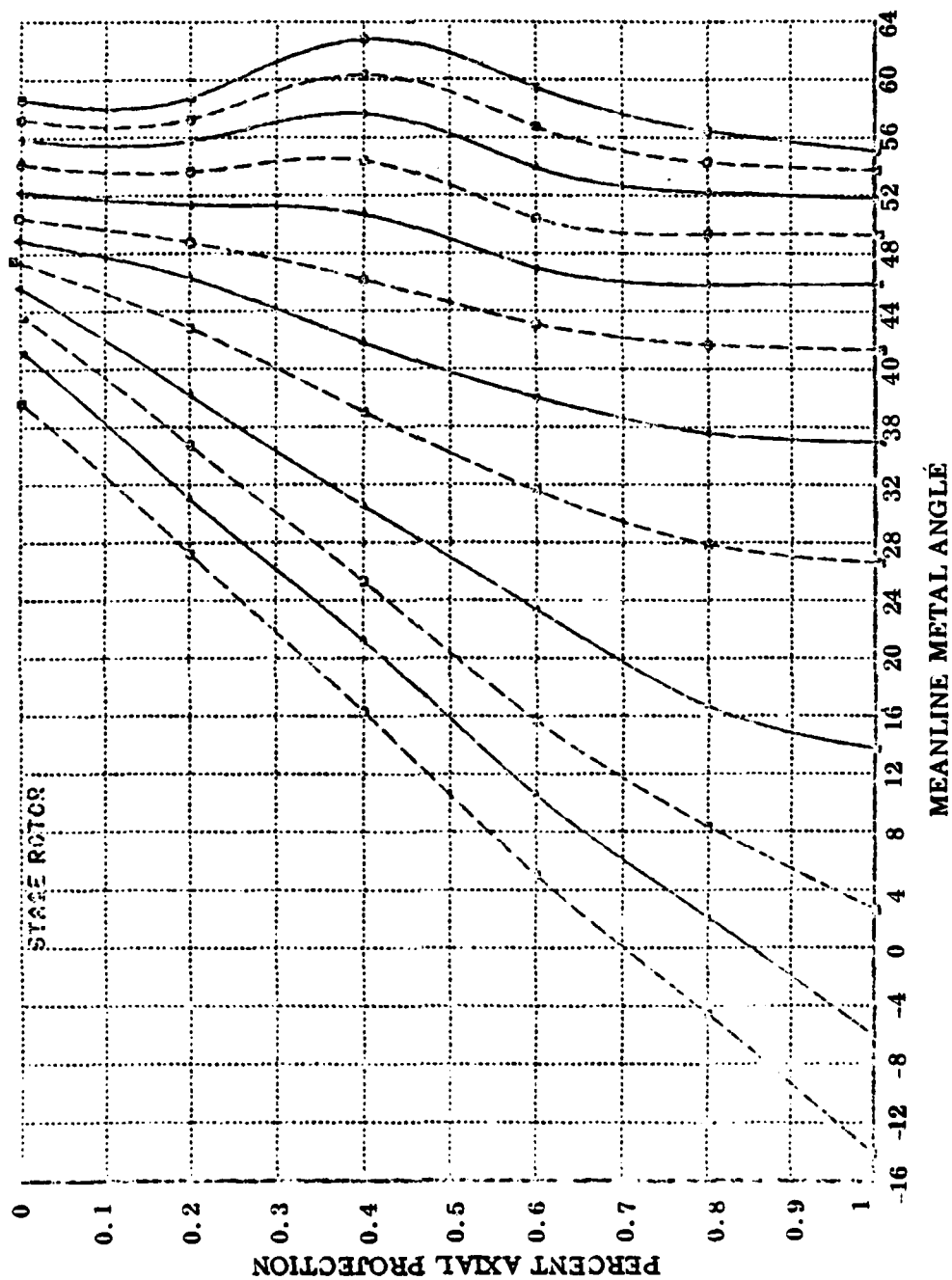


Figure 60. Meanline Metal Angles

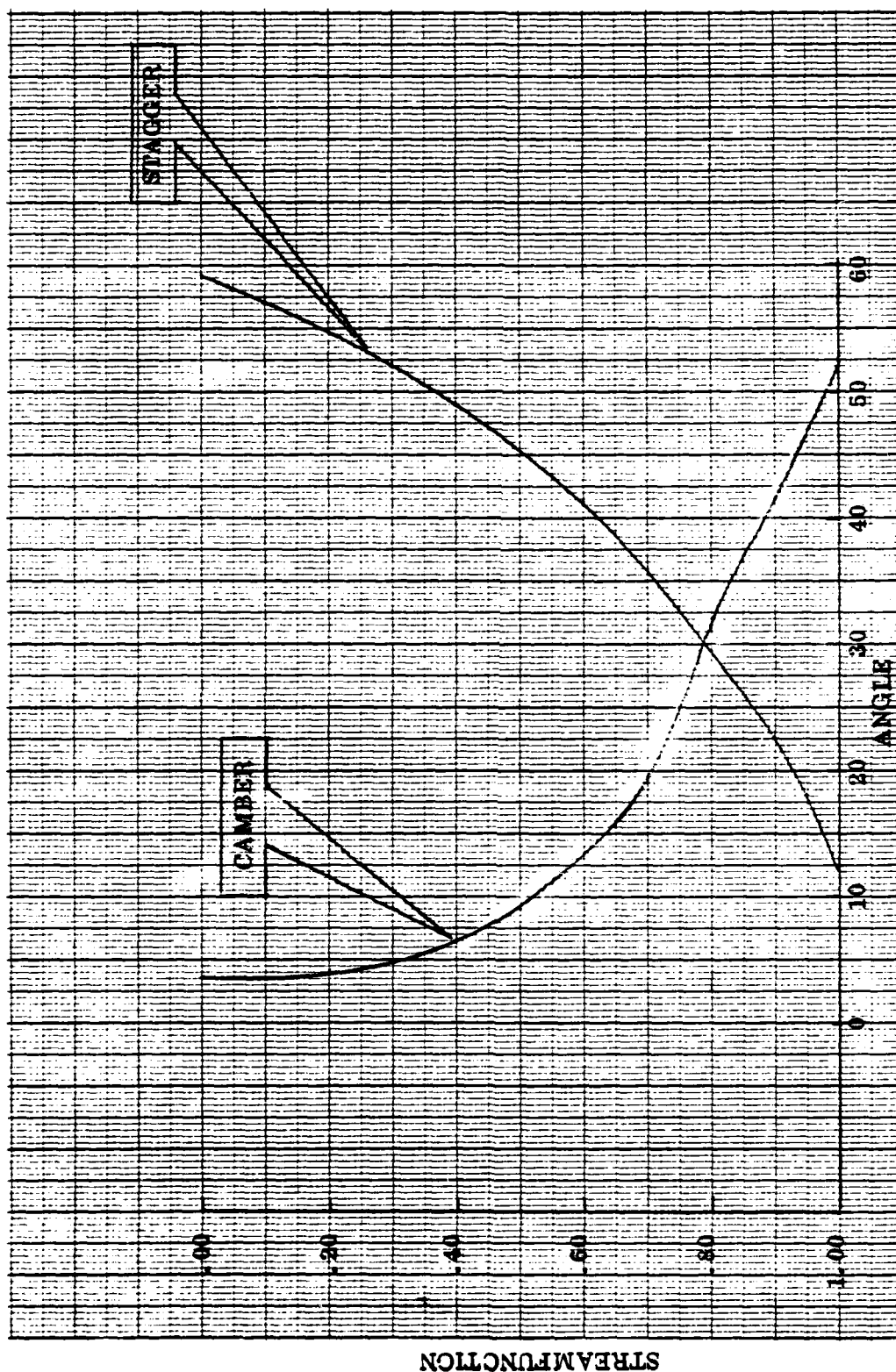
stagger are shown as a function of stream function in Figure 61. The streamline values of camber and stagger will differ from stagger and camber used for aeromechanical analysis and manufacturing which are defined on plane sections cut through the stacking axis. The rotor streamline blade-to-blade passage shapes are shown for tip pitch and hub in Figures 62, 63, and 64, respectively. The rotor blade passage area ratios are shown in Figure 65. The ratio AT/AI to that for normal shock at $M1$ indicates throat margin. The ratio AT/AM vs MM is blade passage internal contraction and indicates whether the shock structure can operate in the started mode. The ratio AT/AD vs MD indicates whether the blade will provide the desired work input. The rotor suction surface incidence angle is shown in Figure 66.

The stator meanline metal angles are shown as a function of percent axial projection for each streamline in Figure 67. Stator streamline camber and stagger are shown as a function of stream function in Figure 68. The stator tip streamline blade-to-blade passage shapes are shown to OD, pitch and ID in Figures 69, 70, and 71.

The vane passage throat to inlet area ratio is shown in Figure 72 as a function of inlet Mach No. and indicates throat margin.

HIGH BYPASS FAN

ROTOR STREAMLINE CAMBER AND STAGGER



GENERAL ELECTRIC COMPANY
AIRCRAFT ENGINE GROUP

Figure 61. Rotor Streamline Camber And Stagger Angles Distribution

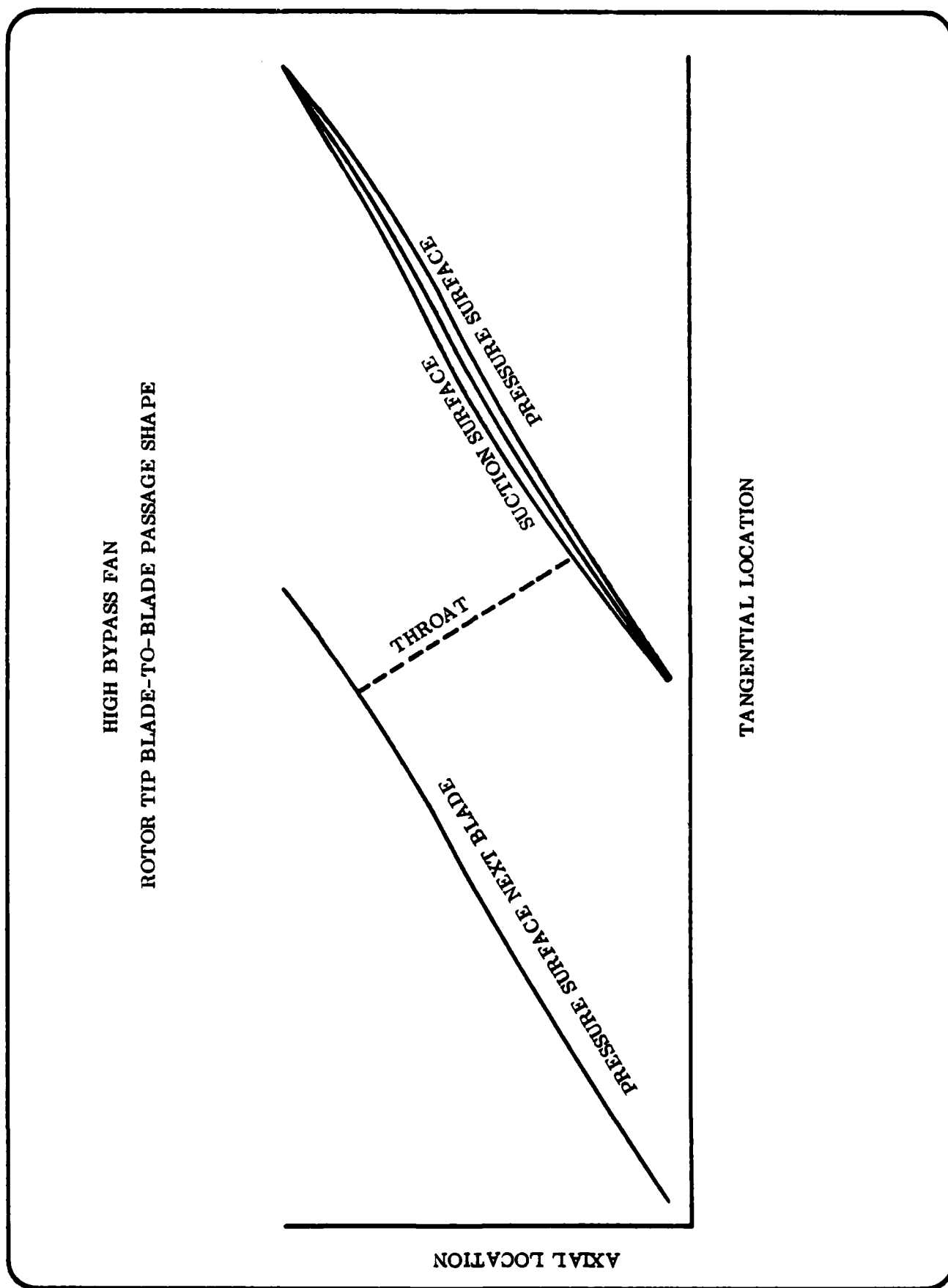


Figure 62. Rotor Tip Blade-to-Blade Passage Shape

HIGH BYPASS FAN
 ROTOR PITCH BLADE-TO-BLADE PASSAGE SHAPE

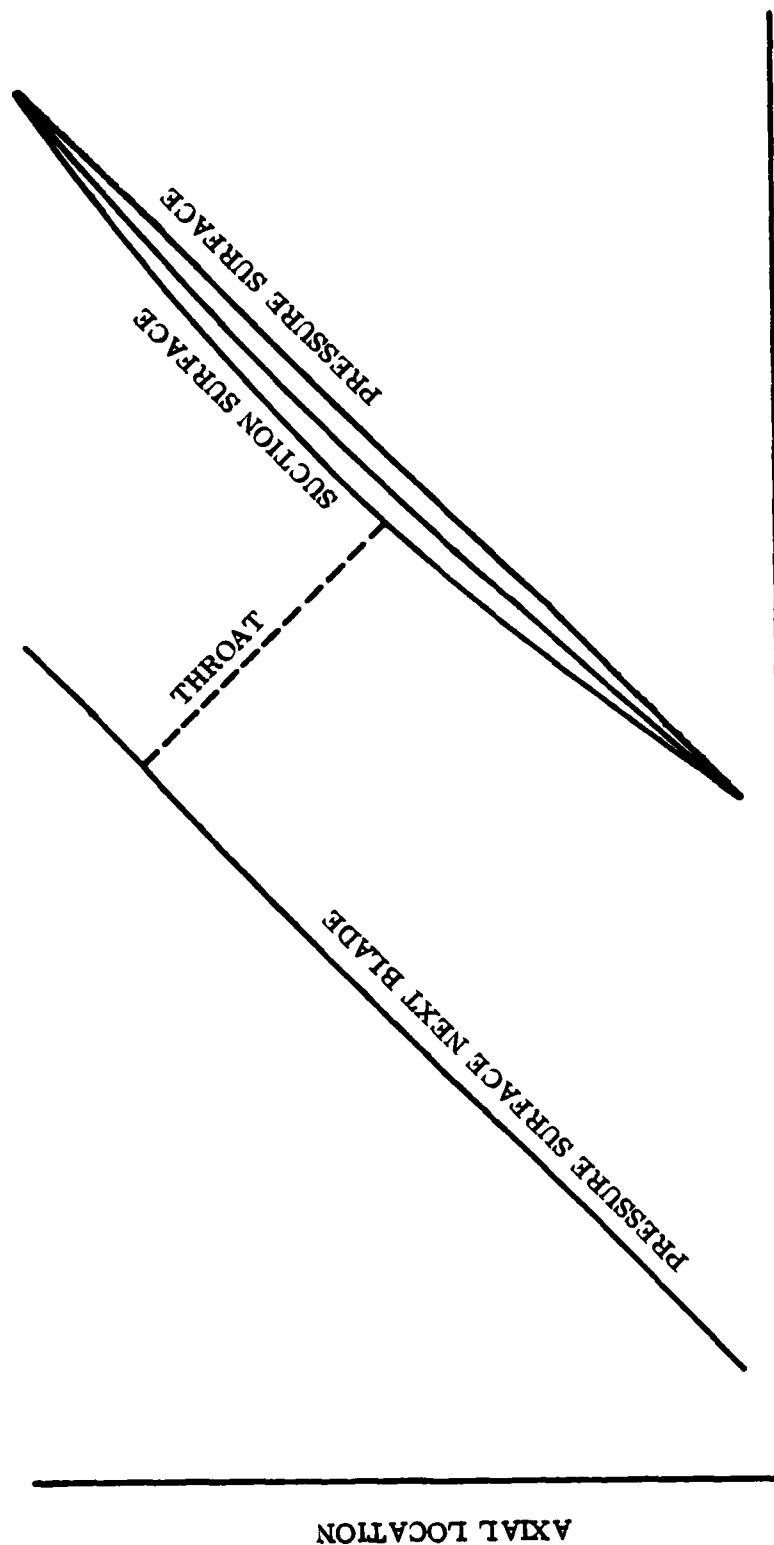


Figure 63. Rotor Pitch Blade-to-Blade Passage Shape

HIGH BYPASS FAN
ROTOR HUB BLADE-TO-BLADE PASSAGE SHAPE

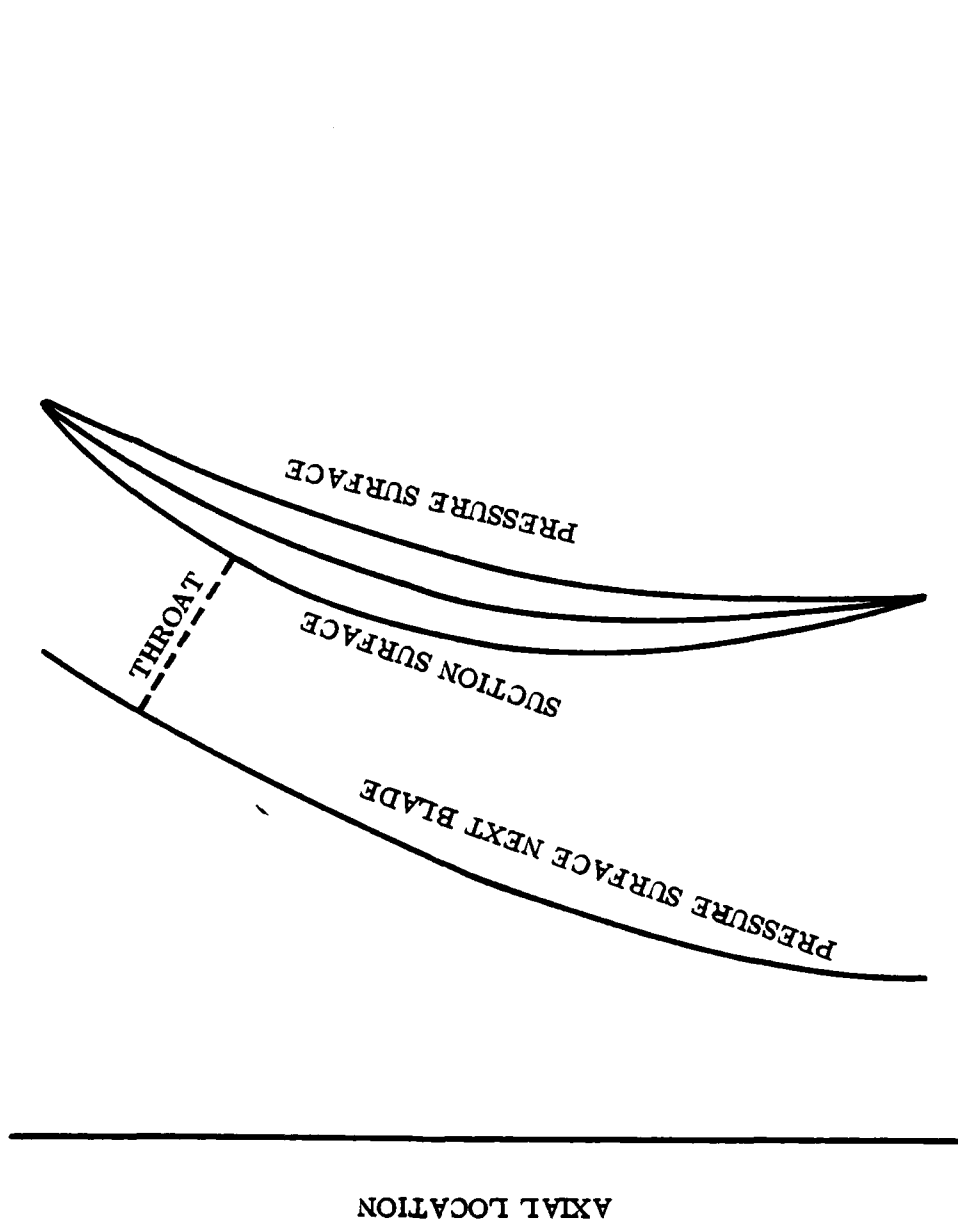


Figure 64. Rotor Hub Blade-to-Blade Passage Shape

HIGH BYPASS FAN ROTOR DESIGN PASSAGE AREA RATIO

THROAT TO CAPTURE AREA RATIO

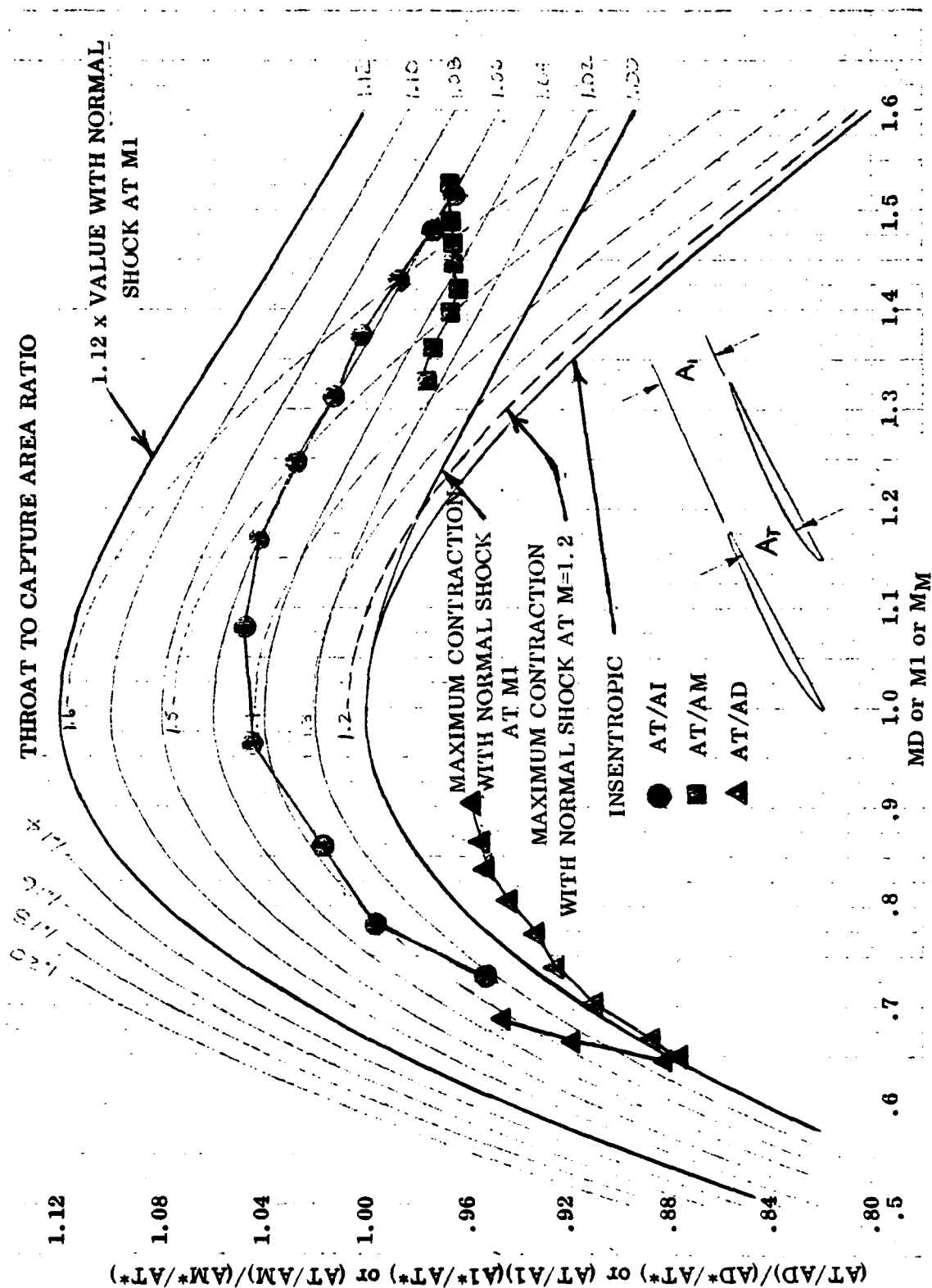


Figure 65. Rotor Blade Passage Area Ratios

GENERAL ELECTRIC COMPANY
AIRCRAFT ENGINE GROUP

HIGH BYPASS FAN

ROTOR SUCTION SURFACE INCIDENCE

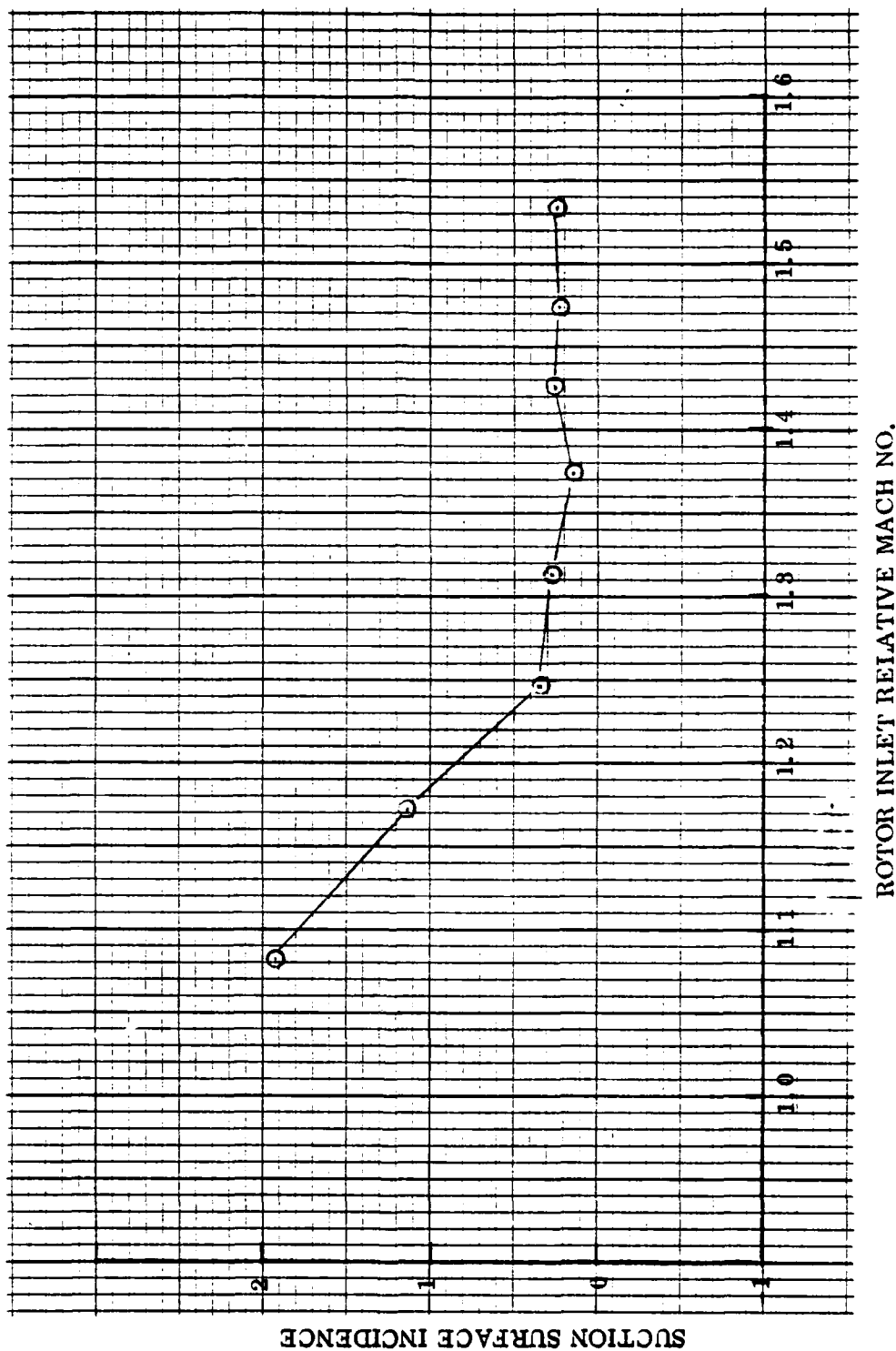


Figure 66. Rotor Suction Surface Incidence Angle

HIGH BYPASS FAN STATOR MEANLINE METAL ANGLES

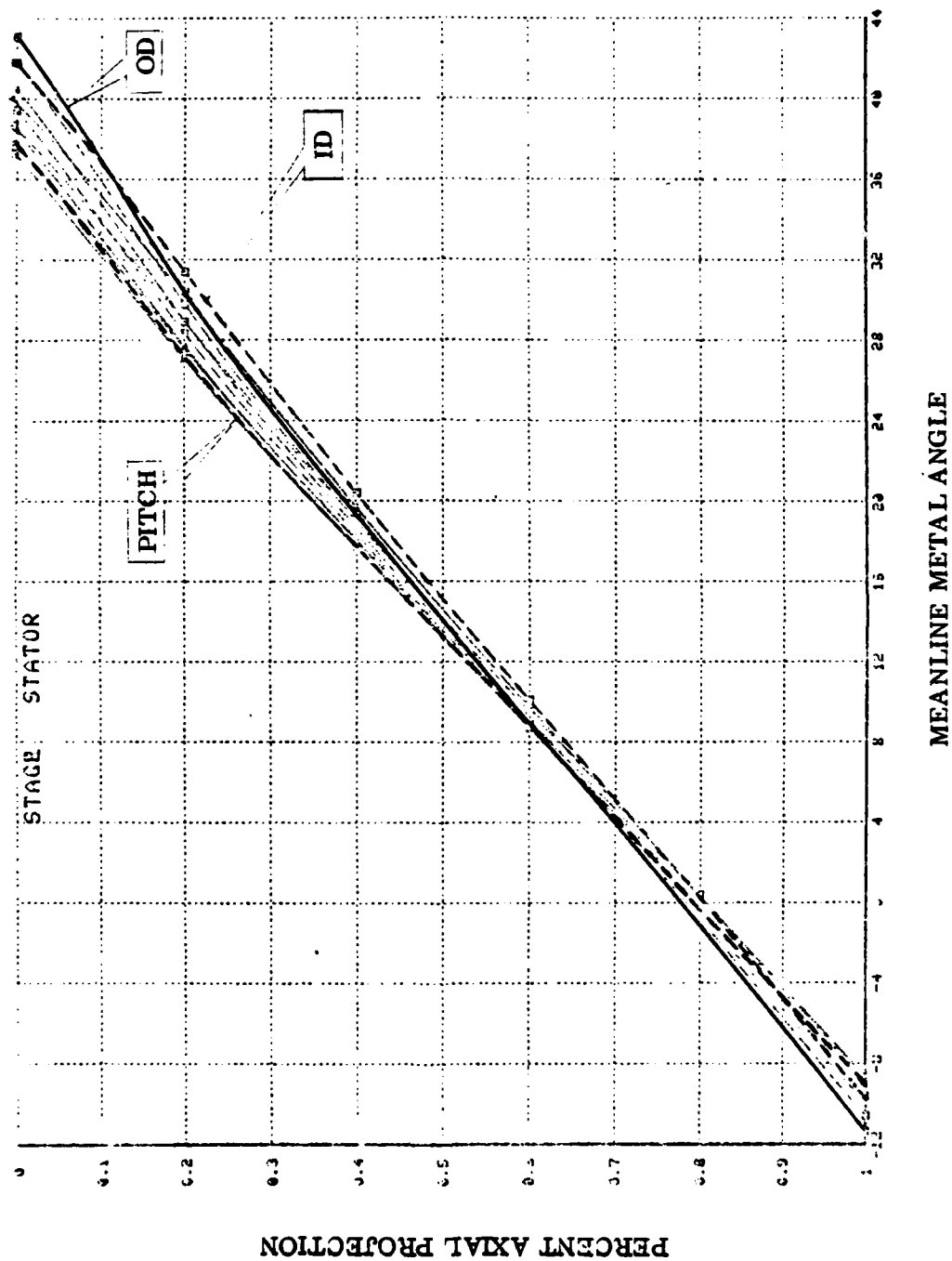


Figure 67. Stator Meanline Metal Angles

HIGH BYPASS FAN STATOR SCHEDULE CAMBER AND STAGGER

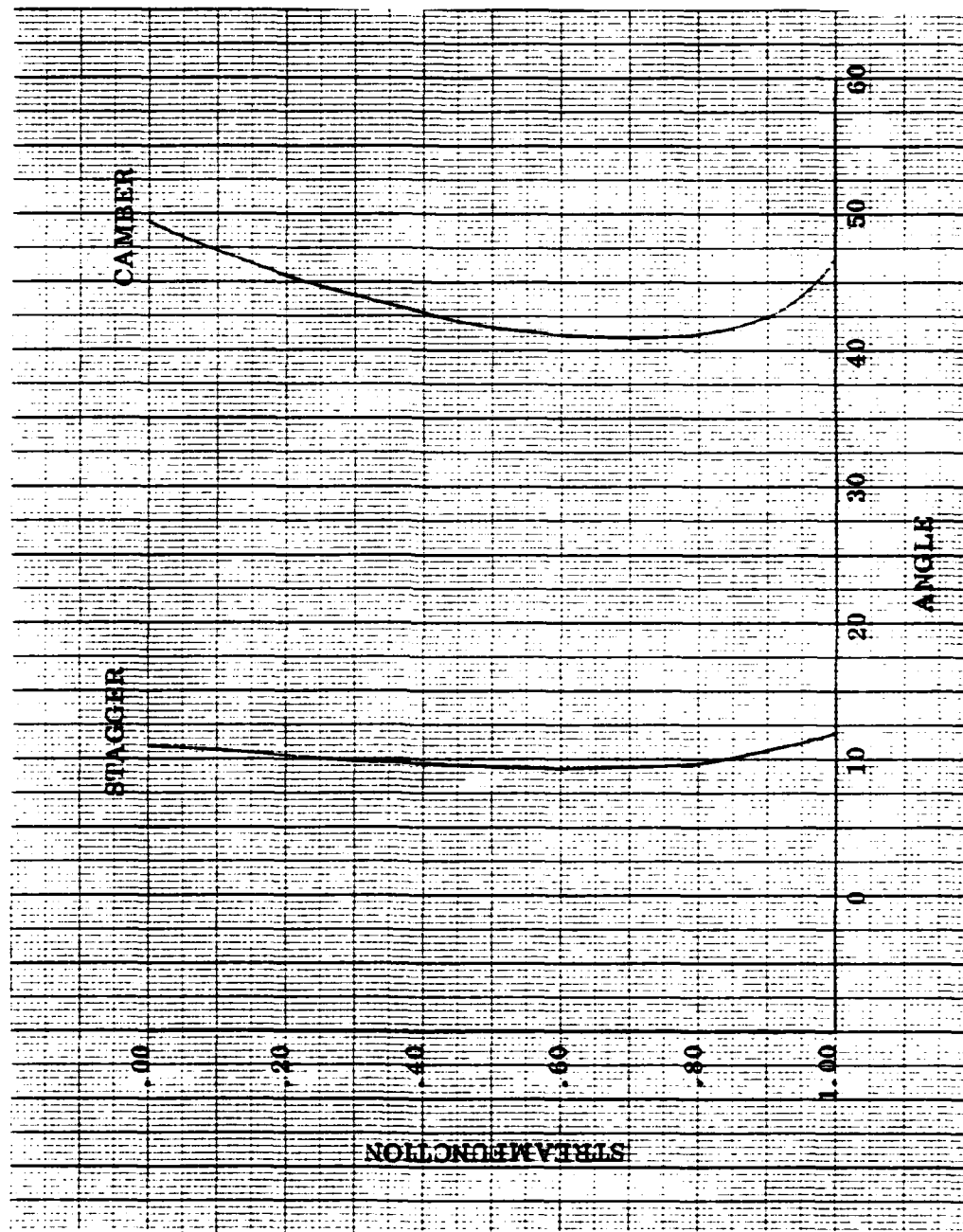
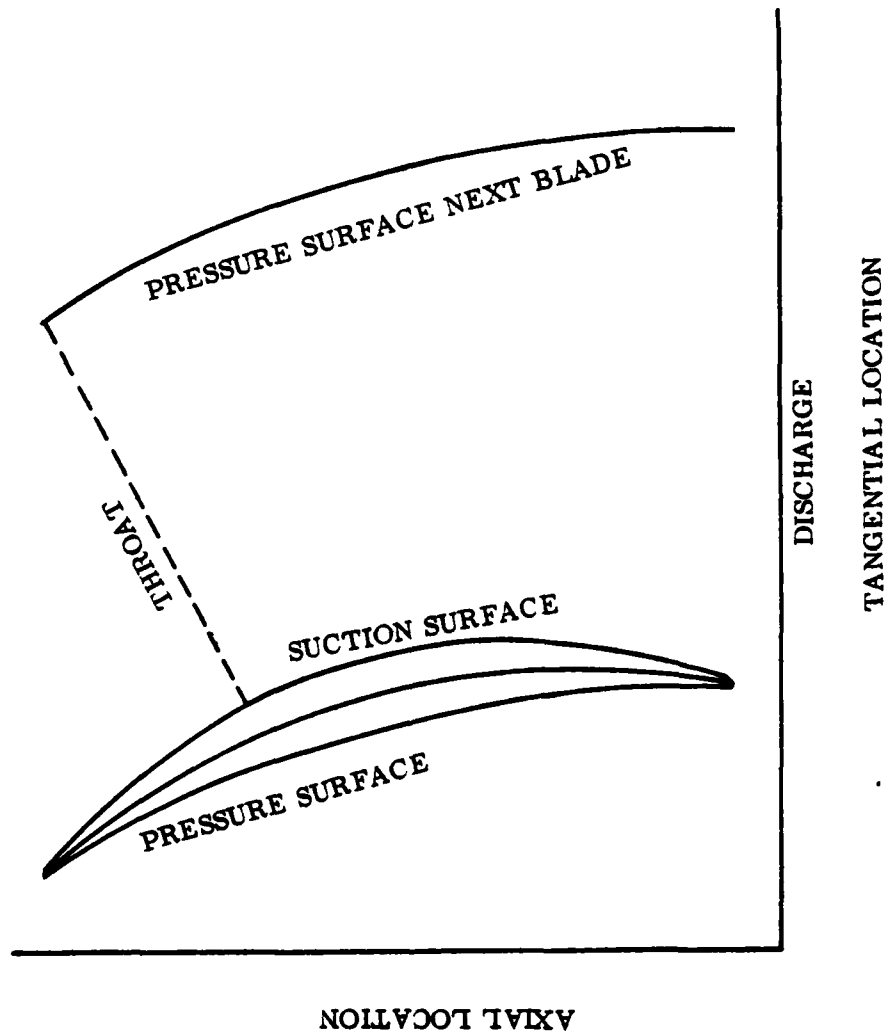


Figure 68. Stator Streamline Camber And Stagger Angles

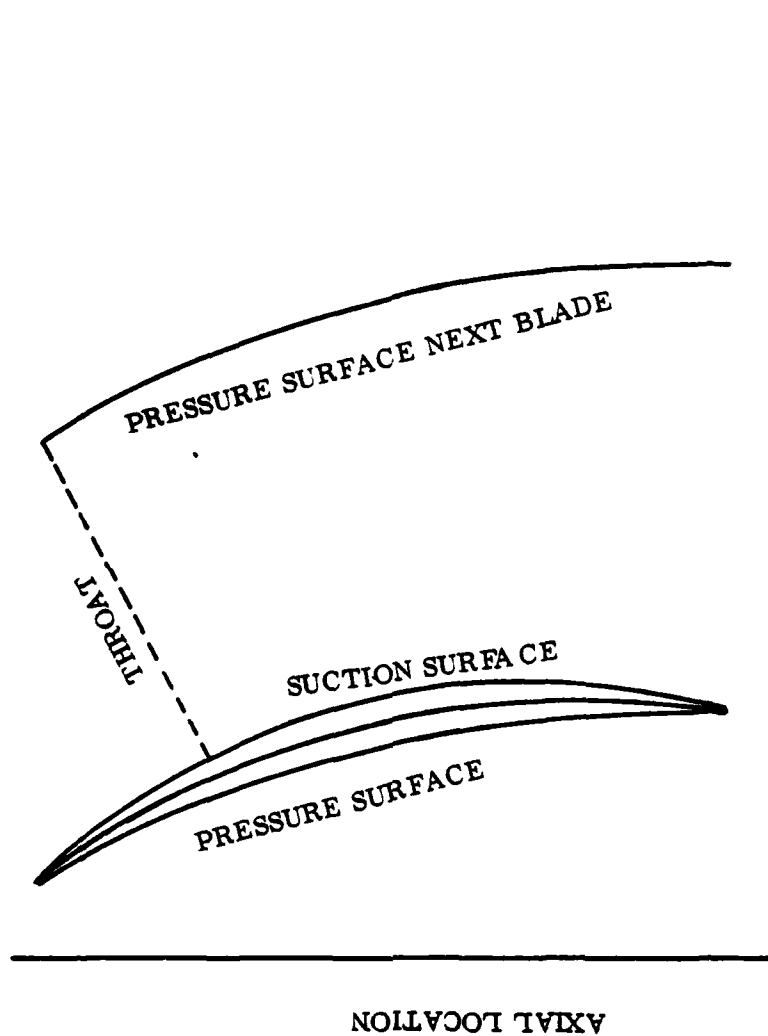
HIGH BYPASS FAN
STATOR OD BLADE-TO-BLADE PASSAGE SHAPE



GENERAL ELECTRIC COMPANY
AIRCRAFT ENGINE GROUP

Figure 69. Stator OD Blade-to-Blade Passage Shape

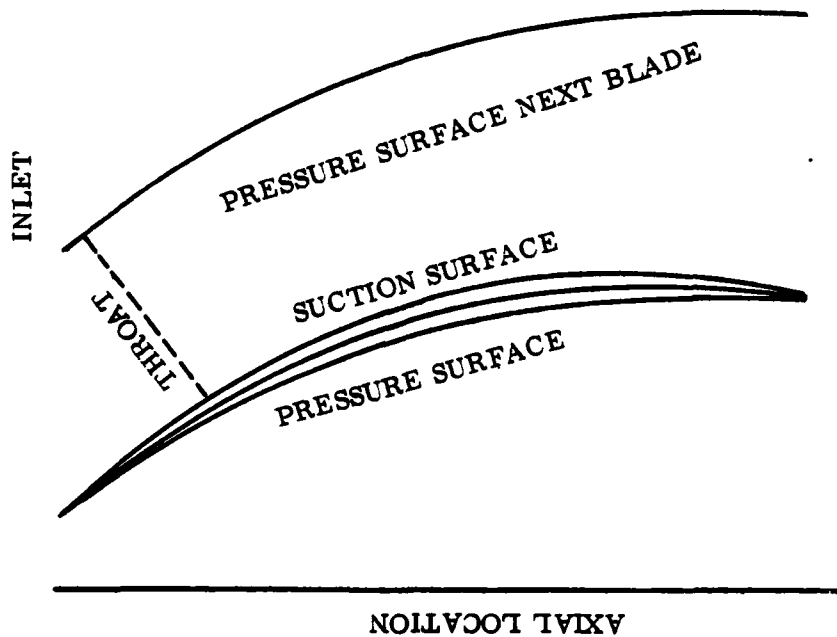
HIGH BYPASS FAN
STATOR PITCH BLADE-TO-BLADE PASSAGE SHAPE



TANGENTIAL LOCATION

Figure 70. Stator Pitch Blade-to-Blade Passage Shape

HIGH BYPASS FAN
STATOR ID BLADE-TO-BLADE PASSAGE SHAPE



TANGENTIAL LOCATION

Figure 71. Stator ID Blade-to-Blade Passage Shape

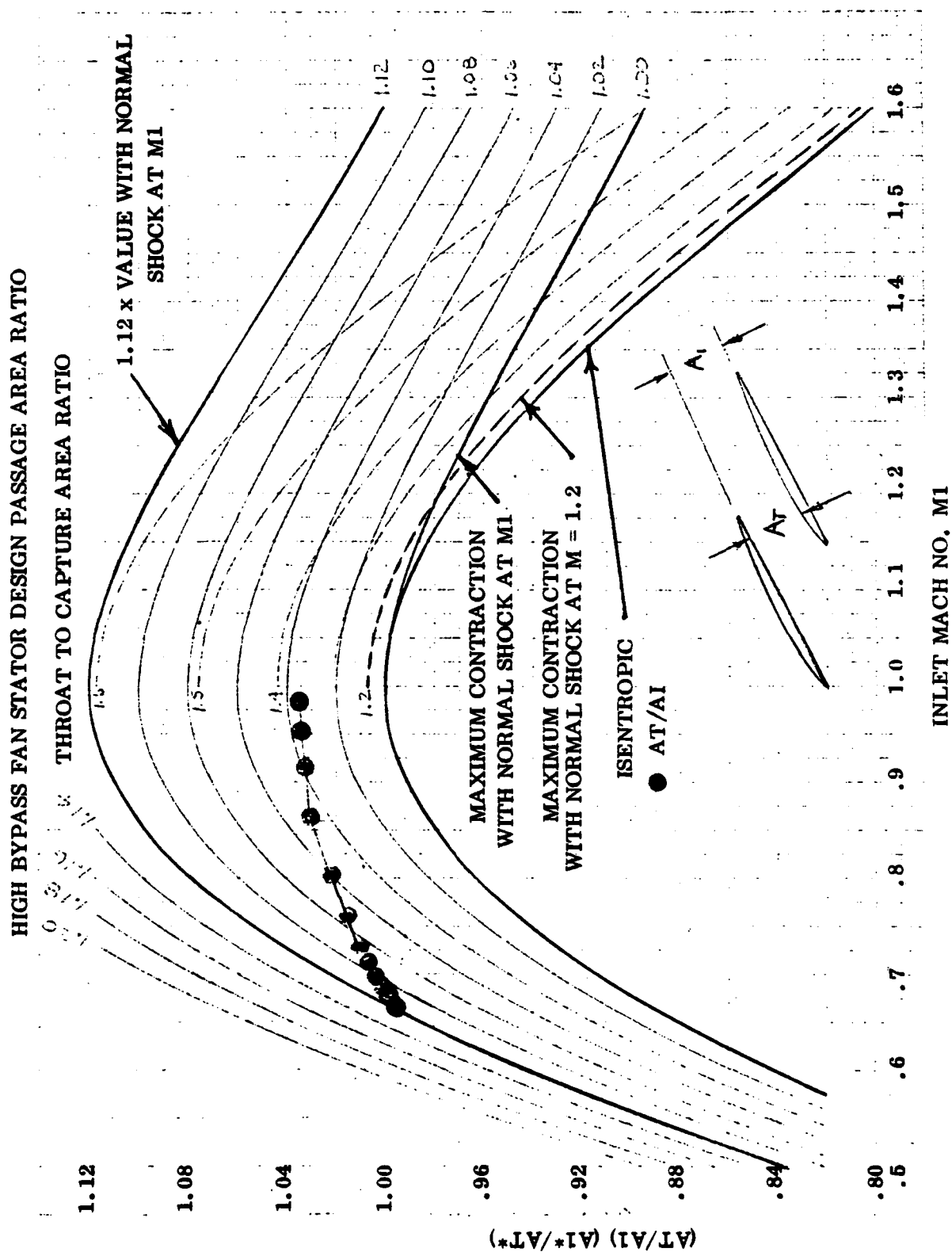


Figure 72. Stator Passage Throat to Inlet Area Ratio

3.4 FAN AEROMECHANICAL ANALYSIS

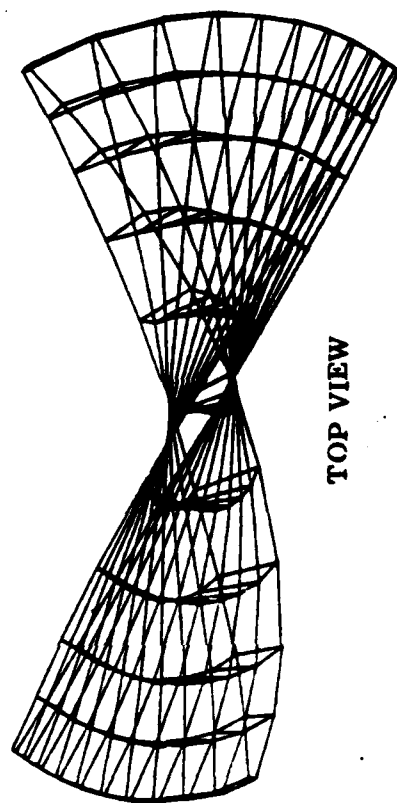
This subsection describes the detailed aeromechanical design-analysis procedure essential to provide a basis for the selection of a final fan design which simultaneously satisfies the prime aerodynamic (aeromechanical/mechanical) design objectives including MIL-E-5007D. The detailed analytical results and trade-offs involved in the selected final fan design are presented.

3.4.1 Fan Rotor Design Analysis

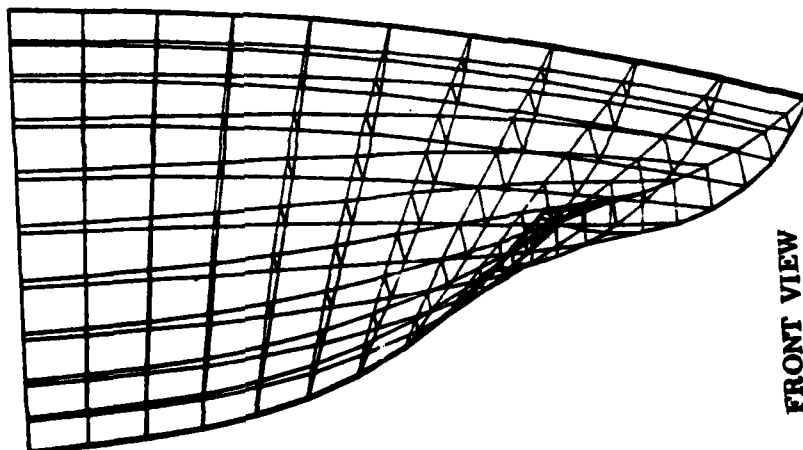
Having proceeded through the iteration/parametric cycle and arrived at a mutually satisfactory aerodynamic/aeromechanical/mechanical design, a detailed design analysis was conducted for the rotor airfoil. This analysis identified the stress, vibration, stability characteristics and the bird impact tolerance of the chosen airfoil design. It also determined the airfoil geometry modifications necessary to achieve the design objectives imposed upon the design. A description of the airfoil, in terms of pertinent aerodynamic parameters and geometry plots, is shown in Figure 73. The frequency, stability and stress characteristics are shown in Figures 74, 75, and 76, respectively. In addressing the FOD tolerance of a fan blade, a fundamental approach is to insure that the leading edge is close to or in compression due to centrifugal effects. This maximizes the ability of damaged edges to absorb stress risers and minimizes crack growth rates. Since tangential tilt can be incorporated to place the leading edge in compression, Figure 76 shows the implications of incorporating airfoil tilt. While the tangential tilt helps the leading edge, i. e., place more of the leading edge in compression, it increases the root convex stress to an undesirable level. For this reason, tilt was not considered to be an effective ingredient in the airfoil design.

Evaluation of the airfoil design for bird impact tolerance, Figure 77, suggests that ingestion of a 4 oz. bird impacting the blade tip area at takeoff conditions satisfies the design intent. Specifically, the bird impact would be expected to develop shear stress levels (τ_{max}) no greater than the material shear strength capability (τ_{crit}). This suggests the avoidance of having airfoil fragments punched out of the airfoil. As the engine is throttled back or the bird speed is increased, (cruise type flight conditions) the bird impact problem becomes less severe as shown by the lower developed shear stress levels. Since a 4 oz. bird is expected to reside over 40% of the blade span, placing the bird centroid at 80% span implies that the bird footprint extends radially from the blade tip to 60% blade height - thus, the notation of bird impact at 80% span for the 4 oz. bird fragmentation problem. Also noted is the number of blades (as a percentage of 20) expected to be impacted. The significance here is that a great many blades could undergo severe damage/deformation. For a given size engine, as the bird weight is increased, the impact problem shifts from one of preventing loss of airfoil fragments to one of avoiding loss of entire airfoils. For the GE26/F4 design, this is the situation when addressing ingestion of 2 lb. vs. 4 oz. bird sizes. Because the 2 lb. bird is expected to reside

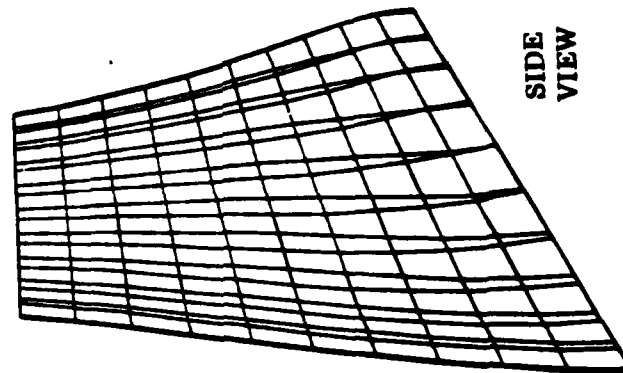
GE26/F4 FAN ROTOR 3-D FINITE ELEMENT MODEL



TOP VIEW



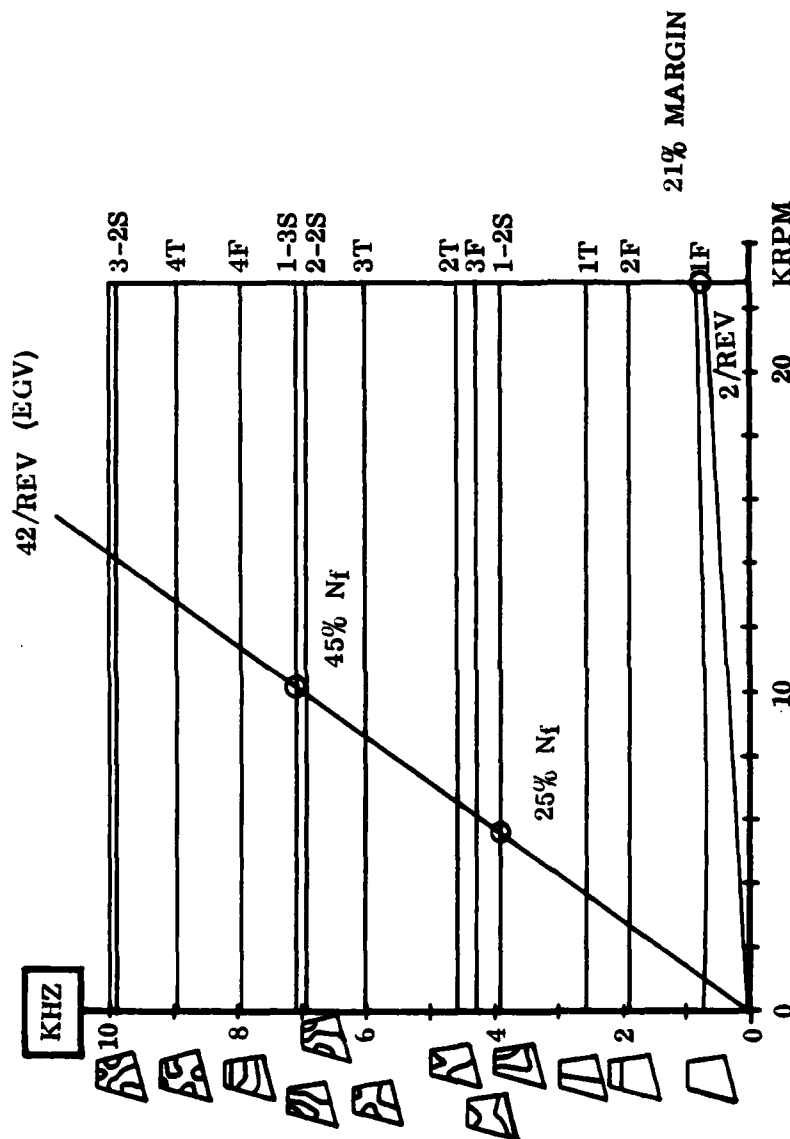
FRONT VIEW



SIDE VIEW

Number of Blades	20
$W/\bar{\rho} / \mathcal{L}$ (pps)	41.6
W/A (Annulus) (pps/ft ²)	41.5
P/P (Hub/Tip)	1.8/1.75
Tip MREL	1.53
Tip Speed, U _T (fps)	1440
Tip Diameter (in.) avg.	14.5
Inlet Radius Ratio	.360
Avg. Radius Ratio	.46
Root Aspect Ratio	1.43
Solidity:	1.36
Tip	2.65
Hub	.030
Tm/c:	.093
Tip	
Hub	

FAN ROTOR CAMPBELL DIAGRAM



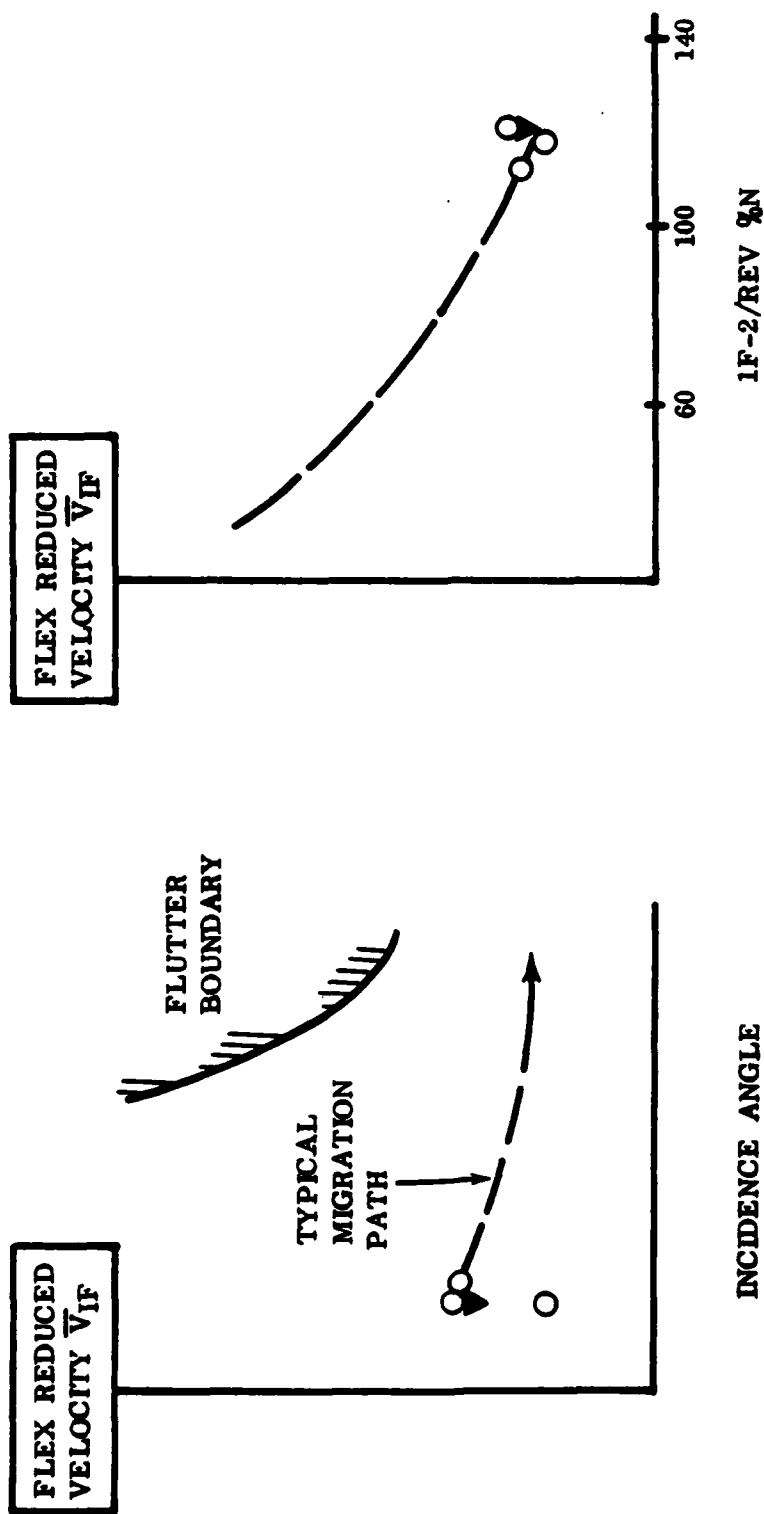
SIGNIFICANCE

DESIGN OBJECTIVES MET:

- 21% 2/REV IF MARGIN
- 1-2S 42/REV AT 25% N_f
- 1-3S 42/REV AT 45% N_f

Figure 74. Rotor Airfoil Frequency Characteristics

INTERDEPENDENCY OF 1F-2/REV MARGIN AND STABILITY PARAMETER



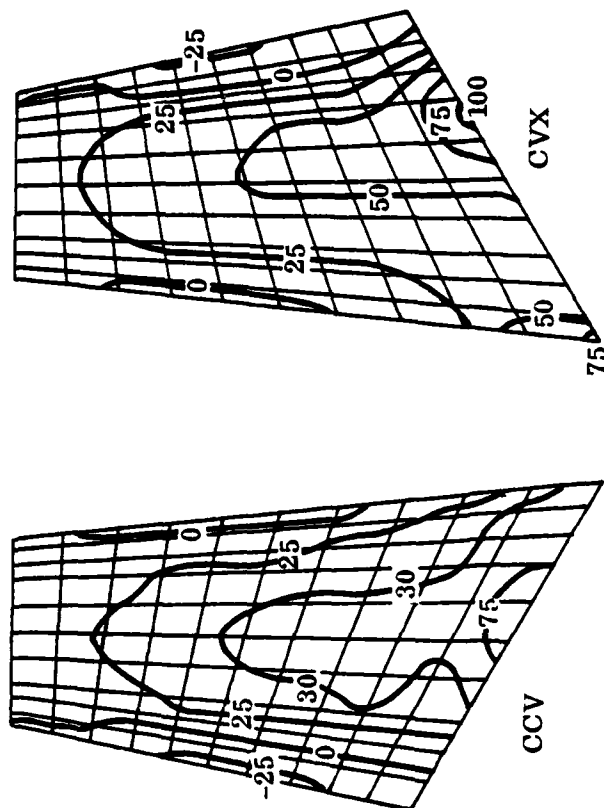
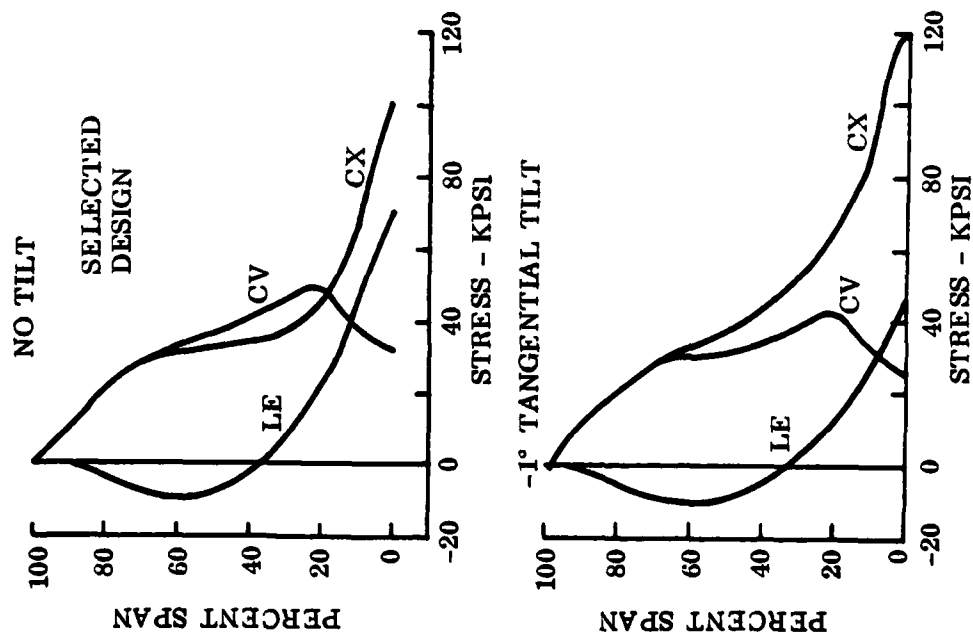
SIGNIFICANCE:

- OTHER SUCCESSFUL ENGINES
- ▼ GE26/F4
- GE26/F4 FAN DESIGN MEETS 1F-2/REV AND STABILITY CRITERIA OBJECTIVES.
- OBJECTIVES BASED ON SUCCESSFUL PREVIOUS ADVANCED FAN BLADE DESIGNS

Figure 75. Rotor Airfoil Stability Margin

GENERAL ELECTRIC COMPANY
AIRCRAFT ENGINE GROUP

GE26/F4 FAN, ROTOR AIRFOIL STRESS



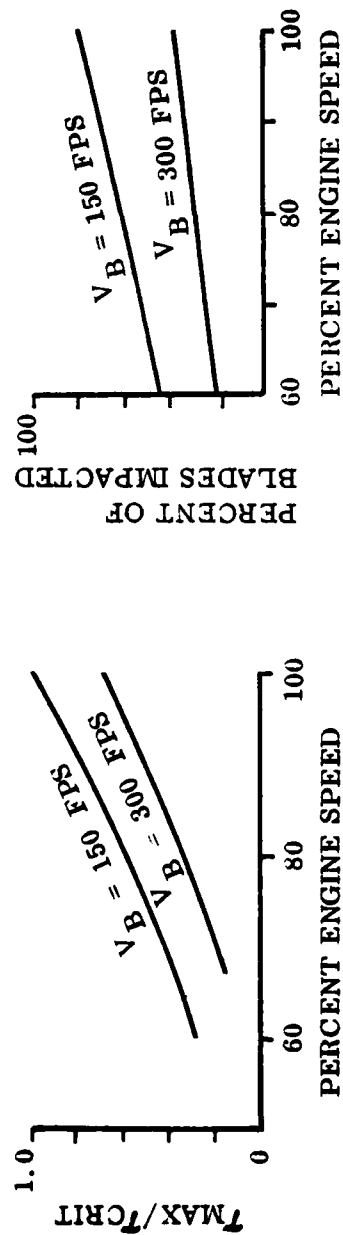
- Design for balanced stress: for F. O. D. resistance, leading edge compressive stress desirable.
- Steady state stress levels consistent with production engine experience.

Figure 76. Rotor Airfoil Stress Characteristics

BIRD INGESTION CAPABILITY/EVALUATION

FRAGMENTATION

- AIRFOIL AS DESIGNED MEETS FRAGMENTATION REQUIREMENTS
... 4 OZ IMPACT @ 80% SPAN



FRACTURE

- AIRFOIL AS DESIGNED MEETS FRACTURE REQUIREMENTS
... 2 LB IMPACT AT 60% SPAN

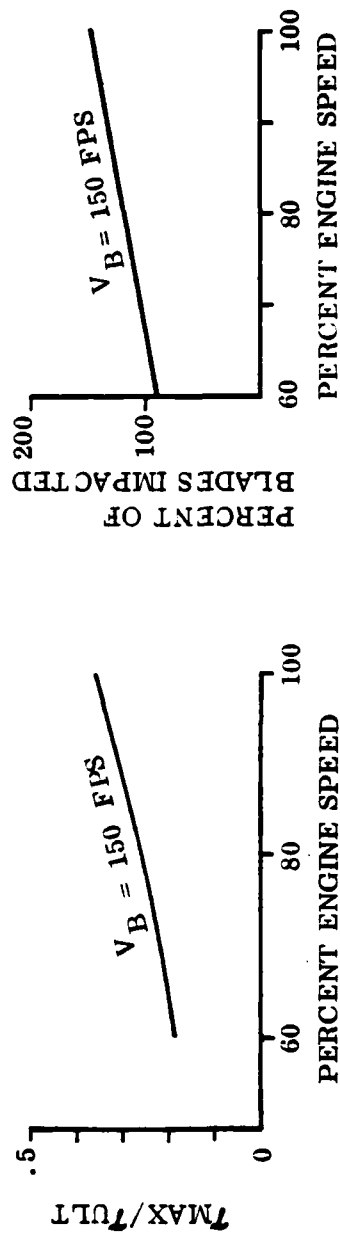


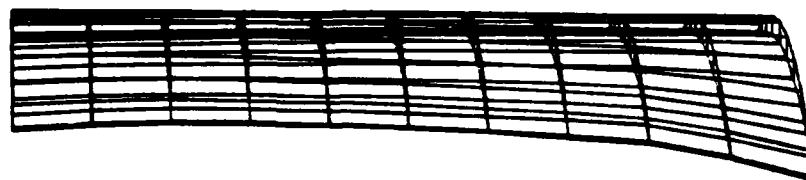
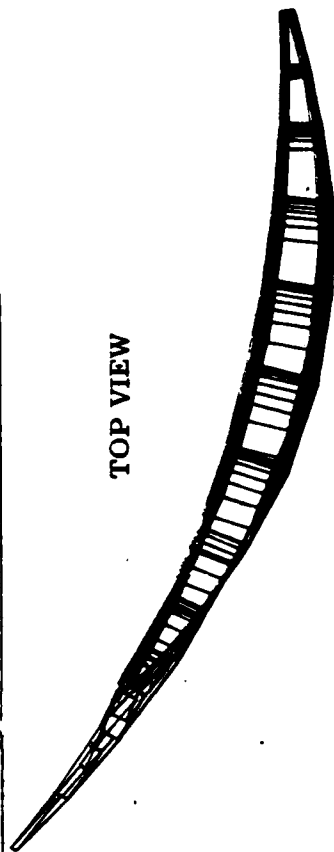
Figure 77. Rotor Airfoil Bird Impact Tolerance Capability

over 80% of the blade span, this suggests a fracture (loss of entire airfoil) rather than a fragmentation problem. As such, Figure 77 also presents the results of the fracture analysis suggesting that the developed shear stress (τ_{\max}) remains lower than that needed for fracture (τ_{ult}). Once again, the concern is the number of blades impacted with some blades undergoing multiple hits from the same bird, i.e., it takes more than one wheel revolution to ingest the whole bird. The large number of blades impacted combined with the relatively large footprint size raises the spectre of very severe airfoil damage/deformation. The fan blades may remain intact but be incapable of sustaining very much of a flow pumping capability. The rationale then for designing small engines for ingestion tolerance to large birds may be counter-productive - that is, severe weight/performance penalties are required to contain fan airfoil damage to a level where reasonable post strike flow pumping capabilities exist. Even then, experimental data would be the key ingredient since the analytical evaluation procedure would be questionable at best.

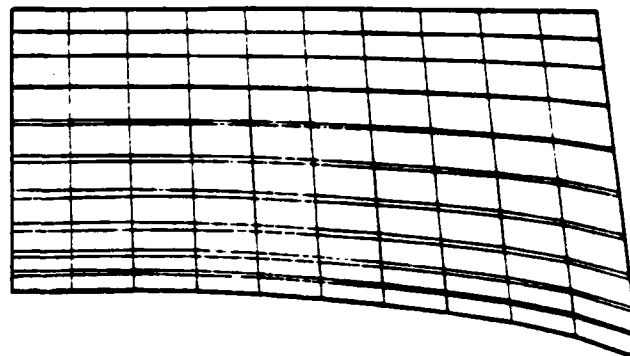
3.4.2 Fan Stator Design Analysis

The main ingredient in the design evolution of the fan stator is the avoidance of forced vibration problems through frequency/stimulus control. As such, fewer iterations are required to identify a mutually satisfactory design. A description of the vane airfoil in terms of pertinent aerodynamic parameters and geometry plots is shown in Figure 78 with the resulting frequency characteristics shown in Figure 79. The design objective for the selected vane configuration is to avoid fundamental mode resonances excited by the rotor passing frequency (20/rev) in the high engine speed region, and to insure that the fundamental bending and torsion modes are uncoupled. The uncoupling of the modes indicated will be done by insuring that the mechanical construction of the vane attachment has sufficient foundation flexibility so as to suppress the airfoil bending mode frequency while at the same time, rendering the torsion mode frequency unaltered. Design of the vane attachment scheme is still underway, but no problems are expected.

GE26/F4 FANSTATOR 3-D FINITE ELEMENT MODEL

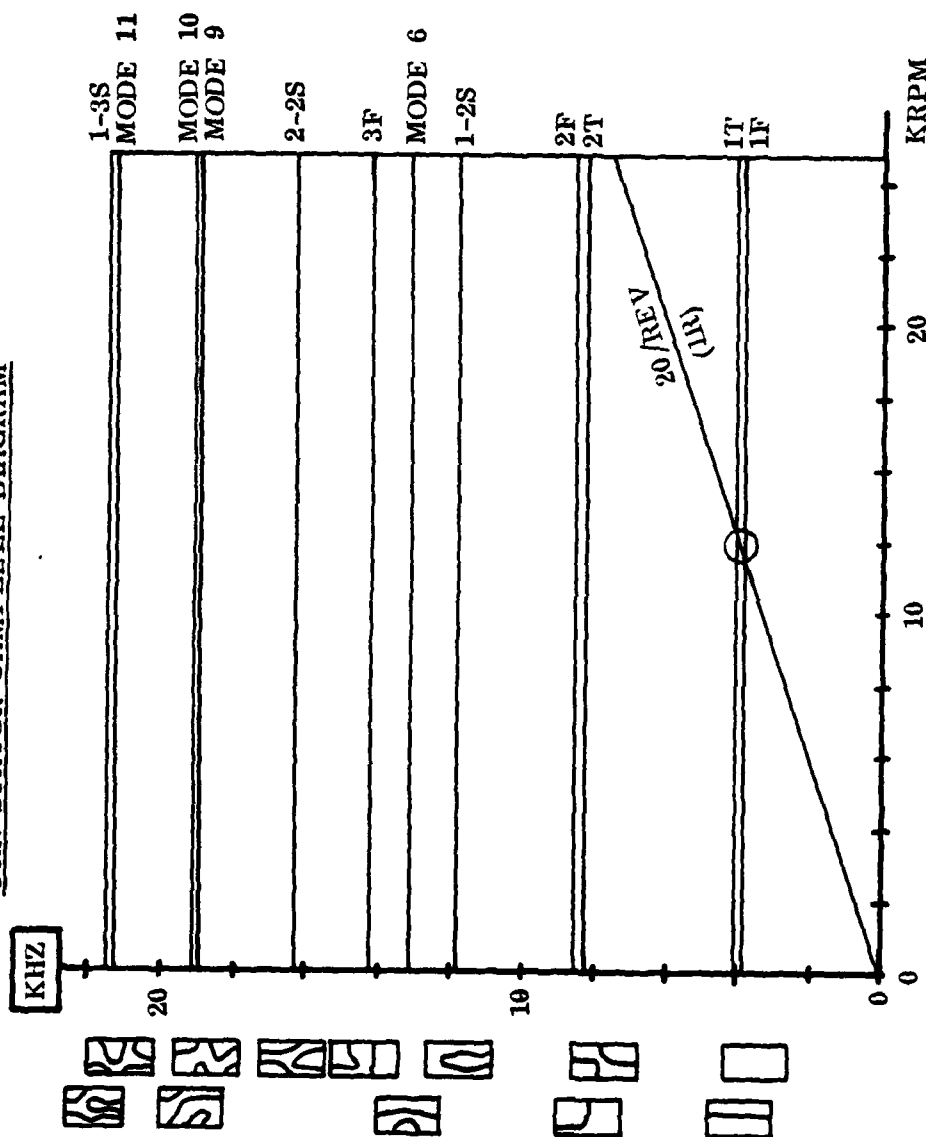


NUMBER OF VANES	42
INLET RADIUS RATIO	.59
AVERAGE RADIUS RATIO	.62
PITCH ASPECT RATIO	1.93
SOLIDITY - OD	1.29
- ID	2.50
TM/C - OD	.099
- ID	.046
CHORD - OD	1.40
- ID	1.69
MATERIAL	A286



ATTACHMENT FIXED OD / ID SIDE VIEW

FAN STATOR CAMPBELL DIAGRAM



SIGNIFICANCE

- FURTHER ITERATION NECESSARY:
- x SEPARATE 1F/1T MODE FREQUENCIES

Figure 79. Stator Airfoil Frequency Characteristics

GENERAL ELECTRIC COMPANY
AIRCRAFT ENGINE GROUP

3.5 FAN MECHANICAL DETAIL DESIGN

3.5.1 Fan Blisk Overall Design

A full scale cross section of the high bypass turbofan blisk is shown in Figure 80. The disk design takes advantage of the fact that absence of blade dovetails allows the blisk rim to carry substantial circumferential stresses. Thus the disk bore diameter could be increased significantly resulting in a lightweight design.

Torque transfer from the drive shaft into the blisk occurs via a bolted flange using ten 1/4" high strength hook bolts.

The blisk was designed to represent flight type hardware. The requirement of instrumentation lead routing in the component vehicle dictates a slightly different aft flange configuration. However the flange can be reworked to update the demonstrator fan blisk into a flight type engine part. Figure 81 shows the similarity between demonstrator and flight type designs. Detail blisk drawing number 17A138-297 has been issued for procurement purposes in Phase III.

3.5.2 Fan Blisk and Spinner Stress Levels

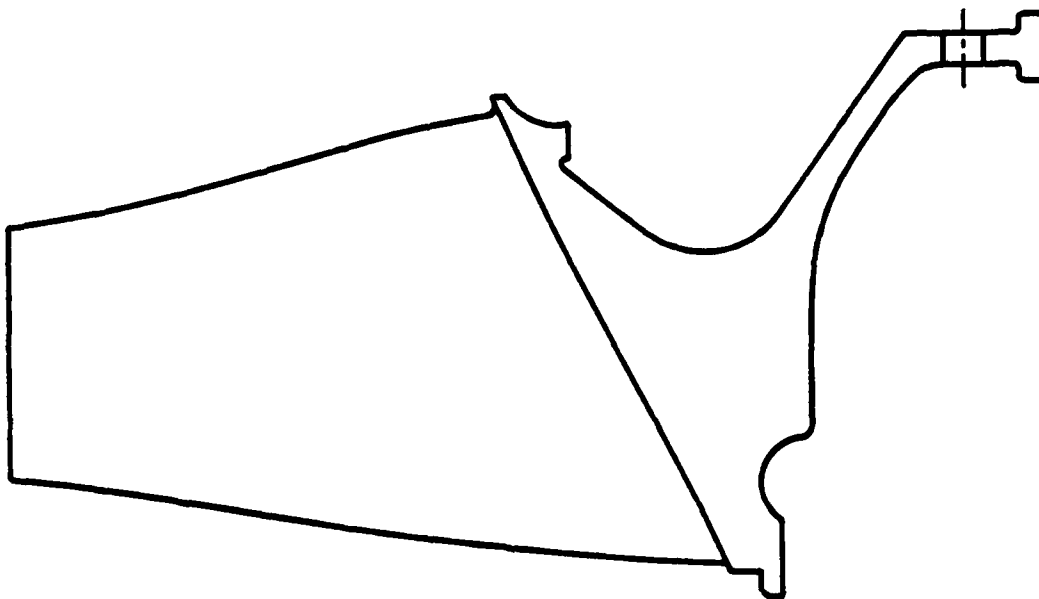
The high bypass turbofan blisk stress analysis was performed using the following guidelines:

- o Rim load distribution non uniform in axial direction. Load distribution from aeromechanical design calculations uprated to 103% NG.
- o Blisk in combination with spinner modeled for finite element stress analysis. Boundary condition in zero axial movement at rear bolt circle.
- o Large bore radius chosen to load up rim and thus to keep weight down. Design is not limited by bore stresses but by overspeed requirements.
- o Blisk/spinner fit was chosen such that interference increases with increasing speed.

The results of the stress analysis are summarized in Figure 82. Conclusions are:

- o Stresses are well within the capabilities of the chosen material (see Para. 3.5.3).
- o Interference fit at blisk/spinner interface plus loads introduced into the spinner result in acceptable stresses in the spinner.

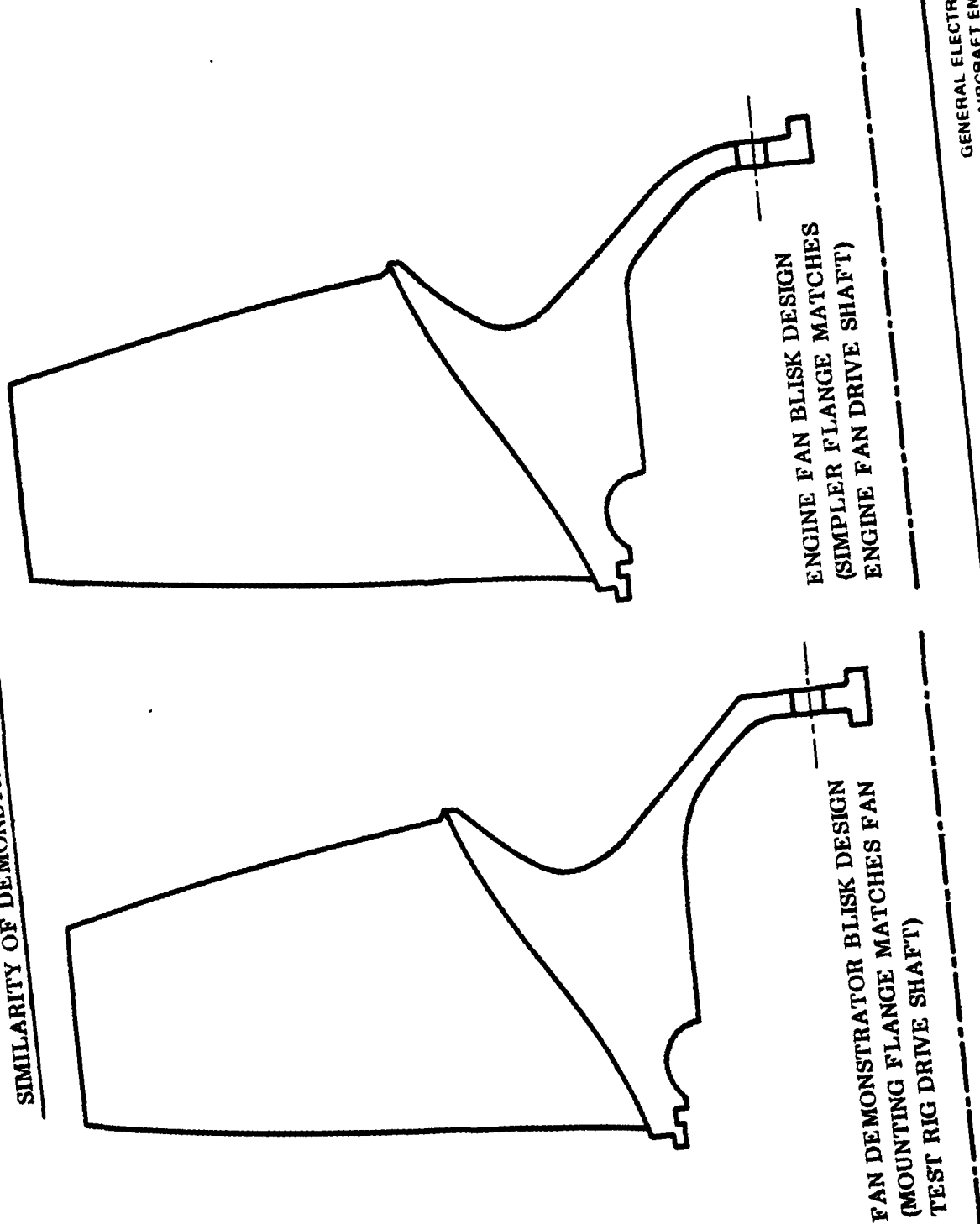
HIGH BYPASS TURBOFAN BLISK DESIGN
FULL SCALE CROSS SECTION



GENERAL ELECTRIC COMPANY
AIRCRAFT ENGINE GROUP

Figure 80. Fan Blisk Full Scale Cross Section

SIMILARITY OF DEMONSTRATOR VS. FLIGHT BLISK DESIGNS



GENERAL ELECTRIC COMPANY
AIRCRAFT ENGINE GROUP

Figure 81. Comparison Between Demonstrator and Flight Blisks

HIGH BYPASS TURBOFAN BLISK AND SPINNER

LINE OF CONSTANT EFFECTIVE STRESS

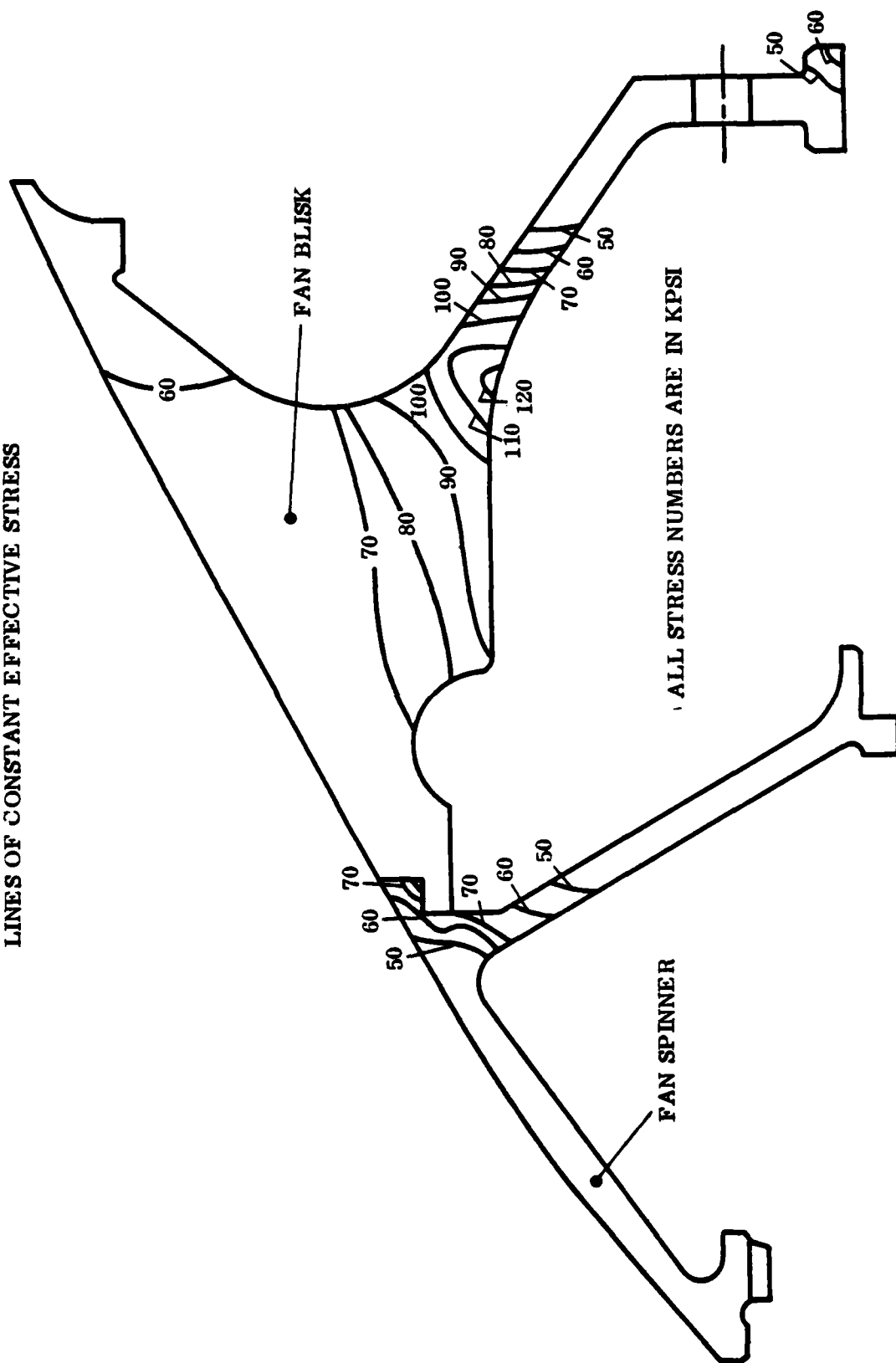


Figure 82. Fan Blisk and Spinner Stress Distribution

3.5.3 Fan Blisk Material Selection

Selection of the high bypass turbofan blisk material was based on the following criteria:

- o cost
- o weight
- o fatigue strength
- o material and process availability
- o FOD and corrosion resistance
- o sand erosion resistance.

With these criteria in mind four material candidates were evaluated, a summary of this study is shown in Table 20.

GE AM355 was selected because it possesses the best balance of the desired criteria and is predictably available from several reliable vendors.

3.5.4 Fan Exit Guide Vane Overall Design

The fan exit guide vane airfoils which resulted from the aeromechanical analysis were integrated into an assembly which becomes a part of the test rig.

The overall design of the exit guide vane assembly is shown in Figure 83. The assembly consists of 42 individually machined vanes with integral outer and inner platforms. The vanes are assembled with .004 nominal gaps all around. Mating surfaces of select exit guide vanes will be ground until the cylindrical aero outer flowpath is met. After final assembly and tack welding the part will be brazed to yield a full 360° vane ring. Design advantages of the chosen design are shown in Figure 83. Detail fan exit guide vane drawing number 17A 138 - 325 has been issued.

3.5.5 Fan Exit Guide Vane Material Selection

The airfoil material selection process followed the same general procedure as that described for the blade (Table 20). The major ingredients, however, in the selection process were high cycle fatigue (HCF) and overstress capability. For this reason the choices involved INCO 718 and A286. The choice of A286 was arrived at considering cost and machineability.

3.5.6 Fan Weight

The total fan weight was estimated in the Phase I preliminary design report to be 43 lbs. The weight calculation of the proposed design shows this estimated weight to be correct.

HIGH BYPASS TURBOFAN FAN BLISK

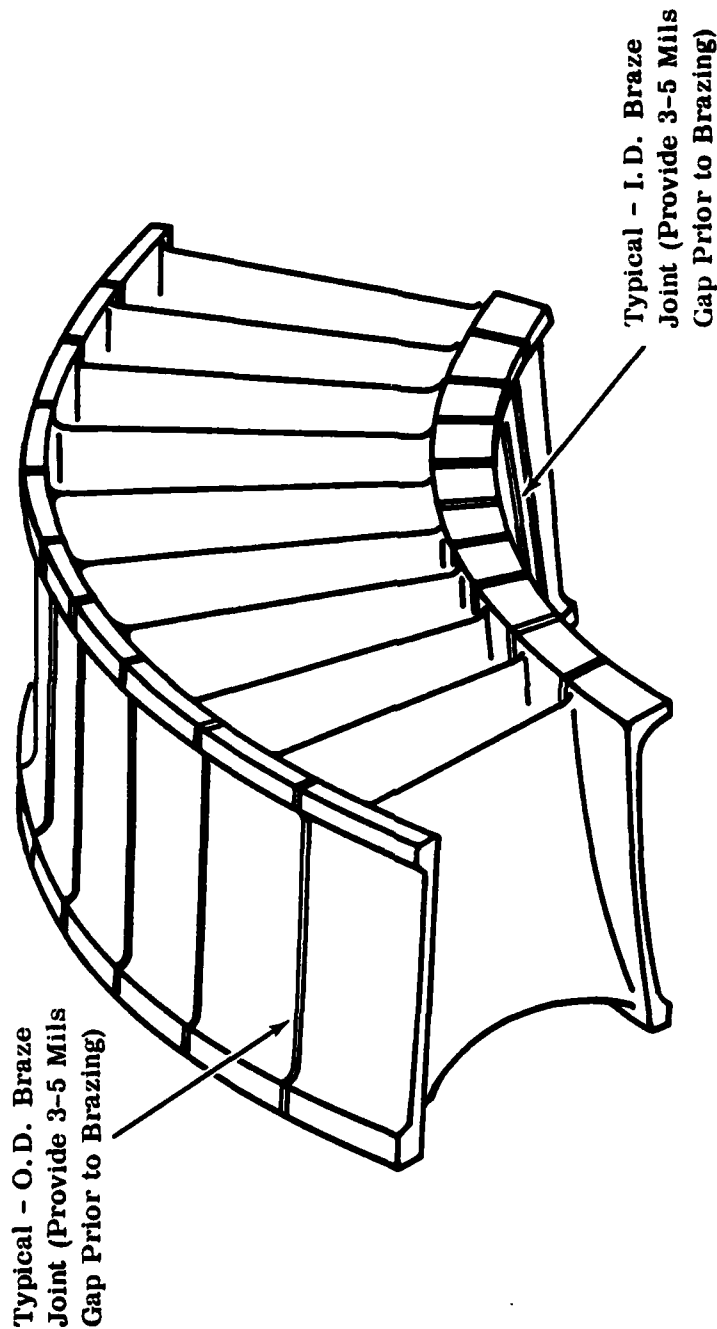
MATERIAL CANDIDATES:

<u>MATERIAL</u> GE AM355	<u>FABRICATION</u> <u>PROCESS</u> MACHINED	PRELIMINARY EXTIMATE OF COST OF 250TH BLISK, \$	EST. WEIGHT, LBS	ADVANTAGES/DISADVANTAGES
		6000.-	23	GOOD BALANCE BETWEEN COST, WEIGHT, DESIGN INTEGRITY AND FOD/EROSION RESISTANCE. GOOD MATERAIL PROPERTIES OF LARGE FORGINGS
CUSTOM 450	CAST	4000.-	23	PROPERTIES COMPARABLE TO AM 355. NEEDS PROCESS DEVELOPMENT. \$2000 COST REDUCTION ANTICIPATED.
TI 6-4	MACHINED	8000.-	13	HIGH PROCUREMENT COST, LOWEST, WEIGHT. EROSION AND FOD RESISTANCE POORER THAN STEEL. POOR MATERIAL PROPERTIES OF LARGE FORGINGS.
INCO 718	MACHINED	10000.-	23	BEST DESIGN INTEGRITY AND FOD/EROSION RESISTANCE. POOR MACHINEABILITY AND HIGHER MATERIAL COST THAN AM355.

MATERIAL SELECTED

GE AM355 WAS SELECTED FOR THE DEMONSTRATOR PROGRAM AND FOR PRODUCTION UNTIL
CUSTOM 450 PROCESS IS READY FOR PRODUCTION.

OVERALL EXIT GUIDE VANE MECHANICAL DESIGN (PARTIAL VIEW OF 360° ASSEMBLY)



Design Advantages

- Good Dimensional Control.
- Good Control Over Fillet Radii.
- Brazing Joints are Easily Accessible for Good Cleanup.
- Design Allows "Soft" Inner and Outer Supports.

Figure 83. Exit Guide Vane Assembly Overall Design

3.5.7 Compliance with MIL-E-5007 Requirements

Several major MIL-E-5007 requirements, applicable to the high bypass turbofan design are listed in Table 21. According to this table all listed requirements are met.

TABLE 21. KEY MIL-E-5007D REQUIREMENTS EVALUATION

TURBOFAN MECHANICAL DESIGN

RELATIVE TO MIL-E-5007D REQUIREMENTS

1)	<u>BIRD INGESTION</u>	AIRFOIL MEETS FRAGMENTATION AND FRACTURE REQUIREMENTS
2)	<u>LCF LIFE</u>	
	REQUIREMENT:	2 * 12 000 CYCLES
	RESPONSE:	DESIGN COMPLIES WITH REQUIREMENT.
3)	<u>DISK BURST SPEED</u>	
	REQUIREMENT:	DISK TO BE ABLE TO RUN SUCCESSFULLY AT 22% ABOVE MAX NG (NG = $1.02 * 1.22 * 22719 = 28\ 270$ RPM)
	RESPONSE:	DESIGN COMPLIES. DEMONSTRATION IN A SPIN PIT AT 28 270 RPM PLANNED.
4)	<u>ANTI ICING</u>	
	REQUIREMENT:	ENGINE MUST BE ABLE TO OPERATE UNDER ICING CONID- TIONS.
	RESPONSE:	EXPERIENCE WITH GENERAL ELECTRIC TURBOFAN ENGINES (TF 34-100, CF6-6, CF6-50 AND CFM 56) INDICATES THAT AN ACTIVE HOT AIR ANTI-ICING SYSTEM TO WARM THE BLISK SPINNER OR EXIT GUIDE VANES IS NOT REQUIRED.

3.6 TEST EQUIPMENT INTERFACE AND DESIGN INTEGRATION

3.6.1 Design Philosophy

The fan component test rig is being designed by the Test Facilities Engineering Group using the following guidelines:

- o Use a simple, rugged and inexpensive design without attempting to simulate flight type designs.
- o Use a two bearing design test vehicle similar to the GE26/F2 vehicle which ran very successfully. Bearings consist of a kingsbury thrust bearing in the rear and a roller bearing in the front.

3.6.2 Fan Interface With Test Rig

Figure 84 shows the high bypass turbofan stage as it will be installed in a test rig which will be set-up in an existing, proven fan test facility. The Test Facilities Engineers are supported by the fan design engineers to assure compatibility with the fan and to help achieve design objectives during the component test. The component test rig, currently in its preliminary design phase will satisfy the following ground rules.

- o Meet engine outer and inner flowpath from spinner through EGV
- o Blisk to be per engine configuration. EGV airfoils will be per engine configuration but the EGV assembly will be designed to conform to test rig configuration.
- o Emphasis to be given to aerodynamic simulation and good instrumentation routing.
- o Use existing test facility and rig hardware wherever possible.

3.6.3 Test Rig Design

The front end of the preliminary design is shown in Figure 84. The back end consists of previously used hardware modified for the high bypass turbofan application. The roller bearing is an existing J85 engine bearing. A layout drawing, Number 17A138-274 has been issued to show the blisk and EGV aerodynamic relationship and flowpath.

HIGH BYPASS TURBOFAN STAGE IN COMPONENT RIG

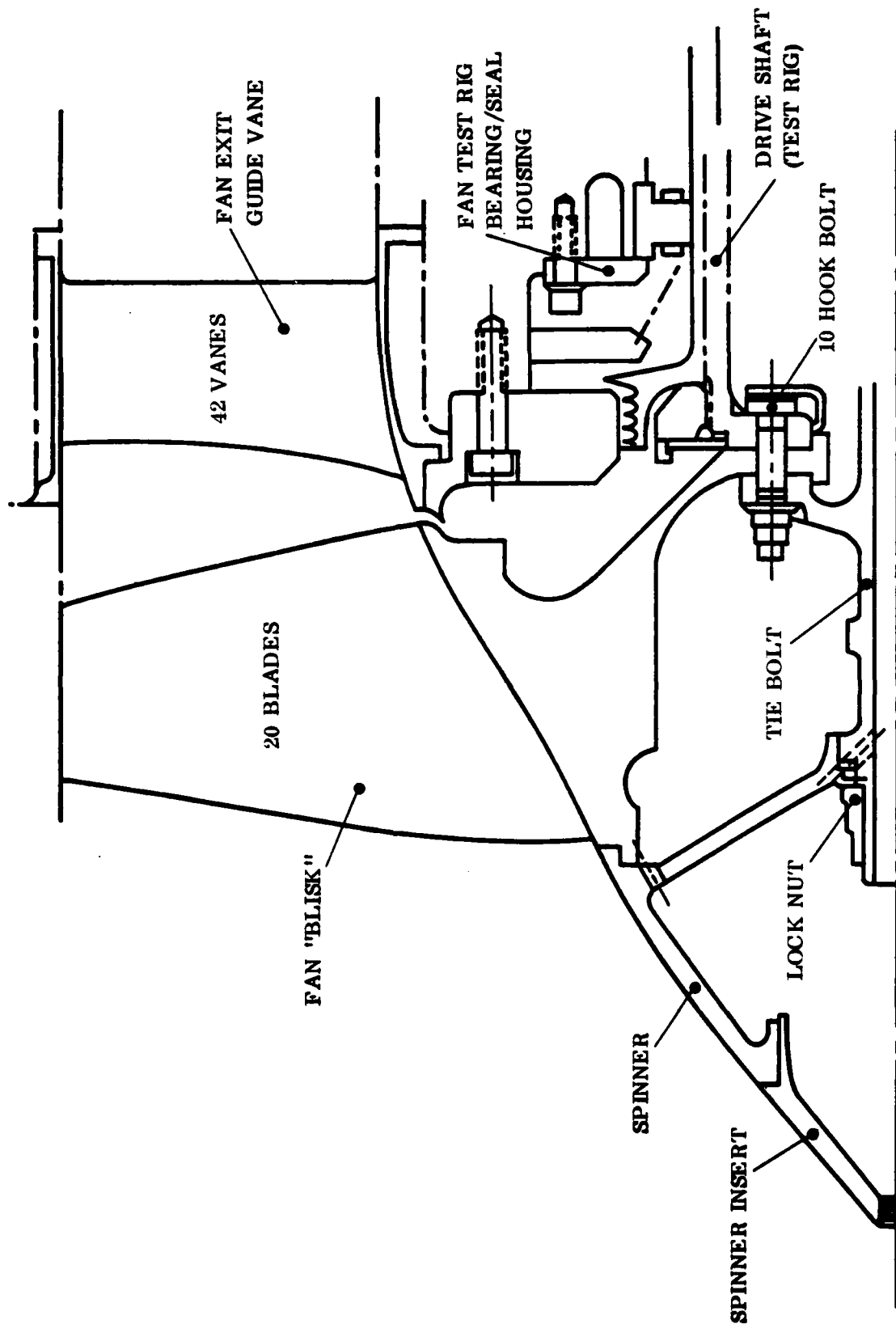


Figure 84. Fan Blisk and EGV Assembled in Test Rig

3.7 RELIABILITY, MAINTAINABILITY, AND SYSTEMS SAFETY

Interim Technical Report #AFAPL-TR-78-109 (Phase I Preliminary Design) concluded that the proposed fan design had satisfactory R&M and Safety characteristics. Since the detailed mechanical design recommended now in this report is essentially the same as the design shown in the Phase I preliminary design report, it is concluded that the R&M and Safety requirements are satisfied. For example, the engine maintainability feature of forward blisk removal without exposure of bearing-sump is included in the component test rig design.

SECTION IV

CONCLUSIONS

The objectives of the Detail Design, Phase II of the Contract Statement of Work, have been met, confirming that the required aerodynamic performance as well as MIL-E-5007D mechanical requirements can both be met simultaneously.

Further, the comparison (in Table 19) of the important design parameters versus those of the originally proposed fan show close agreement.

The High Bypass Turbofan design balanced the aerodynamic and aeromechanical requirements for an operational fan to be used in the engine selected in Phase I so that the original proposed efficiency and stall margin objectives can be met.

SECTION V

RECOMMENDATIONS

The small high bypass fan, designed during Phase II of this contract, meets the aerodynamic and mechanical/life requirements of the Statement of Work, and therefore the Contractor recommends that the Air Force authorize the fabrication and test of the fan stage in accordance with Phase III. (This recommendation was acted upon on 7 May 1979 when the Contractor was authorized to proceed.)

The Contractor recommends that the Air Force consider a critical assessment of the MIL-E-5007D specification of bird strike capability as it applies to relatively small engines.

ABBREVIATIONS, ACRONYMS, AND SYMBOLS

AD	=	discharge area
A1	=	inlet area
AM	=	mouth area
AR	=	aspect ratio
AT	=	throat area
β bird	=	relative angle of bird
β_1	=	inlet relative air angle
β_1^*	=	inlet relative metal angle
β_2	=	discharge relative air angle
C_z air	=	axial velocity of air
C_z bird	=	axial velocity of bird
δ	=	corrected pressure
DFR		rotor diffusion factor
DFS	=	stator diffusion factor
FCW	=	first covered wave
FOD	=	foreign object damage
g	=	gravitational constant
H	=	enthalpy, BTU/lb
HCF	=	high cycle fatigue
i	=	incidence
\hat{i}	=	suction surface incidence
ID	=	inner diameter
J	=	778 ft-lb/BTU
LE	=	leading edge
M _D	=	discharge Mach No.
M _I	=	inlet Mach No.
M _M	=	mouth Mach No.
N	=	rotational speed, RPM
O/L	=	operating line

ABBREVIATIONS, ACRONYMS, AND SYMBOLS

OD	=	outer diameter
PS1	=	inlet static pressure
PS	=	pressure surface
PT1	=	inlet total pressure
PT2	=	discharge total pressure
RR	=	radius ratio
RT _{in}	=	inlet tip radius
RT _{out}	=	discharge tip radius
SS	=	suction surface
$\sqrt{\theta}$	=	corrected temperature
tm/C	=	maximum thickness/chord
U	=	wheelspeed, ft/sec
U _T	=	tip wheelspeed, ft/sec
W	=	airflow
W/A	=	airflow/annulus area
W _{air}	=	relative velocity of air
W _{bird}	=	relative velocity of bird
W _{nor}	=	relative velocity component of bird normal to blade